

**Molecular and Functional  
Characterization of TrkC  
Alternative Splicing Regulation and its  
Impact on the Fate Acquisition of  
Cortical Projection Neurons**

**Inaugural-Dissertation  
to Obtain the Academic Degree  
Doctor rerum naturalium (Dr. rer. nat.)**

**submitted to the  
Department of Biology, Chemistry, Pharmacy  
of Freie Universität Berlin**

**by**

**Andreea-Ioana Weber**

**- 2021 -**

The work presented in this dissertation has been performed between 1.4.2017 and 30.5.2021 under the supervision of Prof. Dr. Victor Tarabykin at the Charité Universitätsmedizin, Institute of Cell Biology and Neurobiology, and under the supervision of Prof. Dr. Florian Heyd at the Freie Universität Berlin, Department of Biology, Chemistry, Pharmacy.

First reviewer: Prof. Dr. Victor Tarabykin

Second reviewer: Prof. Dr. Florian Heyd

Disputation on: May 9th, 2022

# ACKNOWLEDGEMENTS

I am first and foremost grateful for all the fortunate events that led up to me completing this doctoral research project. Humans will always fascinate me, from the molecular bits and bobs that endow us with brains supporting the ability to reason and all the way up to the creation of work that endures across generations. While some of this enduring type of work is in the realm of the arts, humanities and, yes, science, I have substantially benefitted from the less visible but equally important work of people who directly passed down their wisdom to me and supported me. One of my greatest privileges is to have had quite a few such people in my life.

First, I would like to thank Prof. Dr. Victor Tarabykin for giving me the chance to hop aboard the cortex development train, to work in his lab and, last but not least, for having the idea for this project and providing me with the resources needed to pursue it.

Second, my gratitude goes out to Prof. Dr. Florian Heyd, who fuelled my enthusiasm for alternative splicing in cortex development even further and who not only agreed to act as second advisor and reviewer for this project but also provided me with a second “lab home”. I will always remember your outstanding helpfulness! I would also like to thank all the members of the Heyd lab for the very warm welcome, and especially Dr. Marco Preußner for his work on the siRNA screen.

Among the nicest surprises of the last years was getting altruistic support from some very unexpected sources. Thank you, Dr. Marta Rosário and PhD Dr. Michael Depew, for all the mentoring conversations you have chosen to spend your time on for my sake. You made me feel both capable as a scientist and seen as a human, and I will always treasure this. Also, a kind thank you to Prof. Heiner Schaal from U Düsseldorf for reaching out with scientific advice and providing the enhancer reporter plasmids used in this thesis.

The bulk of the PhD would have been far less productive and enjoyable without the excellent company and collaboration of my colleagues from the Tarabykin lab and the Institute for Cell Biology and Neurobiology. I would like to make a special mention of Dr. Ingo Bormuth, who introduced me to the wonderful world of cortex development. Your enthusiasm for science, your patience and kindness are truly unparalleled, Ingo, and I would be a lesser scientist if I hadn't had the luck to work under your guidance, even though it was for such a short period of time. Furthermore, the work presented here would not have been at all possible without the participation of three talented scientists and in utero electroporation specialists: Katya Borisova, Katya Epifanova and Sasha Rusanova. You all are modest and may say that in utero electroporation is “just a one hour thing”, but I am indebted to you for always taking that time out of your very busy PhD lives. I keep my fingers crossed that you get all the recognition you deserve, scientific and otherwise! Dr. Mateusz Ambrozkiewicz also performed a round of IUEs. Thank you very much for that and for your availability to answer my questions! Aside from this, everyday lab life would have been austere without Diana, Pina, Claudia, Ethi, Eva, Andrew and Marni - so long, and thanks for all the fi...uhm, protocols ;)

I have also benefitted from excellent technical support from Denis Lájko, Rike Dannenberg, Roman Wunderlich, Antje Grünwald and Bobby Draegert. Thank you all - lab work would be a million times more stressful without your efforts and expertise.

I would like to thank my parents for being highly atypical Romanian parents and letting me do my thing, whether that was design (if drawing and painting on the walls can be called that) or science or building an unusual life for myself. I still fondly remember the books you gave me that started my scientific journey: the wonderful Larousse pocket encyclopedias on biology, which I read during my childhood so many times over that the pages fell out. Thank you for your continued support!

Last, but certainly not least, I am pleased to thank my “chosen family”: Elena, Iunia, Irina, Laura, and Leo. Without you, my life would feel far less fun, interesting, hopeful and safe, less worthwhile. A special shoutout to Leo for being the most amazing flatmate ever and, among many other things, treating the occasional DNA tube and microscopy slide box in the fridge as a funny and interesting occurrence :D.

## SELBSTSTÄNDIGKEITSERKLÄRUNG

Hierdurch versichere ich, Andreea-Ioana Weber, dass ich die hier vorliegende Arbeit selbstständig verfasst und keine anderen als die von mir angegebenen Quellen und Hilfsmittel verwendet habe. Ich versichere, dass ich meine Dissertation nicht schon einmal in einem anderen Promotionsverfahren eingereicht habe.

Berlin, den 07.09.2021

---

*“Sometimes, magic is just spending more time on something than anyone else might reasonably expect.”*

- RJ Teller

*“The stars we are given. The constellations we make.”*

- Rebecca Solnit

# TABLE OF CONTENTS

<b>1. INTRODUCTION</b> .....	<b>3</b>
1.1. General aspects of cortex development .....	3
1.2. Organization of the neocortex .....	4
1.3. A primer on the prenatal development of the mammalian cerebral cortex .....	7
1.4. Processes involved in neuronal identity acquisition in the cortex.....	10
1.4.1. Biology of the different types of neocortical neural progenitor cells (NPCs) ..	10
1.4.3. Generation of projection neuron subtypes .....	16
1.5. Functions of alternative splicing in prenatal brain development .....	18
1.5.1. Mechanistic aspects of alternative splicing.....	19
1.5.2 Alternative splicing in the brain and its development .....	21
1.6. The role of TrkC alternative splicing isoforms in neuronal identity acquisition	
24	
1.6.1. Neurotrophins and their receptors, the Trk tropomyosin receptor tyrosine ki-	
nases .....	25
1.6.2. The TrkC receptor variant TrkC-T1 is a determinant of deeper layer (CFuPN)	
neuron fate .....	26
<b>2. RESULTS</b> .....	<b>29</b>
2.1. TrkC-T1 exerts its effect on MAPK/Erk1/2 signalling by sequestering p52-ShcA	
to intracellular compartments .....	29
2.2. The ratio of TrkC-T1 to TrkC-TK+ transcripts shifts during cortex development..	
30	
2.3. The ratio of TrkC-T1 to TrkC-TK+ transcripts is not affected by different decay	
rates of the two transcripts .....	32
2.4. TrkC-T1 and TrkC-TK+ transcript quantities are likely not regulated by miRNAs	
in the developing cortex.....	32
2.5. The TrkC-T1 and TrkC-TK+ transcripts are present in different ratios in NPCs	
and neurons .....	34
2.6. Srsf1 and Elavl1 alter the ratio of TrkC-T1 to TrkC-TK+ in an antagonistic man-	
ner .....	36
2.7. Srsf1 and Elavl1 alter choice between CFuPN and CPN fate in the developing	
cortex.....	40
2.8. Srsf1 and Elavl1 directly influence the ratio of TrkC-T1 to TrkC-TK+ on both the	

transcript and protein levels .....	43
2.9. The effects of Srsf1 and Elavl1 on the CFuPN-CPN fate decision are dependent on the levels of TrkC-T1.....	45
2.10. Srsf1 and Elavl1 are differentially expressed in the histological compartments of the developing cortex .....	47
2.11. Srsf1 and Elavl1 are expressed in different NPC- and neuron-specific ratios in the developing cortex .....	49
2.12 Bioinformatic analysis of the Ntrk3 primary transcript suggests the presence of an Srsf1-dependent exonic splicing enhancer in exon 13A.....	50
2.13 Fragment 3 of exon 13A contains a GAR exonic splicing enhancer crucial for the formation of TrkC-T1 .....	52
2.14 The splicing-enhancing effect of fragment 3 of the TrkC-T1-specific exon 13A depends on Srsf1 .....	55
2.15 The SR protein kinases Srpk1 and Srpk2 participate in the CFuPN fate choice, but not by involvement in TrkC alternative splicing.....	55
<b>3. DISCUSSION.....</b>	<b>59</b>
3.1. The balance of TrkC alternative splicing isoforms is cell-type specific in NPCs and neurons .....	59
3.2. Srsf1 and Elavl1 co-regulate the balance of TrkC alternative splicing.....	64
3.3. Srsf1 and Elavl1 levels define cell-type specific splicing-regulatory environments in the developing cortex .....	67
3.4. Srsf1 and Elavl1 regulate projection neuron identity acquisition by controlling TrkC alternative splicing .....	71
<b>4. MATERIALS AND METHODS .....</b>	<b>75</b>
4.1. Cell culture and treatment .....	75
4.2. Delivering expression constructs into cultured cells.....	77
Transfection of immortalized cells .....	77
Nucleofection of primary cortical neurons .....	77
4.3. Tissue processing .....	77
4.4. Cell and tissue staining procedures .....	78
Chromogenic RNA <i>in situ</i> hybridization.....	78

Immunofluorescent staining .....	79
4.5. List of antibodies used in this study .....	80
4.6. Image acquisition, processing and quantification .....	80
Image acquisition for <i>in situ</i> hybridization.....	80
Image acquisition for immunofluorescence .....	81
Analysis of fluorescence micrographs.....	81
4.7. Fluorescence-assisted cell sorting (FACS) .....	81
4.8. RNA extraction .....	82
4.9. cDNA first-strand synthesis .....	82
4.10. Quantitative real-time PCR.....	82
TaqMan qPCR.....	83
SYBR Green qPCR .....	83
4.11. Splicing-sensitive PCR.....	83
4.12. Molecular cloning of expression and reporter constructs.....	85
Subcloning of ORFs for expression constructs .....	85
Generation of splicing reporter vectors .....	85
4.13. Knockdown constructs .....	86
4.14. siRNA-based knockdown .....	86
4.15. Protein extract preparation and Western blotting .....	87
4.16. Animal care and husbandry.....	88
4.17. <i>In utero</i> electroporation .....	88
4.18. Statistical analysis.....	89

<b>BIBLIOGRAPHY .....</b>	<b>91</b>
---------------------------	-----------

<b>SUPPLEMENTARY INFORMATION.....</b>	<b>119</b>
---------------------------------------	------------

*The digital version of this thesis is interactive and can be navigated by clicking on the section titles on the right. The table of contents is also interactive and can be used to rapidly access the subsections of interest.*

## SUMMARY

The astonishing cellular diversity and finely tuned neuroanatomy of the cerebral cortex motivates sustained research efforts on the mechanisms that give rise to this intricate tissue. To enable the higher cognitive functions of mammals, various subtypes of cortical projection neurons, distributed in precise ratios and at specific positions in the cortex, participate in the neuronal circuitry of the brain. These positions and ratios are established during embryonic development. Including the neuron's targets and input sources, the subtype identity of a neuron depends on its transcriptomic signature.

Broadly speaking, cortical neuron subtypes project either to the contralateral hemisphere, such as callosal projection neurons (CPN) or outside of the cortex, such as corticofugal projection neurons (CFuPN). Both of these subtypes are generated by neural progenitor cells (NPCs) in the forebrain. During embryonic development, NPCs divide sequentially to generate other NPCs and various neuron subtypes, as dictated by the identity of the NPC itself. The fate decisions of an NPC lineage that determine how many neurons of each subtype it will produce are influenced by a spatially and temporally specified combination of molecular signals. These intra- and extracellular cues jointly intervene in cellular mechanisms, such as division speed, inheritance of fate-determining factors, and many more, ultimately shaping the ratio of neuron subtypes that the lineage produces during differentiation.

One of the mechanisms that can control differentiation is the alternative splicing (AS) of primary transcripts, which can be regulated in a cell type- and stage-specific manner, ensuring adaptation to changing developmental requirements. AS is a way of generating molecular diversity by the context-dependent inclusion or exclusion of exons, introns or parts of exons from pre-mRNAs to form distinct mRNAs. At its simplest, AS is regulated by distinct sequence elements in the pre-mRNA, which are bound by splicing-regulatory proteins, termed splicing factors (SFs). SFs themselves respond to intra- and extracellular cues by being expressed or activated according to the needs of the developing tissue. Examples of AS regulating cell differentiation in other biological systems abound, but, even though AS is implicated in an increasing number of processes in the adult brain, its functions in cortex development are largely unexplored.

The focus of this work are two isoforms of the neurotrophin-3 receptor, TrkC, which result from alternative splicing. The better studied of the two isoforms, the kinase-active TrkC-TK+, has been shown to act as a recipient of survival signals in neurons. Our research group previously showed that the less studied isoform, TrkC-T1, is a determinant of CFuPN fate, present in the development of the cortex in specific cell types and time windows. As the levels of TrkC-T1 in NPCs coordinate the numbers of CFuPN that are produced at the expense of CPN, the aim of this project was to explore how the AS of TrkC is regulated, in order to further our understanding of the factors that shape the NPC transcriptome and hence fate.

In this work, we show that the balance between TrkC-T1 and TrkC-TK+ is cell type-specific in the developing cortex and primarily established at the level of AS regulation. We find that the splicing factors Srsf1 and Elavl1 regulate this isoform balance in an antagonistic manner. To our knowledge, this is the first described instance of these splicing factors co-regulating an AS event. In addition to this, we bring direct *in vivo* evidence that implicates both of these SFs in the CFuPN-CPN fate choice, a biological process they had not been previously linked to. We also find that Srsf1 and Elavl1 have different expression patterns in the developing cortex, a feature that contributes to the different cell type-specific splicing-regulatory environments that give rise to distinct ratios of TrkC-T1 to TrkC-TK+. Taken together, these findings further our knowledge of how cortical projection neuron fate is regulated at the posttranscriptional level.

# ZUSAMMENFASSUNG

Die außerordentliche Vielfalt an Zellen und die präzise Neuroanatomie der Großhirnrinde (Kortex) führt immer wieder zu neuen Forschungsbemühungen, um die Mechanismen zu verstehen, welche diese komplexe Gewebeorganisation hervorbringen. Um die höheren kognitiven Funktionen der Säugetiere zu ermöglichen, beteiligen sich diverse Untertypen von kortikalen Neuronen an neuronalen Netzwerken, in präzise abgestimmten Verhältnissen und an definierten Positionen. Diese Verhältnisse und Positionen werden während der Embryonalentwicklung festgelegt. Zusammen mit den Zielzellen und Input-Quellen eines Neurons hängen diese Eigenschaften von dessen transkriptomischen Signatur ab.

Im Allgemeinen projizieren die Untertypen von kortikalen Neuronen entweder zur gegenüberliegenden Kortexhämisphäre, wie z.B. callosale Projektionsneurone (CPN), oder außerhalb des Kortex, wie z.B. kortikofugale Projektionsneurone (CFuPN). Beide Untertypen werden von neuronalen Vorgängerzellen (engl. "neural progenitor cells", kurz NPCs) im Vorderhirn generiert. Während der Embryonalentwicklung teilen sich die NPCs sequentiell, um andere NPCs oder unterschiedliche Neuron-Untertypen zu generieren, so, wie es die Identität der NPC an sich bestimmt. Die Schicksalsentscheidungen einer NPC-Abstammungslinie werden von einer zeitlich und räumlich bestimmten Kombination an molekularen Signalen bestimmt. Diese intra- und extrazelluläre Auslöser greifen gemeinsam in zelluläre Mechanismen ein, wie die Teilungsgeschwindigkeit, Vererbung von schicksalsbestimmenden Faktoren u.v.m., um letztlich das Verhältnis der Neuron-Untertypen zu bestimmen, welche die Abstammungslinie während der Differenzierung produziert.

Eines der Mechanismen, welche zelluläre Differenzierung beeinflussen können, ist das alternative Spleißen (AS) der Primärtranskripte, welches basierend auf dem Zelltyp oder Entwicklungsstadium reguliert werden kann, um die Anpassung an sich verändernden Entwicklungsanforderungen zu ermöglichen. AS generiert molekulare Diversität durch die kontextabhängige Inklusion oder Exklusion von Exone, Introne oder Teile von Exone der Prä-mRNA, um unterschiedliche mRNAs hervorzubringen. In der einfachsten Form wird AS von Sequenzelementen reguliert, die von spleiß-regulierenden Proteinen, genannt Spleißfaktoren (SFs) gebunden werden. SFs reagieren an sich auf intra- und extrazelluläre Reize, indem sie unterschiedlich exprimiert oder aktiviert werden, so, wie das sich entwickelnde Gewebe es benötigt. Es gibt viele Beispiele von AS-geregelten Zelldifferenzierung aus anderen biologischen Systemen. Trotz der Tatsache, dass AS mit einer steigenden Zahl an Prozessen des adulten Gehirns in Verbindung gebracht wird, sind dessen Funktionen im sich entwickelnden Kortex größtenteils unerforscht.

Der Fokus dieser Arbeit stellen zwei Isoformen des Neurotrophin-3-Rezeptors TrkC dar, welche aus AS resultieren. Die umfangreich studierte Isoform, die Kinase-aktive TrkC-TK+ Isoform, wurde mit dem Empfangen von Überlebenssignale in Neuronen in Verbindung gebracht. Unsere Forschungsgruppe hat gezeigt, dass die weniger bekannte Isoform, TrkC-T1, ein bestimmender Faktor für das CFuPN-Schicksal ist. Sie ist in dem sich entwickelnden Kortex in genau definierten Entwicklungszeiträumen und Zelltypen vertreten. Da die Niveaus an TrkC-T1 in NPCs die Anzahl produzierten CFuPN, im Gegenzug zu CPN, bestimmen, war das Ziel dieser Arbeit zu erforschen, wie das AS von TrkC geregelt ist, um unser Wissen über Faktoren zu erweitern, welche das NPC-Transkriptom und damit deren Schicksal gestalten.

In dieser Arbeit zeigen wir, dass die Balance zwischen TrkC-T1 und TrkC-TK+ zelltypspezifisch im sich entwickelnden Kortex ist, und dass dies primär auf der Ebene der AS-Regulation bestimmt wird. Wir beschreiben, dass die SF Srsf1 und Elavl1 diese Isoform-Balance auf antagonistischer Art und Weise regeln. Nach bestem Wissen ist das die erste beschriebene ko-regulierende Interaktion dieser Faktoren. Zusätzlich erbringen wir direkte in vivo-Evidenz, dass die beiden SFs an der CFuPN-CPN-Schicksalsentscheidung beteiligt sind, ein biologischer Prozess, mit dem sie bislang nicht in Verbindung gebracht worden sind. Außerdem beschreiben wir, dass Srsf1 und Elavl1 unterschiedliche Expressionsmuster im sich entwickelnden Kortex aufweisen, was zur zelltypspezifischen Balance von TrkC-T1 zu TrkC-TK+ beiträgt. Zusammengenommen erweitern diese Befunde unser Wissen über wie das Schicksal kortikaler Neurone auf dem posttranskriptionellen Niveau geregelt ist.

# 1. INTRODUCTION

## 1.1. GENERAL ASPECTS OF CORTEX DEVELOPMENT

Some of the most complex processes that have arisen in the evolution of animals are cognitive abilities, made possible by the brain. Among these are learning, memory, and voluntary motor control, expanded in humans by language and reasoning and culminating with conscious self-awareness. Cognitive abilities depend strongly on the most recent evolutionary addition to the brain, the cerebral cortex. Its mammalian-specific portion, the neocortex<sup>1</sup>, also known as isocortex, is comprised of two interconnected sheets of neural tissue that take up most of the outer surfaces of the brain hemispheres. In each hemisphere, the isocortex is adjacent and in direct continuation to its evolutionarily older counterparts, the lateral cortex, or archicortex, and the medial cortex, or paleocortex. These types of cortex are responsible mainly for olfaction and include parts of the limbic system such as the hippocampus and the cingulate cortex (reviewed in Rakic, 2009; Geschwind & Rakic, 2013; Cárdenas & Borrell, 2020).

The neural<sup>2</sup> tissue of the neocortex is a complex, three-dimensional lattice of different neuronal and non-neuronal cell types, encompassing an estimated 16 billion individual nerve cells and 164 trillion synapses in humans. The cortical neurons are interlinked in both local microcircuits and also in large networks spanning the two hemispheres and beyond: some axons of cortical neurons form fiber tracts that reach as far as the spinal cord (Azevedo et al., 2009; Tang et al., 2001). To understand how this network accounts for advanced cognitive abilities and how one could aid its regeneration or alleviate neurodevelopmental disorders, one has to understand, among others, what cell types it is composed of and how these interact under physiological conditions. Studying how the plethora of neural cell types arise during embryonic development and how different neuron subtypes reach their terminal positions and mature functionality in relaying and processing information significantly supports these efforts.

Since the overwhelming majority of cell types in the cortex originate from the same

---

1) For better reading flow, the remainder of the text will employ „cortex” to refer to the neocortex, unless otherwise indicated.

2) “Neural” refers to all cells of neuroectodermal origin, “neuronal” strictly to neurons.

pool of neural progenitor cells (Florio & Huttner, 2014), one of the intensely researched questions in cortex development is: how is it ensured that the correct neural cell types are produced in the correct numbers and at the right time and position, all from these progenitor cells that, outwardly, seem highly similar? Research in cortex development, therefore, strives, among other things, to elucidate the cell-intrinsic and -extrinsic factors that regulate how neural stem cells differentiate into several lineages of neuronal and non-neuronal cells and how the terminal identity of this cellular progeny is consolidated and maintained.

Along with transcriptional controls and epigenetic processes, alternative pre-mRNA splicing can contribute in many ways to the dynamics of how genetic information is processed and deployed during cell type specification. Exploiting AS mechanisms, as will be discussed in this work, can grant developmental processes the necessary degree of transcriptomic and proteomic flexibility in order to attain a high measure of histological complexity in a precisely orchestrated manner, leading to a cognitively functional cortex.

## 1.2. ORGANIZATION OF THE NEOCORTEX

From a bird's eye view, the adult mammalian cerebral cortex consists of projection neurons, interneurons (GABAergic), subplate neurons, macroglial cells (astrocytes and oligodendrocytes), and blood vessels lined by an endothelium with brain-specific permissiveness. The focus of this work lies on projection neurons, with an often pyramid-shaped soma extending a main apical dendrite towards the *Pia mater* above and axons innervating cortical and subcortical targets. Cortical projection neurons are represented in the bulk of the adult cortex and make up 80% of neocortical neurons, employ L-glutamate for excitatory signal transmission, and are positive for NeuN (Rbfox3). Interneurons represent the second class of neurons that is crucial for the cortical circuitry. They primarily serve inhibitory functions, using  $\gamma$ -aminobutyric acid as a neurotransmitter, and are Gad65-positive. Finally, glial cells do not participate in relaying information but provide vital support to the neurons they surround (Götz & Huttner, 2005; Geschwind & Rakic, 2013; Sun and Hevner, 2014; Lodato et al., 2015; Mukhtar and Taylor, 2018; Uzquiano et al., 2018)

At a more detailed look, the processing of information in the cortex is made possible by its transmission and integration through an extensive array of projection

neuron subtypes, together with their selective inhibition by interneurons. Historically, projection neuron subtypes have been classified by their localization in one of the layers of the cortex (Figure 1.1), as visualized microscopically after employing classical staining techniques (Golgi staining and Nissl staining, see Zaqout & Kaindl, 2016; Paletzki & Gerfen, 2019). Classical characterizations of cortical cytoarchitecture show six layers across the radial (inside-out) axis, each dominated by specific neurons when classified by cell morphology and hodology (connective properties) (Rakic, 2009, Geschwind & Rakic, 2013).

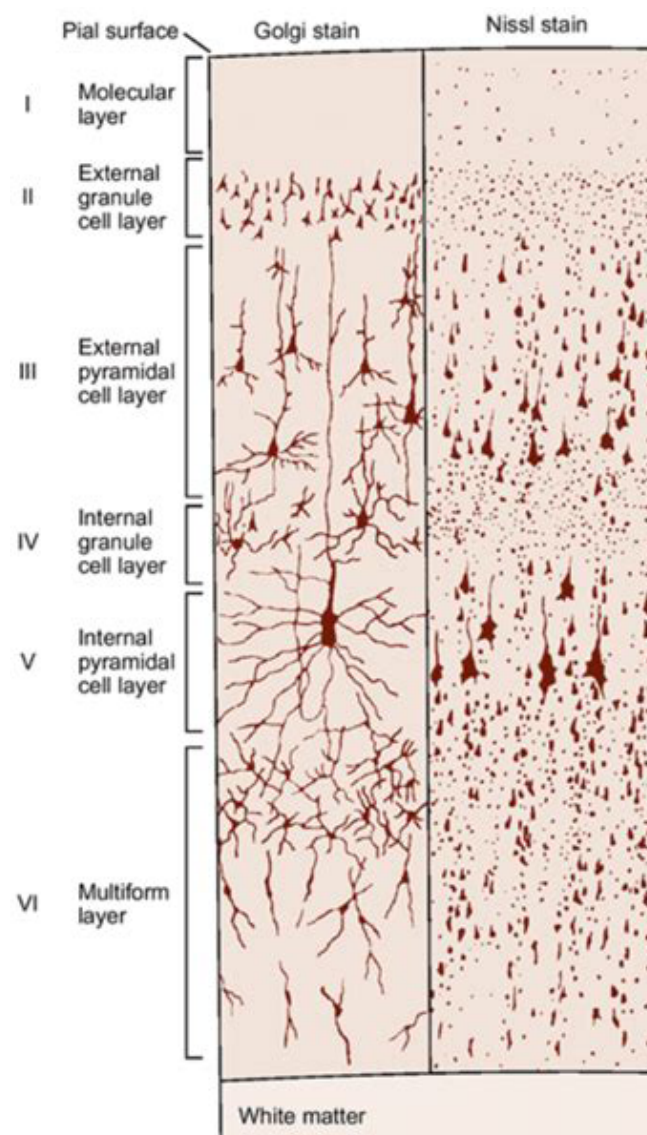


**Figure 1.1** Classic nomenclature and aspect of cortical layers, as depicted by K. Brodmann. Layer numbers as currently used are indicated in Roman numerals. The original drawing was first published in in 1909 in “Vergleichende Lokalisation: Lehre der Grosshirnrinde in ihren Prinzipien dargestellt auf Grund des Zellenbaues”, Leipzig, by JA Barth. The copyright expired in 1988, 70 years after the author’s death in 1918 (EU Directive 2006/116/EC, art. 12)

- Layer I is the first layer under the *Pia mater*, devoid of pyramidal cells but containing Cajal-Retzius cells that secrete Reelin, a chemoattractant that guides pyramidal neuron migration during development;
- Layer II consists of stellate cells and pyramidal neurons;
- Layer III is dominated by small and medium-sized pyramidal neurons;
- Layer IV primarily harbors stellate neurons and pyramidal neurons;
- Layer V is highlighted by conspicuously large pyramidal cells;
- Layer VI, the most deeply set layer, contains small pyramidal cells and multi-form neurons.

In time, the projection neuron subtype classification based solely on laminar position has been abandoned in favor of a currently still intensely researched and expanding identity definition that takes into account morphology, hodology, electrophysiological properties, and the presence of different combinations of transcripts, transcription factors, and epigenetic properties. The redefining of neuron subtype definitions is sped up by the advent of transcriptomic profiling of either purified neuronal populations or single neurons via deep sequencing of RNA, which showcases the astounding molecular complexity of cortical neuron subtypes. However, for the purposes of

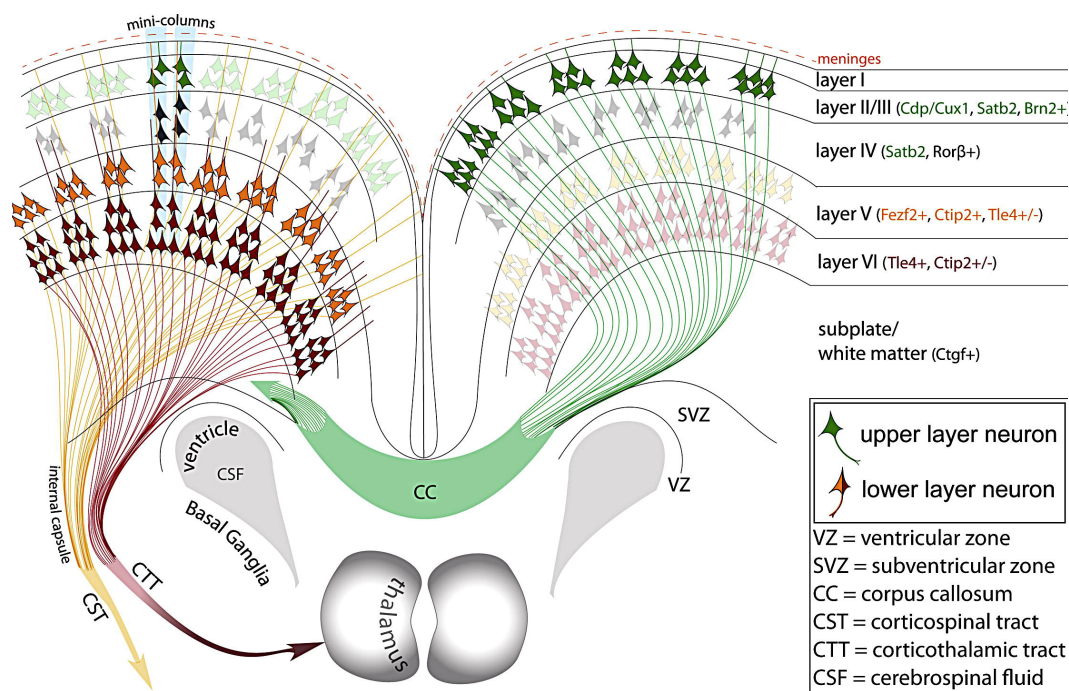


**Figure 1.2** Organization of the postnatal cortex with major projection targets of excitatory neurons. Major markers of the neuron subtypes present in these layers are indicated on the right. Note that callosal projection neurons (Satb2-positive) are, in reality, also present in the deep layers. Reproduced from DeBoer et al., 2013.

this dissertation, a lower amount of granularity in the definition of subtypes suffices. In a broad sense, layers II-III will be referred to as superficial (upper) layers and layers V and VI as deep layers (see Figure 1.2). The definitions of projection neuron subtypes will be restricted to callosal projection neurons (CPN), which project their axons to the contralateral cortical hemisphere, and corticofugal projection neurons (CFuPN), that project to subcortical structures, such as the thalamus (corticothalamic projection neurons, CThPN) or even as far as subcerebral targets in the medulla oblongata (subcerebral projection neurons, SCPN). Greig et al., 2013 offers a more in-depth categorization of classes within these broad projection neuron subtypes.

CPNs are primarily represented in the superficial layers, but some can also be found in the lower portion of layer V (Vb) and layer VI. They are an evolutionary novelty in mammals, allowing extensive bilateral transfer of information between cortical hemispheres (Fame et al., 2011; Jabaudon, 2017). In contrast, CFuPN and the layers they inhabit, V and VI, are thought to be evolutionarily older but are of equal importance for cortical function (Cárdenas & Borrell, 2020; Montiel & Aboitiz, 2015). The proportion of the cortical thickness that the cells of individual layers occupy differs between the functional areas of the cortex, requiring finely tuned local control over neuron subtype numbers (Arai & Pierani, 2014).

### 1.3. A PRIMER ON THE PRENATAL DEVELOPMENT OF THE MAMMALIAN CEREBRAL CORTEX

The brain and, by extension, the cerebral cortex is formed prenatally by progenitor cells that can generate a range of differently fated cellular progeny. These cell lineages birth the majority of cell types present in the cortex. The neural and non-neural cells that result from these lineages proceed to arrange so as to form the functional laminar cytoarchitecture described in the previous section. The potential of a lineage, or the cell types a lineage can birth, is usually sequentially restricted through molecular processes that control a stepwise, cascading series of events, namely, fate induction, fate specification, commitment to a fate, and terminal differentiation (McConnell, 1995; Dang & Tropepe, 2006; Greig et al., 2013). In the cortex, the exact output in terms of fates is controlled by factors extrinsic and intrinsic to the neural progenitor cells (NPCs). This section will succinctly describe the processes that lead up to the formation of the neocortex, whereas fate choice mechanisms directly relevant to cortical projection neurons are introduced in section 4.

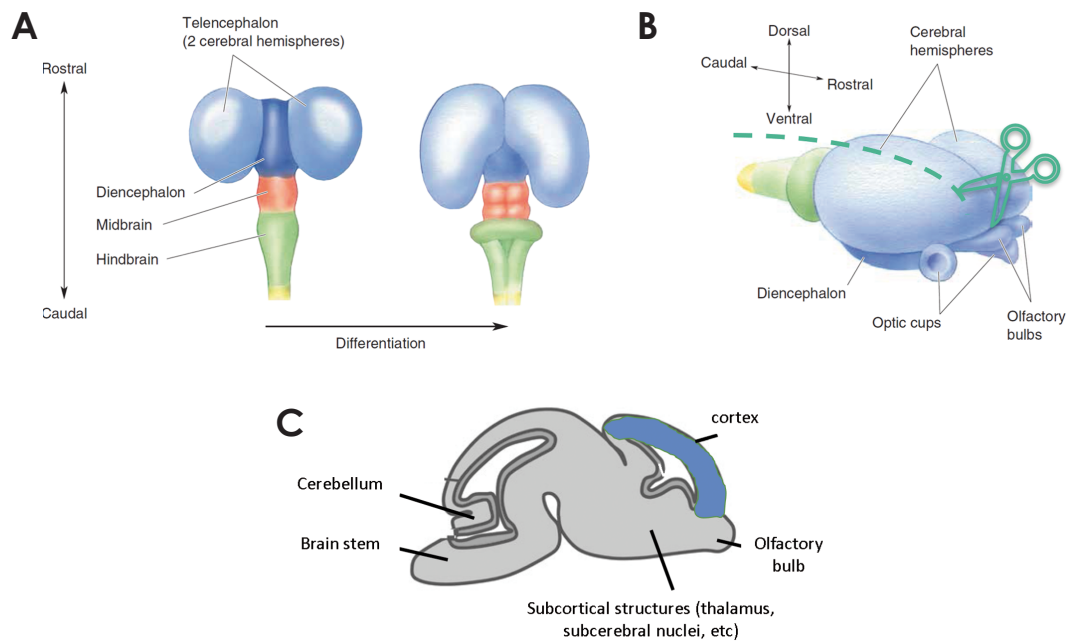


**Figure 1.3 Overview of the rodent brain.** **A** The developing rodent brain and its subdivisions. The telencephalon gives rise to the cerebral cortex. **B** Fronto-lateral view of the embryonic brain. **C** Model of the postnatal rodent brain in a sagittal section, as indicated by the dotted line in B. A and B: modified from and Bear et al., 2016 and C from Temple & Shen, 2013.

The entire central nervous system (CNS), comprised of the brain and spinal cord, and the peripheral nervous system (PNS) result from the folding, fusing, and evagination of the neural tube. The neural tube forms from an elongated part of the ectodermal layer termed neuroectoderm. The neuroectoderm is located on the dorsal surface of the embryo and folds longitudinally towards the interior of the embryo. The two resulting edges, the neural folds, fuse dorsally, thus giving rise to an internal canal, and this hollow cylinder then separates from the ectoderm and descends into the embryo. This cylinder is the neural tube, initially consisting of a thin sheet of neuroepithelial cells (NECs), which then closes at both the anterior (rostral) and the posterior (caudal) end (Puelles et al., 2013; Cohen et al., 2013). The caudal portion of the neural tube gives rise to the spinal cord, while the anterior protrusion is the precursor of the brain. In the next step towards brain formation, the neural precursor cells in this anterior area differentiate into three longitudinally arranged domains, of which the most rostral one, the prosencephalon (forebrain), precedes brain formation (Figure 1.3). Subsequently, the neuroepithelial cells of the prosencephalon undergo a further specialization step into telencephalic and diencephalic cells. The telencephalon contains the anlagen of the cortex and of further structures, as outlined below (Schoorjans and Guillemot, 2002; Bulfone et al., 2005; Moreno et al., 2009; Nowakowski et al., 2017).

The differentiation of the ventral versus dorsal and anterior versus posterior aspects of the neural tube is achieved through an interplay of signaling activators and inhibitors, also called morphogens, which are secreted from patterning centers inside and outside the neural tube and can then diffuse in the histological surroundings of the source. As is also later the case for cortical progenitors, the tangential (anteroposterior and lateromedial) positional identity of a neuroepithelial cell is determined by its competence to respond to the specific combination of morphogens present at its location. A successful response then activates intracellular signaling pathways and leads to transcriptional changes in patterning genes or cell sorting by migration or apoptosis, ultimately creating sharply defined territories of cells with different fates. The formation of the telencephalon depends first on the definition of an anteroposterior directionality of the body axis, which is achieved through the differential distribution of activators and repressors of Wnt, BMP, Fgf, and retinoic acid (RA) signaling along the neural tube (Muhr et al., 1999; Faravelli et al., 2014; Allodi & Hedlund, 2014; Hébert & Fishell, 2008; reviewed in Cohen et al., 2013). Further refinement of the cerebral vesicle boundaries is ensured by the expression of distinct combinations of Wnt pathway ligands (Mulligan & Cheyette, 2012). Next, proper development of the telencephalic vesicle is guided by dorsoventral differentiation of the neural tube, which is instructed by opposing gradients of BMP and Shh (Hébert & Fishell, 2008; Wang et al., 2016). Finally, the telencephalon is also patterned lateromedially by two sets of bilateral signaling centers: the cortical hem, situated at the interhemispheric midline, and the antihem, a portion of tissue that separates the dorsal and ventral telencephalon, which secrete Wnt and BMP ligands, or Fgf8 and EGF, respectively (Grove, 1998; Assimacopoulos et al., 2003).

The cortical hemispheres develop from the pallium, the dorsal part of the telencephalic vesicles. The adjoining ventrally positioned subpallium gives rise to a variety of other brain cell types (reviewed in Moreno et al., 2009). Most notably, the medial and lateral ganglionic eminences derived from the subpallium generate the inhibitory interneurons of the cortex, which migrate and settle in the cortical layers among the projection neurons between embryonic day (E) 12.5 and 15.5 (Anderson et al., 1997; Marín & Rubenstein, 2001).

At this point, the cortex consists of a thin sheet of progenitors. Between E 10.5 and E 17.5 in the mouse, the NPCs of the cortex must self-amplify and, at the same time, generate the cortical projection neurons in a stereotyped temporal order. These neurons migrate outwardly towards the pia mater and progressively settle above the progenitor zones in the layers as mentioned above, splitting the cortical sheet (corti-

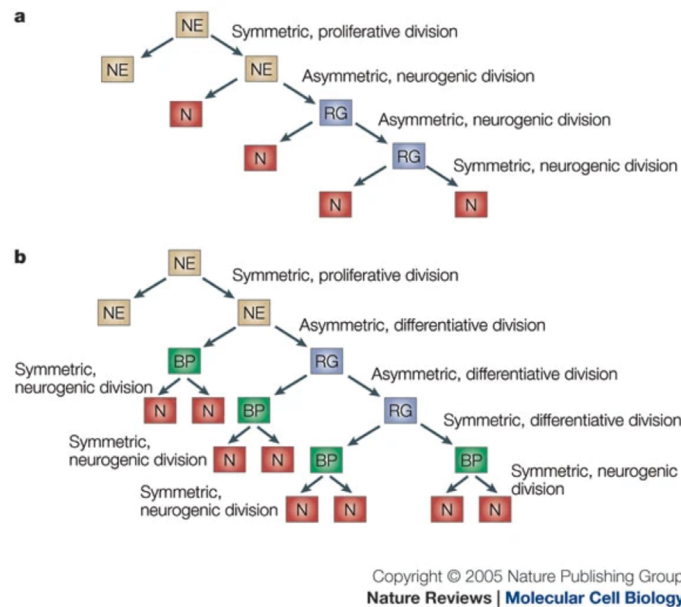


**Figure 1.4** Lineages generated by cortical neural progenitor cells. Neuroepithelial cells (NE) birth the cortical radial glia (G), which, in turn, can either directly (a) generate neurons (N) or indirectly (b), through the production of basal (intermediate) progenitors (BP). Reproduced from Götz and Huttner, 2005.

cal pre-plate) into the marginal zone (future layer 1) towards the pia mater and the germinal zones at the ventricular surface (discussed in more detail in 4.2). To form the final cortical plate, the neurons settle in an inside-out fashion: late-born neurons migrate outwardly through the already generated deep layers (V-VI) and position themselves above in order to become the superficial layers (II-III) (Angevine & Sidman, 1961; Berry & Rogers, 1965; Rakic, 1971, 1972; Greig et al., 2013). The timing of production for the different projection neuron subtypes is discussed in more detail in section 4.2.

## 1.4. PROCESSES INVOLVED IN NEURONAL IDENTITY ACQUISITION IN THE CORTEX

### 1.4.1. Biology of the different types of neocortical neural progenitor cells (NPCs)

Before addressing the state of the knowledge on NPC fate acquisition, it bears mentioning that many aspects of NPC biology are observed across the entirety of the cortex. Some of these aspects are relevant to the process of committing to producing

particular neuronal lineages and will be briefly outlined here. For more details, Florio and Huttner, 2014, and Uzquiano et al., 2018 provide extensive reviews of NPC biology.

The cortical NPC niche consists at first of a thin neuroepithelium that lines the dorsal side of the lateral ventricles. Up to around E 10.5, the neuroepithelium consists of progenitors called neuroepithelial cells (NECs), which proliferate by symmetric division in order to expand the progenitor pool (Chenn and McConnell, 1995, Götz and Huttner, 2005). As they undergo further differentiation to cortical neural progenitor cells (NPCs) (Figure 1.4), they maintain epithelial characteristics and also assume astroglial properties and are hence known as radial glial cells (RGCs or RGs). Like many other epithelial cells, RGCs express the intermediate filament protein Nestin and exhibit apical-basal polarity. While the cell bodies remain close to the ventricular surface and form the ventricular zone (VZ), the RGCs also have apical endfeet, located at the ventricular surface, and a strongly elongated process spanning the thickness of the cortex. This process provides the scaffolding along which the neurons produced by the RGCs migrate outwardly to their final laminar positions (Rakic, 1972, 2009). In addition to these epithelial properties, RGCs express astroglial genes, such as glial fibrillary acidic protein (GFAP), brain lipid-binding protein (BLBP), S100 $\beta$ , a Ca<sup>2+</sup>-binding protein, and GLAST, an astrocytic L-glutamate transporter. They are identifiable by the expression of the transcription factor (TF) Pax6 (reviewed in Mukhtar & Taylor, 2018, Florio & Huttner, 2014).

RGCs are not only a direct source of excitatory projection neurons but also generate them indirectly by giving rise to intermediate progenitor cells (IPs), which are essential for producing the entire range of projection neurons. Early-born cortical projection neurons result from the asymmetric, neurogenic divisions of the RGCs situated in the VZ, also often termed apical radial glial cells or aRGCs. In later stages of cortex development, neurogenesis is also indirect: the aRGCs generate IPs, which then undergo neurogenic divisions. IPs downregulate Pax6 and express the TFs Tbr2 and Cux2 (Zimmer et al., 2004; Englund et al., 2005). These progenitors are primarily located above the VZ and form the subventricular zone (SVZ) and can also be found interspersed in the basal portion of the VZ (Haubensak et al., 2004; Kowalczyk et al., 2009; Pontious et al., 2008). As IPs are thought to produce 2-4 neurons each (Wu et al., 2005), they are thought to have been instrumental in amplifying the neurogenic potential of the cortical progenitors during evolution, especially through the highly proliferative subset termed basal radial glia (bRGs) that are particularly enriched in

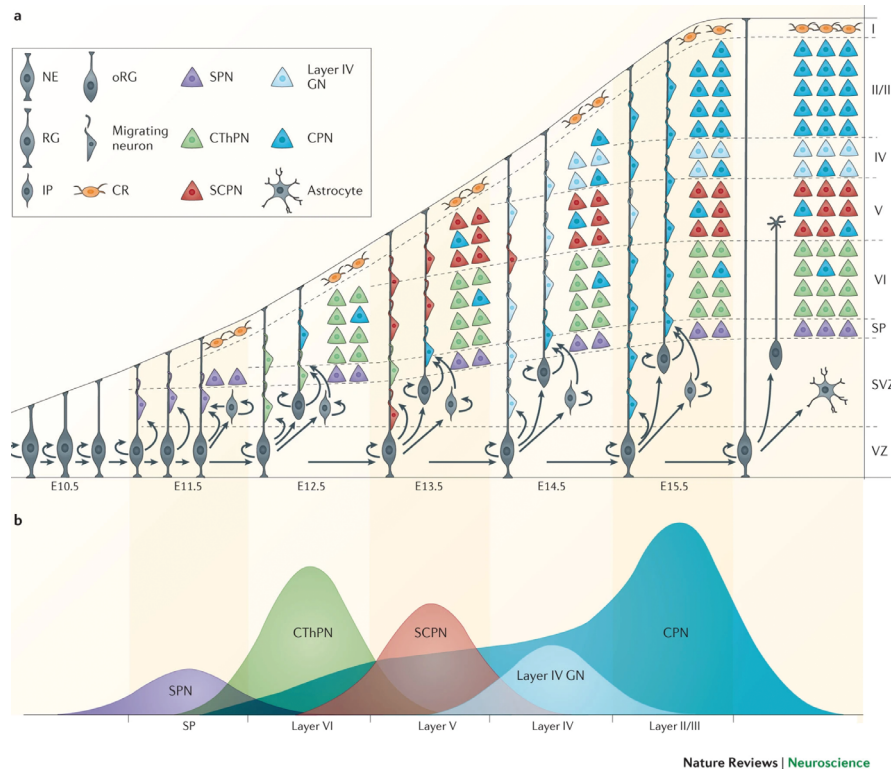


**Figure 1.5** **Timing of neuron subtype production in the developing cortex.** Neuron subtypes are generated in sequential, partially overlapping waves and settle as layers in an inside-out manner. NE- neuroepithelial cell, RG - radial glia, IP - intermediate progenitor, oRG - outer radial glia, CR - Cajal-Retzius cell, SPN - subplate neuron, CThPN - corticothalamic projection neuron, SCPN - subcerebral projection neuron, GN - granule neuron, CPN - callosal projection neuron Reproduced from Greig et al., 2013.

the cortices of primates and humans (Florio et al., 2015, Stahl et al., 2013, Wang et al., 2016).

#### 1.4.2. Fate refinement of neocortical progenitor cells (NPCs) and its impact on neuronal subtype fate acquisition

aRGs and IPs generate projection neurons in a precisely ordered sequence of subtype identities, which spans from around E 10.5 to E 17.5 in the mouse (Figure 1.5). This can be thought of as a sequence of temporally overlapping production waves of neurons of different fates. Corticothalamic projection neurons (CThPNs) of layer VI are produced between around E 11.5 to around E 13.5, subcerebral projection neurons (SCPNS) of layer Vb from around E 12.5 to 13.5, while granule neurons of layer IV are generated from around 13.5 to 14.5. The production of callosal projection neurons (CPNs), located in both deep and superficial layers, overlaps these time periods, with a starting point as early as E 12.5, but only peaks around E 15.5 and continues after

all the other fates have been produced. Around E 17.5, neurogenesis is completed, and the progenitor pool switches to producing the astrocytes and oligodendrocytes that populate the postnatal cortex.

Considered *in toto*, cortical NPCs produce over 50 subtypes of cortical projection neurons (Heavner et al., 2020). The key question that remains incompletely elucidated is: what are the molecular programs that dictate the temporally stereotyped fate switches during corticogenesis? The prevalent model is that the fate of the progeny is specified by characteristics of the progenitor at the time of the terminal mitosis that produces the neurons and is subsequently refined by transcriptional programs in the newborn neuron. The characteristic identity of a progenitor is, as for all other cells, imparted by its transcriptome and proteome. In the case of a cortical NPC, it is thought that its transcriptome and proteome are defined by a temporally shifting combination between cell-autonomous and non-cell-autonomous processes. (Reillo et al., 2017; McConnell, 1995; Florio and Huttner, 2014; Schuurmans and Guillemot, 2002).

Cortical NPCs are exposed to several extrinsic cues in the form of gradients of signaling molecules produced by the patterning centers mentioned in section 3. The combinations of these gradients lead to NPCs adopting regional positional identities, identifiable as expression domains for the transcription factors Pax6, Sp8, Emx2, and COUP-TFI in the progenitors. This ultimately determines cortical arealization (reviewed in Greig et al., 2013). Aside from morphogen signaling, extrinsic feedback mechanisms have been described through which NPC fate switches are instructed once certain thresholds in neuron numbers are reached. As a general switch from neurogenesis to gliogenesis, cardiotrophin-1 secreted by cortical projection neurons is necessary to shift the NPCs to astrocyte production at E 17.5 (Barnabé-Heider et al. 2005). A similar feedback mechanism, based on Fgf9 secretion, was described by our research group (Seuntjens et al., 2009). In the same study, our research group showed that the accumulation of neurotrophin-3 secreted by postmitotic deep layer neurons promotes the switch in NPCs towards the genesis of superficial neuron subtypes. Other kinds of non-cell-autonomous signaling found to regulate NPC behavior are related to bioelectrical properties and cell-cell contacts. Calcium ion pulses travel along the NPC process from the cortical plate, containing postmitotic neurons, into the NPC cell bodies located in the ventricular zone and have been found to regulate proliferation and the onset of cortical neuron migration (Weissman et al., 2004; Rash et al., 2016). Additionally, apical progenitors hyperpolarize in order to switch the

type of neurons produced during corticogenesis (Vitali, 2018). Cell-cell contacts can also play a role in NPC proliferation, as well as signals from the extracellular matrix (Stenzel et al., 2014; Fietz et al., 2010, 2012) or the progressive innervation of the developing cortex by thalamocortical afferents (Reillo et al 2017).

The exact intracellular consequences of these extrinsic signals are not elucidated in all cases. Furthermore, NPCs exhibit several cell-autonomous properties that influence their competence to respond to these extracellular cues. Some of the well-characterized cell-autonomous factors affecting NPC fate choices are epigenetic controls of the transcription of fate regulators. One such instance is the requirement of H3K27 trimethylation at the promoter of the SCPN-inducing *Fezf2* for terminating the production of layer V neurons (SCPN) (Morimoto-Suzuki et al., 2014). Another well-characterized actor in NPC fate decisions and arealization is the methyl-CpG-binding protein 2 (MeCP2), whose developmental malfunctions lead to Rett syndrome (Bedogni et al., 2016; Cobolli-Gigli et al., 2018). Other well-studied cell-intrinsic properties conducive to fate changes are the length of the NPC cell cycle, which increases as the NPCs differentiate during corticogenesis and is required for the switch to differentiative divisions (Calegari et al., 2005; Lukaszewicz et al., 2002; Pilaz et al., 2016) and is also impacted by progenitor polarity and division plane angulation (reviewed in Fietz and Huttner, 2011). The number of previous divisions in the lineage producing an NPC also influences progeny fate (Caviness & Takahashi, 1995; Caviness et al., 2003).

In addition to the described autonomous factors, some intrinsic properties depend on regulatory layers that are, thus far, less rigorously defined. A critical sub-question of that regarding molecular fate controls is whether cortical progenitors are homogeneous across space and time in their potential to generate all projection neuron subtypes. This question arose in part due to observations related to the gradual loss of multipotency of the progenitor pool in bulk and in part due to the expression in NPCs of some transcripts previously related to fate specification in postmitotic neurons. Concerning the stage-related potency of a progenitor, studies in which early progenitors were inserted into a late progenitor population and vice versa in both ferrets (Frantz & McConnell, 1996; Desai & McConnell, 2000) and mice (Mizutani and Saito, 2005) showed that, when analyzed in bulk, only early progenitors can adapt the neuron subtype type produced to match that produced by the surrounding progenitors. Early progenitors in a late cortical context switched to producing neurons of the superficial layers, but late progenitors in an early context did not exhibit the same degree of plasticity and did not switch to deep layer neuron production. It was there-

fore thought for some time that all cortical progenitors undergo a progressive fate restriction process as developmental time passes, gradually losing their capability of generating all neuron subtypes. Other studies found that NPCs could be partially reprogrammed to an earlier fate (Hanashima et al., 2004; Molyneaux et al., 2005). A more recent study (Oberst, 2019) partially reconciles the previous contradictory findings by showing that this fate restriction depends on the progenitor type. The authors found that, indeed, IPs from later stages are fate-restricted, but not the coterminous late-stage aRGCs, which are able to revert to deep layer neuron production.

Another potential layer of NPC fate regulation was uncovered by findings that subsets of NPCs express transcripts tied to specific projection neuron fates. *Cux2* and *Svet1* transcripts were detected in both SVZ cells and some neurons of layers II-IV (Tarabykin et al., 2001; Nieto et al., 2004; Zimmer et al., 2004), prompting models in which either IPs or other subsets of progenitors exclusively produce neurons of the superficial layers. While initial studies employing *Cux2*-based lineage tracing (Franco et al., 2012) supported the idea that the expression of neuron subtype-characteristic transcripts in progenitors indicates the commitment to that fate, other studies using the same genetic system could not confirm these findings (Guo et al., 2013; Eckler et al., 2015). In addition, lineage tracing studies that employed the IP-specific *Tbr2* promoter found that this progenitor type can also generate neurons residing in all cortical layers (Vasistha et al., 2015, Mihalas et al. 2016; Mihalas and Hevner, 2018), leaving the question of superficial layer specification at the progenitor level open. Notably, there were no reports of intrinsic factors expressed in the VZ and implicated in the fate decisions of NPCs towards CFuPN production up to our research group's identification of *TrkC-T1* as a fate determinant for deep layer neuron production. This finding will be detailed in section 6.

Taken together, our understanding of the biological processes that contribute to establishing the differential transcriptomes and proteomes of NPCs of different ages and lineage potentials covers a broad spectrum but is still incomplete. Due to the influx of deep single-cell and single-nucleus transcriptomic profiling studies over the last decade, there has been a recent surge in discoveries of fate-steering mechanisms that are centered around posttranscriptional controls. Such mechanisms operate at the level of RNA processing, stability, and translation (Mazin et al., 2013; Dillman et al., 2013; Hu et al., 2014; Ziats & Rennert, 2014; Camp et al., 2015; Mora-Bermúdez et al., 2016; Kageyama et al., 2018; Rosenberg et al., 2018; Zhong et al., 2018; Fan et al., 2018; Welch et al., 2019; Polioudakis et al., 2019; Loo et al., 2019; Najafi et al., 2019;

Duan et al., 2020; Huang et al., 2020). From the evidence gathered so far, the availability of fate-determinant mRNAs is regulated through their localization in subcellular compartments (Chowdhury et al., 2021) and through altering their stability by N6-methyladenosine modification (Yoon et al., 2017) or miRNA binding (Bian et al., 2013; Mao et al., 2014; Fededa et al., 2016; Martins et al., 2021). Furthermore, the translation of *Cux2* and *Fezf2* (see section 4.3; Zahr et al., 2018) and many other transcripts (Rodrigues et al., 2020; Kraushar et al., 2014) is developmentally regulated and repressed at crucial time points for fate switching. Aside from these mechanisms, alternative splicing of NPC and neuron pre-mRNAs has been shown to regulate nearly all steps of cortical neurogenesis, as will be described in detail in section 5.2.

### 1.4.3. Generation of projection neuron subtypes

Even though it is not clear where exactly the commitment of a newborn neuron to a subtype fate happens during the differentiation and division of an NPC (Toma et al., 2016; Greig et al., 2013), we know so far that the commitment is ensured by a series of cross-repressive interactions between transcription factors. As this research project dealt primarily with the decision between corticofugal (CFuPN) and callosally projecting neuron (CPN) fate, the remainder of the subsection will consist of an overview of the molecular controls known to participate in this process.

The neurogenic division of an apical or intermediate progenitor produces a postmitotic neuron that is believed to be in a fate-specified state as a result of the processes described in the previous subsection. Depending on this fate-restricted state, the neuron commences a lineage-specific transcriptional program that dictates the final fate of the neuron, suppresses alternative fates, and ensures proper terminal differentiation (Greig et al., 2013; Jabaudon, 2017).

While the molecular controls behind this process are still being explored, we know that they are strongly impacted by the dose and combinations of transcriptional regulators during defined developmental time windows. Presently, the widely accepted model is one of sequential fate refinement. In this model, key transcription factors start the differentiation process towards the projection subtype specified before, followed by the activation of other transcription factors that further this differentiation by various repressive and activating interactions, and which can themselves fine-tune the final neuronal properties, including the projection targets (Greig et al., 2013,

Srinivasan et al., 2012, McKenna et al., 2015, Toma et al., 2014).

The developmental choices leading to CFuPN and CPN fates are particularly interesting because these highly different projection neurons exhibit an overlap of both the time frames they are produced in and their final localization (Greig et al., 2013, Koester & O’Leary, 1993, Srinivasan et al., 2012), in particular, the subcerebrally projecting fraction (SCPN) of CFuPN and the CPN residing in layer Vb. Crucially, their balanced production is necessary for forming healthy cortical circuitry and is misregulated in diseases such as autism spectrum disorders (Fang et al., 2014; Falcone et al., 2021; Zhang et al., 2019).

The SCPN fate is specified by *Fezf2*, the key regulator that antagonizes *Tbr1*, which is the top-level transcription factor for CThPN identity (Molyneaux et al., 2007; Bedogni et al., 2010; McKenna et al., 2015). *Fezf2* simultaneously represses some CPN characteristics (Rouaux & Arlotta, 2013). While it is also expressed at low levels in CThPN, this subtype is significantly less affected by the deletion of *Fezf2* (Molyneaux et al., 2005). *Ctip2*, a postmitotic TF, exhibits a similar expression pattern in SCPN and CThPN (Arlotta et al., 2005, Molyneaux et al., 2005) and likely operates downstream of *Fezf2*, given that it is absent from the cortices of *Fezf2* null mice (Chen et al., 2005, Chen et al., 2008). *Ctip2* regulates subsequent differentiation steps of SCPNs, such as the proper formation of axon bundles (fasciculation) and their outgrowth (Arlotta et al., 2005), and is used in this research project as a marker of CFuPN identity. Various other TFs, such as *Diap3* or *Crim1*, have been implicated in the further delineation of SCPN fate and CFuPN fate, especially concerning the area-specific morphologies of these neurons (Arlotta et al., 2005).

Work from our research groups and others have identified the transcriptional regulator *Satb2* as a critical factor in establishing CPN identity (Britanova et al., 2008, Alcamo et al., 2008). *Satb2*<sup>-/-</sup> neurons have their axons misrouted to the anterior commissure and external capsule instead of the corpus callosum and also express *Ctip2* even when they are located in the superficial layers. This phenotype suggested that *Satb2* is required for repressing the transcriptional program associated with CFuPN. *Satb2* and other top-level CPN fate regulators, such as *Foxg1* and *MeCP2*, likely control properties shared by all CPN, while other factors, such as *Brn1/2*, *Cited2*, or the *Cux* family, function in either defining further specialized CPN identities, the establishment of area-specific projections, or in the final maturation of the dendritic tree (Fame et al., 2016, Cubelos et al., 2015, Hevner et al., 2003, Dominguez et al., 2013, McEvelly

et al., 2002). Based on this research, we use *Satb2* in the current study as a marker of CPN identity.

While these fate specification and determination events occur, the newborn neurons migrate and settle in the previously described layers. Their terminal differentiation involves axon extension to their targets, refining the axonal projections, depending on the cortical area and fate, the formation and maturation of their dendritic tree, synaptogenesis, and, finally, acquisition of subtype-characteristic electrophysiological properties (Rakic, 2009; Reillo et al., 2017).

### 1.5. FUNCTIONS OF ALTERNATIVE SPLICING IN PRENATAL BRAIN DEVELOPMENT

Soon after the discovery of pre-mRNA splicing (Berget et al., 77; Chow et al., 77), it was also found that this process is not strictly limited to removing the (supposedly) non-coding introns from between the protein-coding exons. In response to changes in various extra- and intracellular conditions, the skipped parts of a pre-mRNA can encompass several different stretches, including ones that span several introns and

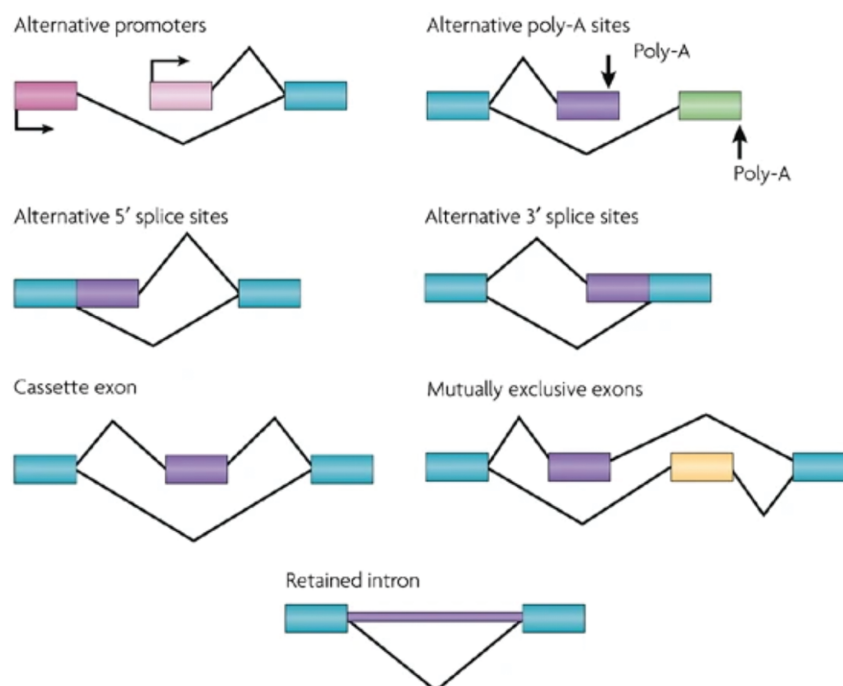


**Figure 1.6** **Patterns of alternative splicing.** Different parts of the pre-mRNA can be skipped or retained in order to generate a variety of mRNAs. Alternative promoters and polyadenylation sites further expand the possible mRNA variants. Reproduced from Li et al., 2007.

exons (Alt et al., 1980; Early et al., 1980). This dynamic selection of the pre-mRNA stretches to be removed was termed alternative splicing. Along with alternative translation initiation sites, alternative splicing accounts for a significant expansion of the protein isoforms that can be generated by individual eukaryotic genes (Miles et al., 2017). Deep RNA sequencing projects have revealed that an overwhelming majority of human multi-exon genes (95%) produce several transcript variants, distinguished by the combinations of introns and exons that are included or skipped during their splicing (Pan et al., 2008; Wang et al., 2008). This variety of isoforms is thought to have contributed to a gradual increase in organismal complexity during evolution (Bush et al., 2017; Gallego-Paez et al., 2017). Given the outstanding intricacy of the central nervous system, it is not surprising that alternatively spliced gene products are particularly prevalent and diverse in the brain (Zaghlool et al., 2014, Barbosa-Morais et al., 2012, Gallego-Paez et al., 2017; Naro et al., 2021), and, as will be presented in this section, in its development. A brief outline of the mechanistic aspects of alternative splicing will precede the overview of the state of the knowledge on neural alternative splicing in order to facilitate a seamless understanding of how the splicing regulators described in the remainder of this work exert their functions.

### **1.5.1. Mechanistic aspects of alternative splicing**

Splicing overall is catalyzed by the major spliceosome and, for a small fraction of introns, by the minor spliceosome (Wahl et al., 2009; Wilkinson et al., 2020; and see Turunen et al., 2013 for a review of the minor spliceosome). These large ribonucleoprotein complexes assemble on the nascent pre-mRNA in order to excise portions of it, and they do so by first recognizing conserved sequence motifs at and close to the intron termini. These are the 5' and 3' splice site sequences at the intron-exon boundaries and, within the intron, the branch point sequence and the polypyrimidine tract. At the 5' and 3' splice sites, the spliceosome catalyzes two sequential trans-esterification reactions that separate the skipped ribonucleotide stretch from the RNA stretches that will be retained in the mature mRNA. Finally, the termini of the remaining RNA stretches are ligated. The recognition and choice of 5' and 3' splice sites flanking different exons guide which parts of the pre-mRNA are maintained and which ones are excised.

It is worth noting that, while alternative splicing in mammals often involves single exons that are facultatively included or excluded, called cassette exons, various other

patterns of splicing exist (Figure 1.6). These include alternative 5' and 3' splice sites, the retention of an intron, but also the use of alternative promoter and polyadenylation sites (Black, 2003), which can all affect the stability, localization, or translation efficiency of the resulting mRNA (Lareau et al., 2007; Mockenhaupt and Makeyev, 2015; Su et al., 2018). A subgroup of cassette exons are exons included in the mature mRNA in a mutually exclusive fashion. This dynamic can encompass merely two exons or groups of several adjacent exons that act as two unitary cassettes. As will be described in section 6, the TrkC pre-mRNA contains two mutually exclusive exon groups that make up the distinct 3' termini of the two transcript variants studied in this work, which endow the two protein products with different signaling capabilities.

The sequence elements at the 5' and 3' splice sites and the branch point are, in and of themselves, not sufficient to single-handedly steer and confidently predict the outcome of an alternative splicing event, but merely a part of an overarching combinatorial regulatory system. First, local chromatin state and RNA polymerase II kinetics impact splice site choice (reviewed in Naftelberg et al., 2015). Second, spliceosomal components must recognize the functional sites on the pre-mRNA several times during the splicing process in order to ensure the necessary fidelity of the process (Wahl et al., 2009). Site recognition is influenced by the exact sequence of the 5' and 3' splice sites, meaning that individual splice sites can compete for being selected by the spliceosome. Several scoring models have been proposed to predict the probability of a splice site to be recognized and used by the spliceosome (Yeo and Burge, 2004; Freund et al., 2003). At the same time, the spliceosome responds to interactions with a plethora of other RNA-bound proteins, which affect the splicing outcome both through intrinsic properties and through the exact positions within introns or exons that they bind at (Wahl et al., 2009; Barash et al., 2010; Lee & Rio, 2015; Fu and Ares, 2014). The trans-acting RNA-bound proteins involved in the splice site selection are termed splicing factors, and they can bind to various cis-regulatory sequences in the pre-mRNA. These cis-regulatory sequences are categorized by their position and by the type of contribution to the alternative splicing outcome as exonic splicing enhancers (ESEs), exonic splicing inhibitors (ESIs), and their intronic counterparts, ISEs and ISIs. Aside from these mechanisms of splice site choice control, many other regulatory layers have been described. Among them are the posttranslational modification and subcellular localization of splicing factors, the presence of RNA secondary structures that ease or prevent the assembly of the spliceosome, or other RNA species (miRNAs) (reviewed in McManus and Graveley, 2011; Heyd and Lynch, 2011; Lee and

Rio, 2015).

In summary, whether an exon or more will be skipped or retained or whether an intron will be included in the mature mRNA depends primarily on the epigenetic context, the exact sequence of the 5' and 3' splice sites, on the net sum influence of cis-regulatory elements, their avidity to bind splicing factors, and on the availability of the splicing factors themselves in the observed cellular context, with the requisite posttranslational modifications.

### **1.5.2 Alternative splicing in the brain and its development**

The inextricable link between alternative splicing and the central nervous system (CNS) has been brought into the spotlight by a recent influx of comparative transcriptomic studies, starting around the turn of the millennium. At that point, the growing availability of completed genomic sequences was met by decreasing costs for analyzing expressed sequence tags and then cDNAs detected by splicing-sensitive microarrays. More recently, whole transcriptomes have become accessible by high-throughput RNA sequencing (RNA-seq), thus allowing the precise mapping of reads to the corresponding genes and the identification of splice variants in a systematic fashion (Chen et al., 2014; Blencowe, 2006; Johnson et al., 2003). The picture that emerged from these efforts was the outstanding contribution of tissue-specific alternative splicing signatures (sets of splicing variants) to phylogenesis and ontogenesis (Matlin et al., 2005; Nilsen and Graveley, 2010; Barbosa-Morais et al., 2012; Merkin et al., 2012).

The CNS, and, in particular, the brain, exhibits the pinnacle of AS pattern complexity (Zaghlool et al., 2014; Ramsköld et al., 2009; de la Grange et al., 2010; Xu et al., 2002). Furthermore, in two comparative high-throughput transcriptomic studies of organs, brain tissue stood out for having the most conserved transcriptomic signature across several vertebrate classes, spanning an evolutionary range from chicken to human. At the same time, neural tissue had the most slowly diverging alternative splicing signature from all the analyzed organs (Merkin et al., 2012; Barbosa-Morais et al., 2012). Also, networks of AS events associated with cellular differentiation are evolutionarily remarkably well conserved (Irimia & Blencowe, 2012; Kalsotra and Cooper, 2011; Calarco et al., 2011). Finally, in the developing cerebral cortex, 90% of the expressed genes are subjected to dynamic AS regulation according to brain region and

developmental stage (Kang et al., 2011). Combined, this evidence suggests that neural cells efficiently peruse the high regulatory flexibility enabled by alternative splicing and that this wide array of physiological AS events in the CNS is subjected to significant evolutionary pressure, thus highlighting the functional importance of these patterns for both developing the histological complexity of the brain and for its adult functions.

Three major themes emerge upon reviewing the known cases in which alternative splicing events regulate physiological brain- and cortex-related processes. In the adult cortex, the main themes are the generation of protein isoforms enabling synapse plasticity and the avoidance of aggregation-prone protein isoforms. In the developing cortex, splicing switches are conspicuously involved in nearly all steps of neurogenic differentiation (Ehrmann et al., 2013; Iijima et al., 2011; Ding et al., 2017; and see reviews of Vuong et al., 2016 and Da Cruz and Cleveland, 2011; Hinrich et al., 2016; Rockenstein et al., 1995; Bueé et al., 2000). Therefore, it is unsurprising that AS misregulation is causally involved in the predisposition and progression of neurodegenerative and neurodevelopmental disorders. Among the latter, instances of AS misregulation abound in the etiology of schizophrenia and autism spectrum disorders (Quesnel-Vallières et al., 2019; Irimia et al., 2014; Voineagu et al., 2011; Xu et al., 2012; Jaffe et al., 2018). These disorders show considerable overlap in terms of genetic risk factors, transcriptomic alterations, and some cognitive symptoms (De Crescenzo et al., 2019; Gandal et al., 2018). Importantly, in both disorders, the brain connectome is miswired, exhibiting changes in the number of interhemispheric connections and *corpus callosum* size (Venkataraman et al., 2012; Anderson et al., 2011; Andriamananjara et al., 2019; Mastrovito et al., 2018). Since a disbalance of cortical projection neuron numbers underlying miswiring has been shown to lead to autism-like symptoms (Fang et al., 2014; Falcone et al., 2021; Zhang et al., 2019), alterations in developmental splicing switches may contribute to these disorders through the involvement in the specification of neuron subtypes. However, this avenue remains largely unexplored. Thus far, alternative splicing switches in the developing cortex have been described at several other steps of neurogenesis. The switches involve shifting the balance between the protein products generated by alternative splicing events from the same immature transcript combined with the levels of different alternative splicing regulators (splicing factors).

Several splicing factors (SFs) and alternative splicing isoforms stand out as crucial for enabling the rapid cellular alterations needed during neurogenic differentiation.

The splicing factors Mbnl1 and Mbnl2, which control the alternative splicing of the pluripotency gene *Foxp1*, must be suppressed for the maintenance of stem cell pluripotency (Han et al., 2013). In the decision between the symmetric (proliferative) and asymmetric (differentiative) division of NPCs, Zhang and colleagues have described a mechanism of centrosomal control relying on the antagonistic effects of the splicing factors PTBP1 and the *Rbfox* family in NPCs and neurons, respectively. The switch from the PTBP1-dominated environment of the NPCs to *Rbfox* expression leads to a shift in a network of alternatively spliced exons related to cytoskeletal organization and, most notably, to changes in the splicing of filamin A, an actin-binding protein, and Ninein, a microtubule-anchoring protein. The combination of the alternative splicing isoforms of filamin A and Ninein guides the type of NPC division and thereby their proliferative capacity and differentiation time point (Zhang et al., 2016). At the same level, *Rbfox1* has been implicated in normal NPC karyokinesis and thereby in the timely onset of neuron production and migration (Hamada et al., 2015). Its orthologue *Rbfox3*, also known as NeuN, undergoes splicing isoform switching during neuronal differentiation. The neuron-specific full-length *Rbfox3* isoform promotes a splicing switch in the *Numb* transcript, generating a more stable variant and thus furthering neurogenesis (Kim et al., 2013). Interestingly, *Rbfox* splicing factors also change binding sequence preference during radial glia to neuron differentiation in a concentration-dependent manner. The higher *Rbfox* concentrations present in neurons enable them to also bind moderate-affinity target sites in pre-mRNAs involved in neurogenesis, adding another fail-safe regulatory layer in the progression towards the neuronal fate (Begg et al., 2020). Another well-known NPC-to-neuron switch in splicing factor combinations is the switch between PTBP1 and PTBP2/nPTB. As mentioned above, PTBP1 fulfills crucial functions in maintaining radial glial cell biology by inhibiting several neurogenic alternative splicing events. Its paralog PTBP2 is normally not present in radial glial cells because PTBP1 suppresses the inclusion of exon 10 in the PTBP2 transcript, producing a short isoform targeted by nonsense-mediated decay. PTBP1 is gradually suppressed during differentiation by RBM4 and the neuron-specific miRNA miR-124, leading to the de-repression of productive PTBP2 splicing. The presence of PTBP2 is therefore restricted to neurons and targets different alternatively spliced exons than PTBP1, which consolidate neuronal identity (Makeyev et al., 2007; Boutz et al., 2007; Su et al., 2017).

After the neuronal identity is established, the newborn neurons begin to migrate out of the germinal zones towards the *pia mater*. The splicing of *Dab-1* changes to enable neuron migration. *Dab-1* is a crucial signaling adaptor mediating the chemoregula-

tion of neuronal migration by Reelin, a glycoprotein secreted by the Cajal-Retzius cells in the marginal zone (Gao et al., 2012; Gao and Godbout, 2013). The balance between two Dab-1 splicing isoforms, modulated by RBM4, allows for timely and correct neuron migration (Dhananjaya et al., 2018).

SRRM4/nSR100, a neural tissue-specific splicing factor, maintains a network of neuron-specific alternative splicing events in the cortex that are required for proper terminal differentiation of neurons (Irimia et al., 2014; Calarco et al., 2009). SRRM4 also favors the inclusion of a stabilizing exon in PTBP2, which then proceeds to regulate the splicing of the cytoskeleton-remodeling Rho GTPase Cdc42. In neurons, two isoforms of Cdc42 are required at approximately equimolar concentrations for the proper generation of one single axon and several dendrites. The NPC environment is dominated by only one of the Cdc42 isoforms, and a splicing switch occurs during neurogenesis in order to achieve the neuron-specific equimolar ratio (Yap et al., 2016). The outgrowth of the resulting axon is co-regulated by the NOVA splicing factors, which alter the splicing of the Dcc receptor and other components of the axon guidance pathways (Leggere et al., 2016; Saito et al., 2016). Axonal projection routes are also steered by two splicing isoforms of the Robo3 receptor, which impart different sensitivities to axon repulsion by Slit (Chen et al., 2008).

In conclusion, thus far, research on alternative splicing in the developing cortex has focused on the fate choices involved in the stem cell-to-neuron transition and the migration and terminal differentiation of the resulting neurons. However, there is a conspicuous dearth of studies regarding the involvement of alternative splicing in the specification of individual projection neuron subtypes.

## 1.6. THE ROLE OF TRKC ALTERNATIVE SPLICING ISOFORMS IN NEURONAL IDENTITY ACQUISITION

It is still not completely understood how the transcriptomes and proteomes of CFuPN-producing and CPN-producing progenitors differ regarding potential-inducing and potential-restricting factors or fate determinants. The most recent contribution of our research group to answering this question is discovering the first progenitor-intrinsic determinant of deep layer neuron fate, TrkC-T1 (Parthasarathy et al., 2021). TrkC-T1 is one of the alternative splicing isoforms generated by the neu-

retrophin-3 tropomyosin kinase receptor locus (*Ntrk3*). A different protein product of the locus had been previously studied extensively: the canonical neurotrophin receptor TrkC, which harbors a kinase-active domain and is hence also termed TrkC-TK+. TrkC-TK+ has been shown to exert critical functions in both CNS and PNS development (Lamballe et al., 1991; Klein et al., 1994; Bartkowska et al., 2007; Huang & Reichardt, 2003). The first part of this section will briefly present an overview of neurotrophin signaling for understanding the role of TrkC-T1 in neuronal subtype fate decisions, as shown in Parthasarathy et al., 2021. Detailed reviews on the subject of neurotrophin signaling are provided by Chao, 2003 and Huang and Reichardt, 2001 and 2003. The second part will summarize the findings of our work in Parthasarathy et al., 2021, in which the research project presented here is rooted.

### **1.6.1. Neurotrophins and their receptors, the Trk tropomyosin receptor tyrosine kinases**

Neurotrophin signaling is an evolutionary innovation that only arose in vertebrates, and Trk receptors exhibit a steady increase in the diversity of isoforms produced through alternative splicing. This increase parallels the development of CNS complexity (the Ensembl project, Howe et al., 2021, von Bartheld & Fritsch, 2006). Neurotrophins themselves are a group of secreted signaling ligands, named so because they act as neuron growth and survival factors (Levi-Montalcini, 1987). The group comprises four ligands: nerve growth factor (NGF), brain-derived neurotrophic factor (BDNF), neurotrophin-3 (NT-3), and neurotrophin-4 (NT-4). Each ligand binds with high affinity to the extracellular immunoglobulin G domains of one of the Trk receptors, with NGF favoring TrkA, BDNF and NT-4 preferentially binding to TrkB, and NT-3 to TrkC (Bibel & Barde, 2000).

Neurotrophin binding to Trk receptors triggers receptor homodimerization and the trans-autophosphorylation on specific tyrosine residues of the intracellular domains (ICDs). Subsequently, signaling mediators, for example, from the Shc family, are recruited to these residues and phosphorylated by the receptors. The phosphorylation enables the signaling mediators to relay the neurotrophic signals and trigger transcriptional and phosphorylation changes in the neuron. Each of the four neurotrophins also exhibits low-affinity interactions with the other two Trk receptors and the pan-neurotrophin receptor p75<sup>NTR</sup>, which can modulate intracellular signaling downstream of the Trk receptors by heterodimerization (Chao, 2003; Huang

and Reichardt, 2001 and 2003; Amatu et al., 2019). In this way, each signaling event through Trk receptors underlies fine control through the numbers and types of receptors present in the neuron at that moment. The main routes through which neurotrophins and the Trk receptors signal are the MAPK/MEK/ERK1/2 pathway, which results in the activation of transcription factors such as CREB, and the PI3K/protein kinase C (PKC) pathway. Both pathways lead to changes in cell cycle progression, neurite outgrowth and, in the postnatal brain, synaptic plasticity. In the developing cortex, suppressing the function of canonical TrkB or TrkC using dominant-negative variants led to decreased NPC proliferation (Bartkowska et al., 2007), a phenotype mirrored, for instance, by the simultaneous disruption of the Shc and the PLC- $\gamma$  docking sites of TrkB (Medina et al., 2004).

The information presented so far pertains to the canonical, kinase-active forms of the Trk receptors. However, both TrkC and TrkB have non-canonical alternative splicing isoforms that lack kinase activity, and which are also expressed in the brain and the cerebral cortex (Klein et al., 1990; Middlemas et al., 1991; Tsoulfas et al., 1993; Valenzuela et al., 1993; Fenner, 2012; Brahimy et al., 2016; Parthasarathy et al., 2021). Surprisingly, the expression patterns of the canonical and non-canonical receptors differ (Menn et al., 1998, 2000; Parthasarathy et al., 2021). This difference in expression patterns pointed to specialized functions of the non-canonical receptor isoforms, and such a division of signaling roles between the canonical and the non-canonical Trk receptors could be confirmed in other biological systems (Cronk et al., 2002; Rose et al., 2003; Renn et al., 2009; Esteban et al., 2006; Postigo et al., 2002) and in the CNS (Brahimi et al., 2016).

### **1.6.2. The TrkC receptor variant TrkC-T1 is a determinant of deeper layer (CFuPN) neuron fate**

Our most recent study on CFuPN versus CPN cell fate determination (Parthasarathy et al., 2021) showed that the non-canonical TrkB receptor is expressed in a static pattern in the developing cortex, as opposed to the non-canonical TrkC receptor, TrkC-T1. TrkC-T1 is expressed in the cortical plate at all investigated stages of cortex development. In stark contrast, the expression level of TrkC-T1 in the ventricular zone follows a flow-and-ebb pattern from E 12.5 to E 14.5. This pattern precisely mirrors the production wave of deeper layer neurons (CFuPN) from the progenitor population. Through in utero gain- and loss-of-function manipulations of the TrkC-T1 lev-

els, we could show that TrkC-T1 levels in the cortical NPCs directly steer the choice between the CFuPN and CPN subtypes that are subsequently produced, with high levels leading to a preference for CFuPN production over CPN and vice versa for low TrkC-T1 levels.

We found that, despite lacking the ability to autophosphorylate, TrkC-T1 can still bind ShcA in cortical neurons but cannot phosphorylate it. Therefore, we posited that TrkC-T1 functions as a sink for ShcA and deprives the MAPK/Erk1/2 signaling pathway initiated by other receptor tyrosine kinases, possibly TrkC-TK+, of this signaling adapter molecule (Figure 1.7). By introducing a constitutively active form of Erk2 in the NPCs, we found that the manipulation of MAPK/Erk1/2 pathway strength affected the CFuPN versus CPN fate decision in a way that is in alignment with this pathway being the mediator of the observed effects of TrkC-T1 on fate.

The effect on cell fate is restricted to TrkC signaling alterations in NPCs, as a TrkC-T1 expression construct driven by the neuron-specific doublecortin (Dcx) promoter did not affect cell fate. Also, when overexpressed ectopically in NPCs at E 14.5, TrkC-T1 had no effect on cell fate but, instead, impaired neuron migration. Therefore,

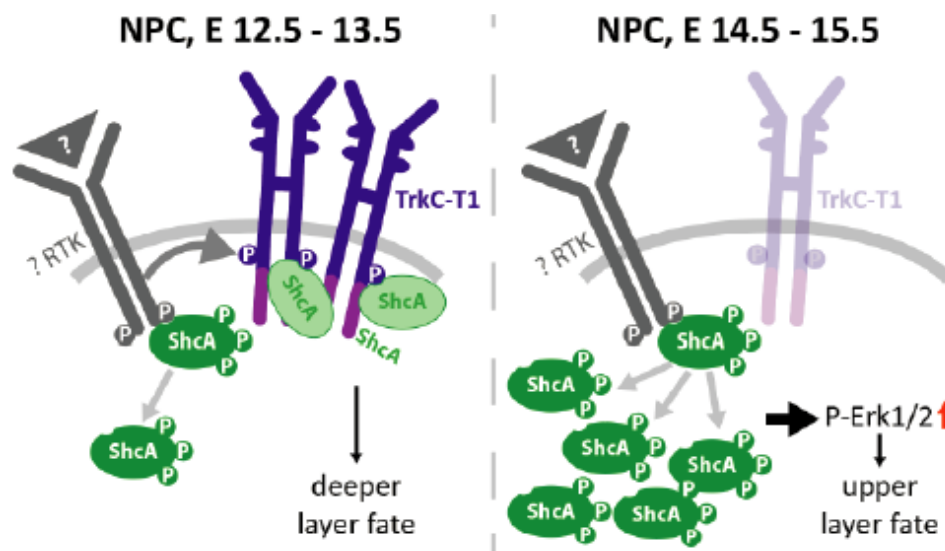


**Figure 1.7 Model of TrkC-T1 function in determining deep layer neuron fate.** Reproduced from Parthasarathy et al., 2021. Based on the research findings presented in this publication from our group, we proposed that the naturally occurring levels of TrkC-T1 in NPCs modulate MAPK/Erk1/2 signaling. Early NPCs generate deeper layer neurons (Ctip2-positive CFuPN) due to high levels of TrkC-T1, which prevent ShcA activation. As the levels of TrkC-T1 decrease in later corticogenesis, ShcA availability increases, and with it, Erk activation, enabling the NPCs to generate superficial layer neurons (upper layer fate).

TrkC-T1 is involved in cell fate decisions in a cell type- and stage-specific manner. TrkC null mutant mice, lacking both TrkC-T1 and TrkC-TK+ ubiquitously, were previously found to exhibit PNS and cardiac phenotypes affecting proprioception and postnatal survival, respectively (Tessarollo et al., 1997), and we could observe no cortical lamination defects in these animals. Furthermore, in another study where TrkC-T1 was stably and ubiquitously overexpressed in mice, it was found that the severity of the phenotypes in the PNS and the heart correlated with TrkC-T1 levels, as judged by the copy number of transgene insertions (Palko et al., 1999). Therefore, TrkC-TK+ and TrkC-T1 have functions that are cell type-specific and dependent on the precise regulation of the levels of and balance between the two isoforms at different stages of development.

Following these findings, the main aim of the research project presented in this dissertation was to investigate the regulatory mechanisms that ensure the appropriate TrkC-TK+/TrkC-T1 balance in the developing cortex, thereby furthering our understanding of the processes controlling neuron subtype fate decisions. To this end, we performed bioinformatic analyses of the two transcripts and the pre-mRNA they originate from and, subsequently, screened for RNA-binding proteins (RBPs) that were deemed likely to regulate the TrkC-TK+ and T1 balance in the developing cortex. *In vitro* and *in vivo* manipulations of the levels of the factors found to regulate TrkC splicing, Srsf1 and Elavl1, allowed us to ascertain the involvement of these RBPs in neuronal subtype fate decisions, a biological process which they had not been brought in connection with before.

## 2. RESULTS

### 2.1. TrkC-T1 exerts its effect on MAPK/Erk1/2 signalling by sequestering p52-ShcA to intracellular compartments

We had previously uncovered in biochemical assays that TrkC-T1 dampens Erk1/2 phosphorylation in a p52ShcA-dependent fashion (Parthasarathy et al., 2021). Since TrkC-T1 lacks the intracellular tyrosine kinase domain but still harbors the tyrosine 516, the docking site for signaling adapters, we wondered whether TrkC-T1 binds p52ShcA, and, because it is unable to phosphorylate it, sequesters it to the Golgi apparatus or other subcellular compartments, thus decreasing the overall amount of p52ShcA available in the cytoplasm. To interrogate this, we analyzed whether TrkC-T1 and p52ShcA localize in similar subcellular compartments in HEK293 cells upon EGF stimulation, which we previously showed to be necessary for TrkC-T1-mediated

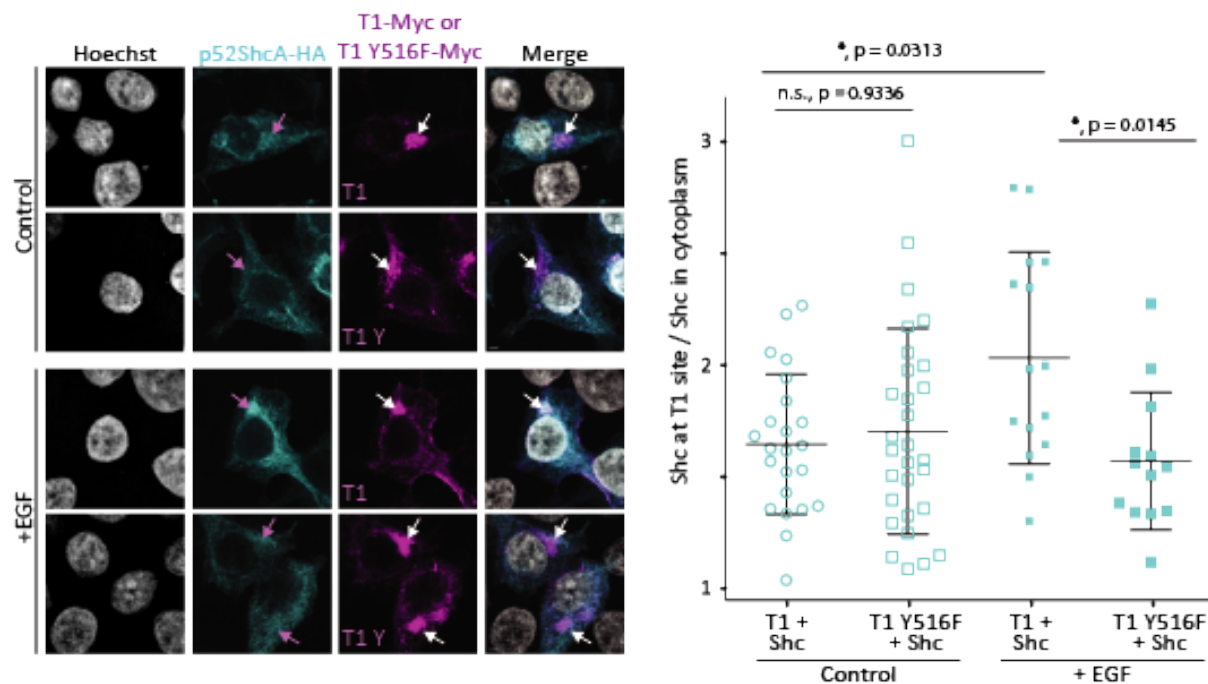


**Figure 2.1 The intracellular localization of TrkC-T1 influences the localization of p52ShcA** (Reproduced from Parthasarathy et al., 2021) **A** HEK293 cells were transfected with CAG promoter-driven constructs expressing p52ShcA with either TrkC-T1 or TrkC-T1 Y516F. Cells were then subjected to EGF stimulation or mock stimulation. **B** Quantification of the mean signal intensity of p52ShcA co-localizing with TrkC-T1 as compared to cytosolic p52ShcA. Identical ROIs were used to determine the mean ShcA signal intensity at TrkC-T1 accumulation sites and in the cytosol. One dot represents one cell. Ratios are reported as mean  $\pm$  SD. T1 + Shc, unstimulated:  $1.67 \pm 0.07$ , N = 23; T1 Y516F+ Shc, unstimulated:  $1.85 \pm 0.19$ , N = 29; T1 + Shc, stimulated:  $2.07 \pm 0.13$ , N = 15; T1 Y516F+ Shc, stimulated:  $1.59 \pm 0.08$ , N = 13. Overarching P value across the samples: 0.0313 (\*), derived from parametric one-way ANOVA (Brown–Forsythe and Welch) test. Arrows point to foci where the TrkC-T1 signal peaks.

effects. An HA-tagged p52ShcA expression construct was transfected together with either TrkC-T1-Myc- or TrkC-T1 Y516F-Myc-expressing constructs into HEK293T cells. After 2 DIV (days *in vitro*), the cells were either left unstimulated or stimulated with EGF. The cells were then stained immunofluorescently for the HA tag, indicating p52ShcA localization, and Myc tag, indicating TrkC-T1 localization (Figure 2.1). P52ShcA localizes in the cytoplasm in unstimulated cells (Wills and Jones, 2012). In the fluorescence micrographs, we observed that, upon EGF stimulation, the p52ShcA signal concentrated at the sites of TrkC-T1 signal, but not at those of TrkC-T1 Y516. This was not seen in the absence of EGF stimulation or for the TrkC-T1 mutant Y516F, which suggests that the activation of TrkC-T1 by extracellular signals and its subsequent phosphorylation at Y516 triggers its ability to bind p52ShcA and concentrate it in areas other than the cytosol and cell membrane. Therefore, the levels of TrkC-T1, in combination with extracellular signals, may control the levels of p52ShcA that are available for signal relaying to MAPK/Erk1/2.

## 2.2. The ratio of TrkC-T1 to TrkC-TK+ transcripts shifts during cortex development

The evidence gathered up to this point from the *in situ* hybridizations for TrkC-T1 and TK+ mRNAs in the developing neocortex (Parthasarathy et al., 2021) and the reported signaling mechanism of TrkC-T1 for fate specification indicated that the quantity of each receptor could be important for corticogenesis. We therefore characterized the ratio of the two receptors throughout cortex development by employing qRT-PCR. To this end, we designed two exon-junction spanning TaqMan® probes, tagged with either VIC (TrkC-TK+) or FAM fluorophores (TrkC-T1). TrkC-T1 and TrkC-TK+ are generated through the mutually exclusive alternative splicing of two exon groups, 13A and 14A for TrkC-T1 and 13-17 for TrkC-TK. Each of the probes is specific to sequences unique to the mutually exclusive exon groups of the two isoforms (Figure 2.2 A). The specificity of the probes enabled us to determine the TrkC transcript ratios at different cortex development stages in a multiplexed fashion.

We then isolated mRNA from microdissected whole cortices of individual embryos across several developmental stages (N = 4 per stage), and quantified the ratio of TrkC+T1 to TK+ using the probes described above (Figure 2.2 B and C). We noticed a change of the quantities relative to one another, with TrkC-TK+ becoming increasingly represented in the total transcript quantity as the cortex matures, at least judg-

ing from a whole-tissue perspective. From E 11.5 to E 18.5, the ratio tilted in favor of TrkC-TK+ with, on average, 16.43 percentage points from the total transcript quantity.

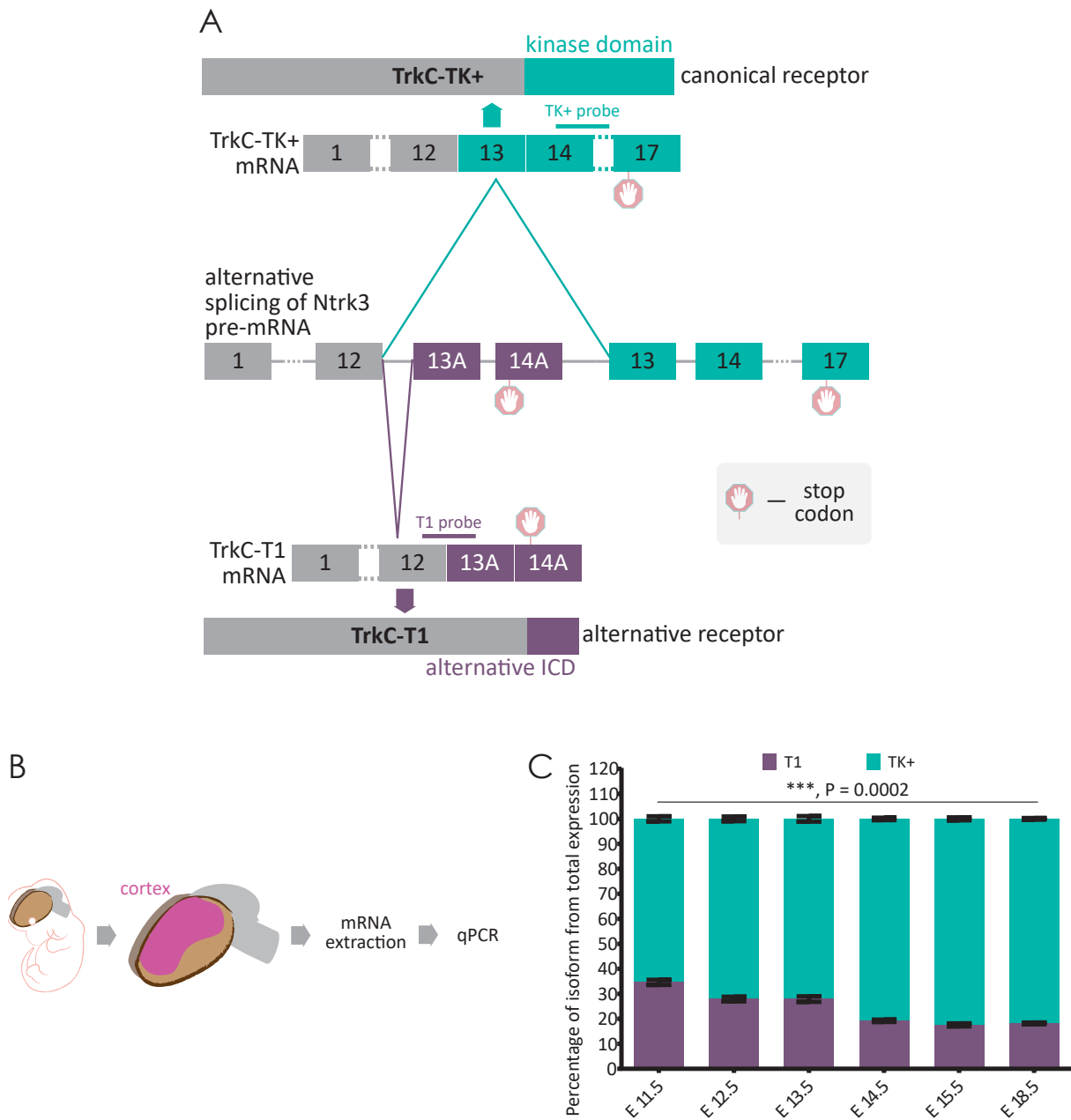


**Figure 2.2 The ratio between the TrkC AS variants TrkC-TK+ and TrkC-T1 changes during cortex development.** **A** Alternative splicing of the TrkC (Ntrk3) pre-mRNA produces the T1 and TK+ variants. Two groups of mutually exclusive exons (13A-14A and 13-17) give rise to the distinct 3' termini of the TrkC-TK+ and TrkC-T1 transcript variants. Correspondingly, these translate to distinct intracellular domains at the N-termini of the protein isoforms, giving rise to either a kinase domain (TK+) or a catalytically inactive domain (T1). Stop codons are indicated and demarcate the start of variant-specific 3' UTRs. Binding sites for the probes used in qRT-PCR are indicated at the respective exon junctions. **B** Experimental setup. **C** TaqMan quantitative real-time PCR for the two TrkC isoforms shows that the balance between TK+ and T1 shifts in favor of TK+ as cortex development progresses from embryonic day (E) 11.5 to E 18.5. N = 4. Bars: mean percentage of isoform from total TrkC expression (T1 plus TK+)  $\pm$  SD. Difference between E 11.5 and E 18.5:  $-16.43\% \pm 1.063$ . P value derived from unpaired, two-tailed Student's t test with Welch's correction.

### 2.3. The ratio of TrkC-T1 to TrkC-TK+ transcripts is not affected by different decay rates of the two transcripts

The stage-specific ratios of the TrkC transcripts to one another led us to wonder what mechanisms control the TrkC isoform ratio. Therefore, we tested whether different transcript decay rates may be the foundation for transcript balance regulation. However, after inhibiting transcription using actinomycin D, we could not see any significant difference in the ratio of T1 to TK+ in qPCR (Figure 2.3 A), despite both transcripts decreasing in quantity upon the treatment (Figure 2.3 B).

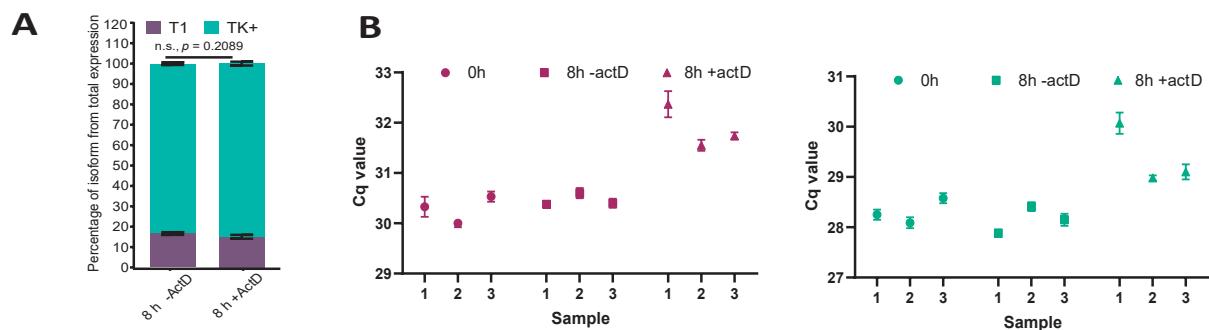


**Figure 2.3 The TrkC-TK+ and TrkC-T1 transcript variants decay at comparable rates.** qPCR was performed on mRNA from N2A cells after 8h either untreated or under treatment with actinomycin D at transcription-inhibiting concentration. **A** The ratio of T1 to TK+ from total TrkC transcript is not significantly affected by 8 hours of actinomycin D treatment.  $N = 3$ . Difference between means:  $-1.596 \pm 1.107$ . P value derived from two-tailed, unpaired Student's t test. **B** 8 hours of actinomycin D treatment led to around 2 cycles delay in reaching fluorescence threshold (Cq values) for both T1 and TK+, as opposed to the no-treatment conditions while using the same amount of cDNA as a qPCR reaction template between conditions.

### 2.4. TrkC-T1 and TrkC-TK+ transcript quantities are likely not regulated by miRNAs in the developing cortex

The mutual exclusion of the last exon groups towards the 3' end of the TrkC pre-mRNA results not just in different intracellular domains for the two receptors, but also in distinct 3' UTRs. MiRNAs are key developmental regulators which act by recognizing specific motifs in the 3' UTR of transcripts, leading to changes in transcript stability or translation (Ha and Kim, 2014). We therefore sought to understand whether the two TrkC transcripts could be differentially regulated by miRNAs. To do this, we employed TargetScan as a tool that predicts miRNA binding to search the 3' UTRs for binding sites while also considering the degree of evolutionary conservation of such binding sites. The binding sites detected by TargetScan can be seen in

Figure 2.4. Additionally, the tables in Figure 2.4 B list all the binding sites found in the aggregate order of the probability of conserved targeting (PCT) score (Friedman 2009, Agarwal 2015).  $P_{CT}$  indicates the probability that a miRNA target site is conserved in order to maintain its targeting by its cognate miRNA, as opposed to conservation by chance or for other regulatory mechanisms. The aggregate  $P_{CT}$  is the probability for a particular miRNA to regulate the transcript, calculated from the  $P_{CT}$  of all its target sites in the respective 3' UTR. Furthermore, it has been shown to correlate with the

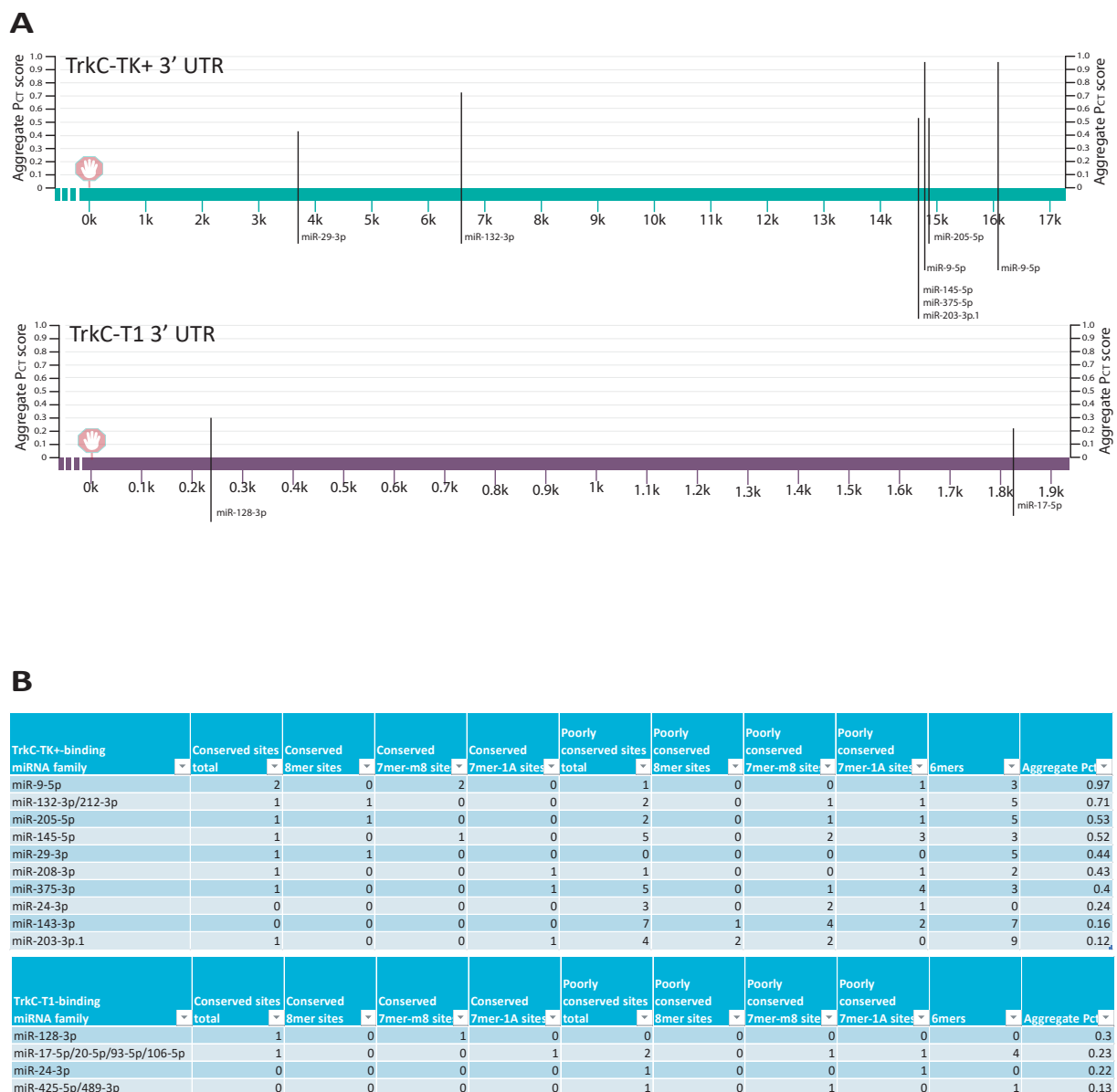


**Figure 2.4 Potential miRNAs targetting TrkC-T1 and TrkC-TK+.** Transcript sequences were analyzed using the TargetScan algorithm (targetscan.org, Agarwal et al., 2015). Putative miRNA binding sites and aggregate  $P_{CT}$  scores are indicated with vertical lines across the length of each 3' UTR, beginning with the stop codon (stop sign). Putative binding miRNA characteristics are summarized in the two tables below.

mean level of mRNA destabilization (Friedman et al, 2009). Since both TrkC-TK+ and TrkC-T1 show a high degree of evolutionary conservation, including the regions encoding their 3' UTRs, we consider the  $P_{CT}$  score to be a good indication of whether a miRNA is likely to regulate these transcripts.

For the two TrkC transcripts, we only found the 3' UTR of TrkC-TK+ to harbor several well-conserved miRNA binding sites (Figure 2.4), of which that of miR-9-5p has the highest  $P_{CT}$  value, 0.97, well above 0.75, which the TargetScan authors consider the cutoff for particularly high preferential conservation.. The second-highest hit was a binding site for miR-132. However, to our knowledge, miR-9 has been shown to be an adult-specific miRNA in the cortex, detectable from E 18.5 on (Miska et al., 2004). Also, the expression patterns of both miR-132 and miR-9 do not match the regulation of the TrkC transcripts in the NPCs, which we showed to be crucial for the fate of the neuronal progeny. MiR-132 is seen to localize in the intermediate zone, but not in the cortical plate, and miR-9 to be uniformly distributed in the cortex at E 12.5 (Zhang et al., 2019). As for TrkC-T1, miR-128-3p had the highest PCT value, but at a mere 0.3, it is unlikely to effectively impact TrkC-T1 levels in the developing cortex. Therefore, we concluded that these miRNAs are not involved in regulating the cell-type specific ratios of the TrkC transcripts in the developing cortex. Taken together, we consider regulation by miRNAs to be an unlikely player in establishing the cell-type-specific ratio of the TrkC transcripts to one another.

## 2.5. The TrkC-T1 and TrkC-TK+ transcripts are present in different ratios in NPCs and neurons

The temporally dynamic behavior of the TrkC-T1 to TK+ ratio during cortex development suggested that it is connected to the cellular composition of the cortex at each of its stages. Furthermore, altering the levels of TrkC-T1 in NPCs from E 12.5 on induces the previously published cell fate changes, and, while both transcript variants are readily detectable in neurons, TrkC-T1 is only detectable in NPCs from E 12.5 to 14.5, with a peak at E 13.5 (Parthasarathy et al., 2021). All of this suggests a cell-type specific regulatory mechanism for the ratio of the two isoforms, which is important for generating and maintaining the physiological levels of TrkC-T1, required for proper neuron fate determination in the cortex.

The most striking change in the cellular composition of the cortex from E 11.5 to E 18.5 is the progression from a tissue formed almost exclusively by NPCs to one

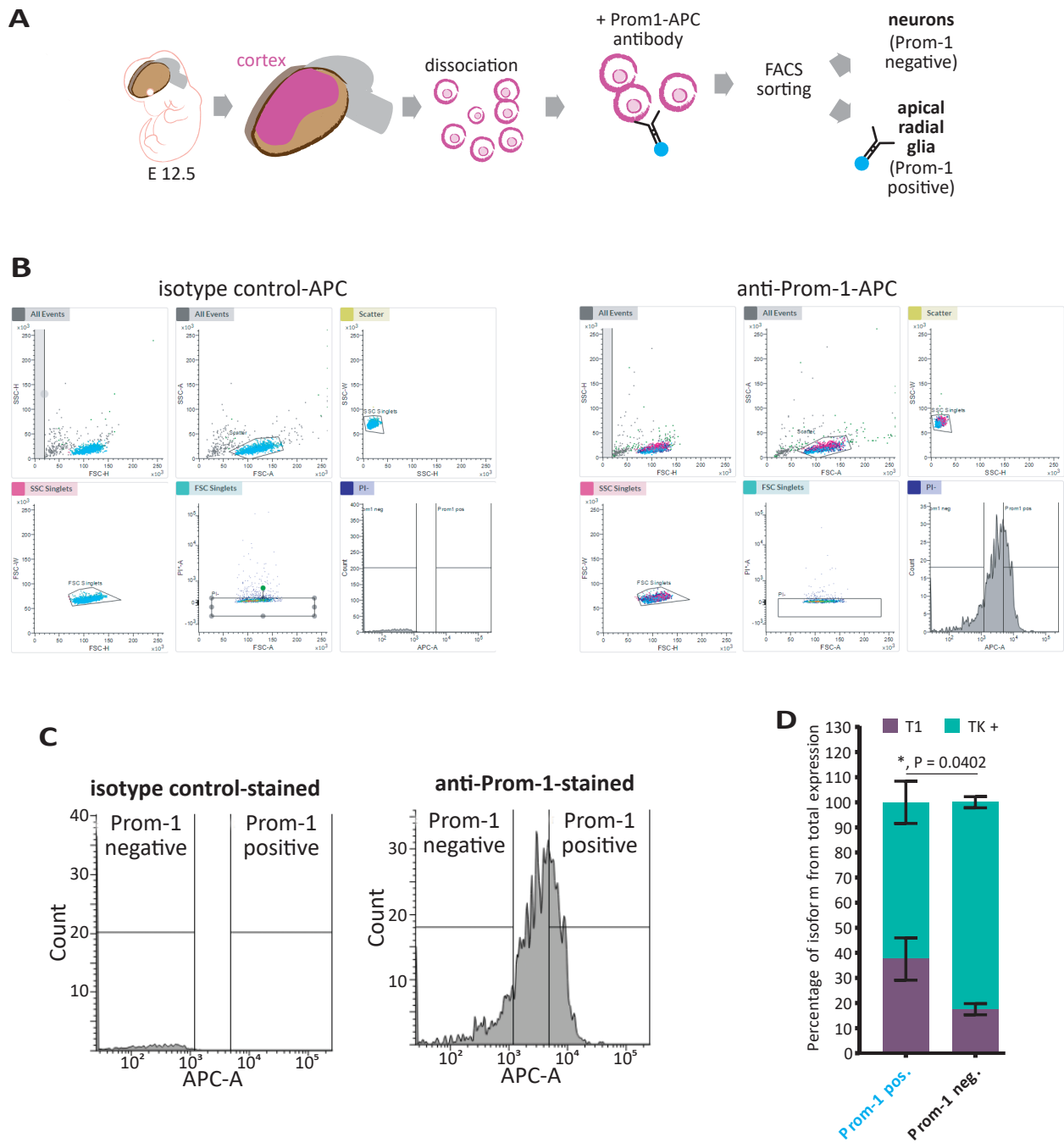


**Figure 2.5 TrkC-T1 and TrkC-TK+ are expressed in a cell type-specific manner in the developing cortex.** **A** Experimental strategy. Primary cortical cells from whole E 12.5 embryo litters were sorted into neuronal and apical radial glial populations by FACS after staining for prominin-1 (Prom-1). **B** FACS gating strategy for the Prom-1-based primary cortical cell sorting. Cells were separated based on the height and amplitude of side scatter (SSC) and forward scatter (FSC) signals in order to discriminate against cell doublets. From the singlets, only propidium iodide (PI)-positive cells were considered viable and included in the sorting based on the APC signal of either the Prom-1 antibody (plots on right side; Prom-1-positive: magenta, Prom-1-negative: dark blue) or a corresponding isotype control (plots on left-hand side; detected singlets: light blue). **C** Final discrimination step between viable Prom1-positive cells and Prom-1 negative ones. **D** Quantification of the ratio of TrkC-T1 and TrkC-TK+. TaqMan qPCR was performed on mRNA from the sorted primary cortical cells, as described under (A).  $N=3$ . P value derived from paired, two-tailed Student's t test. Pairing efficiency between Prom-1+ and Prom-1- results: correlation coefficient ( $r$ ) 0.9962, P value (one-tailed): 0.0019..

formed primarily by neurons (Greig et al., 2013; Rakic 2009). To test whether NPCs and neurons exhibit different ratios of TrkC-T1 to TK+, we sorted primary cortical cells from E 12.5 cortices using an APC-tagged antibody against prominin-1 (Prom-1) (Figure 2.5). Prom-1 is an antigen found exclusively in the membranes of NPCs that have a part of their cell membrane at the cortical-ventricular interface (Sykes and Huttner, 2013). At E 12.5, the cortical environment is dominated by apical radial glia and also contains the subcortically projecting neurons that these NPCs produce (Greig et al., 2013; Rakic 2009). From this, we concluded that Prom-1-positive cells are NPCs and Prom-1-negative ones neurons. We isolated total mRNA from both of the sorted cell categories and quantified TrkC-T1 to TK+ ratios employing the TaqMan assays described above. We observed a difference in the two ratios, with TrkC-T1 being more strongly represented in the total amount of TrkC transcript in Prom-1 positive cells than in Prom-1-negative cells ) (Figure 2.5 D). Conversely, the relative amount of TrkC-TK+ was higher in Prom-1-positive cells than in the negative ones.

## **2.6. Srsf1 and Elavl1 alter the ratio of TrkC-T1 to TrkC-TK+ in an antagonistic manner**

Based on the findings described above, we concluded that the cortical regulation of the TrkC transcript ratio happens most likely at the level of alternative splicing. Alternative splicing involves the binding of splicing factors in and around the alternative exons, which then either recruit spliceosomal components or prevent the binding and/or activity of the spliceosome. This can lead to the recognition of weak splice sites at the exon-intron boundaries of the alternative exons, thus favoring the inclusion of these exons which would otherwise be ignored by the splicing machinery (Fu and Ares, 2014). Embryonic development is rich in examples of differential splicing regulation brought about by spatially or temporally restricted expression, localization or activity of splicing factors, and this also applies to cortex development (see Su et al., 2018, for a review of examples). Because of this, we sought to understand what splicing factors could play a role in regulating TrkC alternative splicing in the developing cortex (Figure 2.6.).

A cursory search for proteins associated with splicing (GO:000039) in the mouse SwissProt database reveals around 100 proteins implicated in splicing and splicing regulation (SwissProt is released under a Creative Commons Attribution International license, CC BY 4.0.). We proceeded to narrow this group down to those splicing

factors that are expressed in the developing cortex and have been shown to exhibit temporal or spatial dynamics fitting a role in TrkC alternative splicing regulation. Since the ratio of T1 to TK+ changes strongly in corticogenesis and especially during the time span of deeper layer neurogenesis, we used two datasets that investigated the dynamics of RNA-binding proteins in the developing cortex, namely the RBP RNA in situ hybridization database from McKee et al, 2005, and the transcriptomic data on RBPs from DeBoer et al, 2013. The datasets show changes in RBPs from E 13.5 to P0 and from E 13.5 to E 15.5 and E 18, respectively. From these databases, we compiled a list of known and putative alternative splicing regulators that may affect TrkC splicing. To this, we added splicing factors that had already been shown to alter the outcomes of alternative splicing in the developing cortex, such as Rbfox2 or the Nova family, and splicing factors known to act in concert with these RBPs, such as the Srsf family.

In addition to this, we queried several RBP binding prediction tools using the splicing-relevant region of the TrkC pre-mRNA. It has previously been shown that alternative splicing cis-regulatory sequences concentrate in the immediate vicinity of exons, notably so in the flanking 100 nucleotides (Zhang & Chasin, 2004). We therefore proceeded to analyze putative RBP binding sites in the sequence region including the TrkC-T1-specific exons 13A and 14A, the interposed intron, and 500 adjacent nucleotides from the flanking introns. As binding prediction tools, we used CISBP (Ray et al., 2013), RBDP (Cook et al., 2011), ATtRACT (Giudice et al., 2016) and RBPmap (Paz et al., 2014). For further analysis, we only considered putative RBP binders that appeared in the results of at least two of the four prediction tools.

At the intersection of developmentally regulated SFs and SFs predicted to bind the TrkC region of interest, we found 27 potential splicing regulators, whose involvement in TrkC alternative splicing we decided to investigate further (Figure 2.6.).

To identify an easily cultured *in cellulo* testing system, we assessed whether the neuroblastoma cell line N2A expresses the TrkC transcript variants of interest and the splicing factors potentially involved in TrkC alternative splicing. We devised a variant-distinguishing PCR for TrkC-T1 and TrkC-TK+ (Figure 2.7 A), which we performed on cDNA from N2A cells with a radiolabeled forward primer shared between the two transcripts and distinct reverse primers. We found that N2A cells indeed express both TrkC-T1 and TrkC-TK+ (Supplementary Figure 1). Therefore, we investigated whether this cell line also expresses the splicing factors we were interested in.

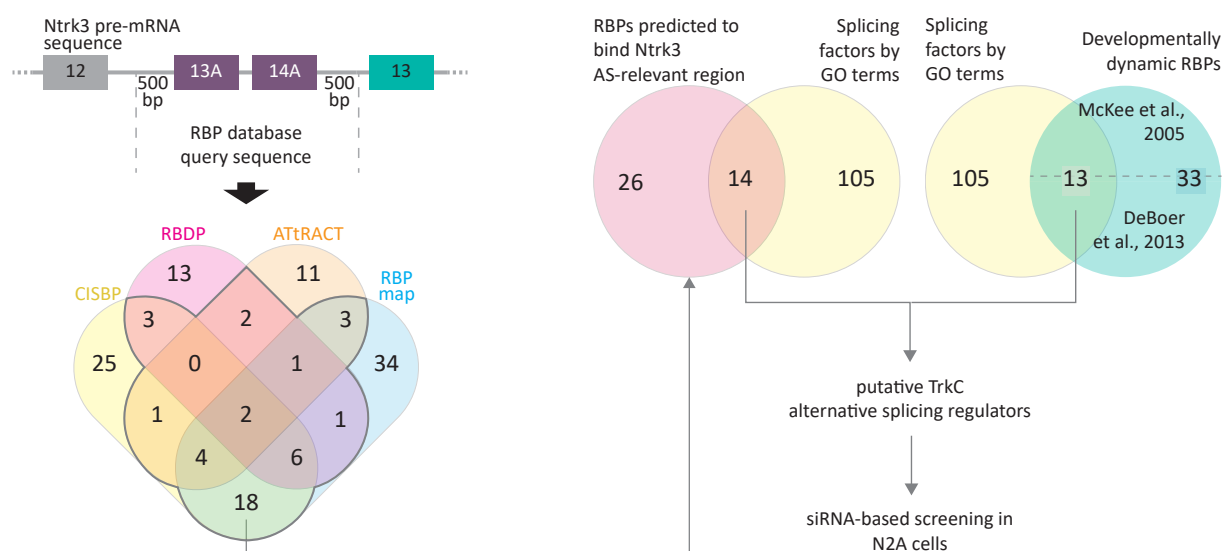


**Figure 2.6. Selection of SFs and other RNA-binding proteins (RBPs) with potential involvement in TrkC AS.** The sequence environment around the cassette exons 13A and 14A was used to query four tools predicting RBP binding. RBPs appearing in the results of at least two of the binding prediction tools were scanned for association with the GO term “splicing”. Additionally, the same GO term analysis was performed on RBPs described to have developmentally dynamic expression patterns in the developing cortex (McKee et al., 2005; DeBoer et al., 2013). We assessed the involvement of RBPs from these two analyses in TrkC alternative splicing.

To this end, we interrogated the wild type N2A microarray data provided by Chakrabarti et al. (GSE45160 on GEO, Chakrabarti et al., 2013) for each of these splicing factors (Supplementary Table 1). This showed that the vast majority is highly expressed in N2A cells, with expression values equal or higher than the 80th percentile rank of N2A transcripts.

With these tools, we performed a screening for splicing factors that affect the balance of TrkC-T1 to TrkC-TK+ using siRNA pools against each factor. We found that, of all the splicing factors tested (Figure 2.7 C), Srsf1 and Elavl1 (HuR) have a strong and significant effect on the TrkC transcript variant ratio (Figure 2.7 D). Furthermore, these two splicing factors have effects of double the magnitude of any of the other splicing factors tested, leading to mean changes of TrkC-T1 formation of around 20%, compared to control siRNA-transfected samples (Supplementary Table 2).

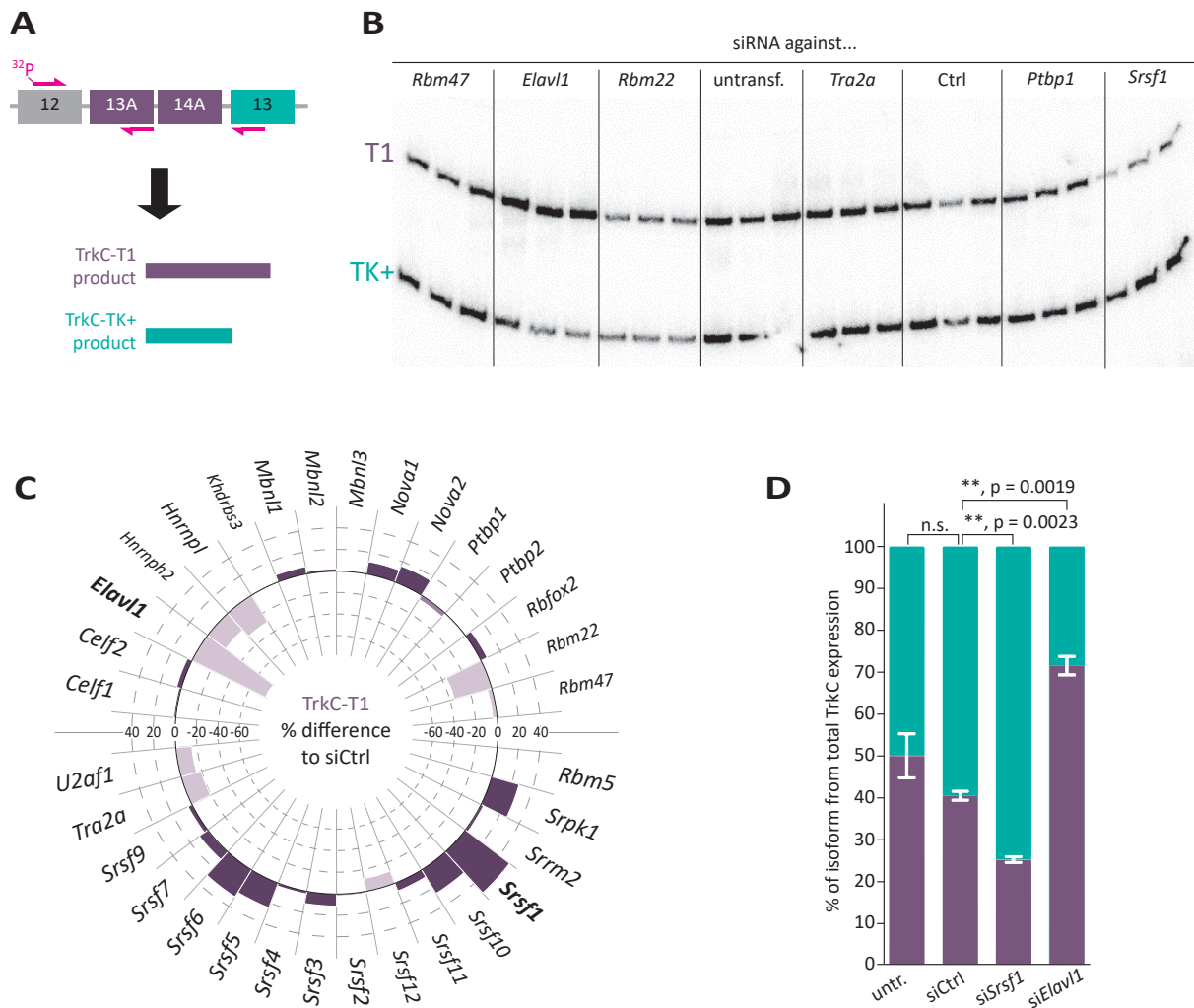


**Figure 2.7 Testing involvement of putative TrkC RBPs in TrkC AS reveals *Elavl1* and *Srsf1* as potent regulators of this AS event.** **A** Strategy for radioactive splicing-sensitive PCR for evaluating the TrkC-T1 and TrkC-TK+ splicing event. Reverse primers specific for either TrkC-T1 or TrkC-TK+ were employed in the same reaction with a radiolabelled forward primer, giving rise to radiolabelled products of easily resolved lengths. TrkC AS was assessed in samples where previously identified RBPs were knocked down using siRNAs. **B** Exemplary result of a radioactive splicing-sensitive PCR for TrkC-T1 and TrkC-TK+ on material from N2A cells treated with the indicated siRNAs. Percentage of TrkC-T1, as represented in (C) and (D), was assessed based on these captures. untransf – untransfected, Ctrl – siCtrl. **C** Summary plot for all tested RBPs and their effect on the proportion of the TrkC-T1 transcript variant from total TrkC transcript, normalized to TrkC-T1 percentage in the control siRNA samples. Gray dotted circles graduate the plot, indicating increases (positive values, outside of “0” circle) or decreases (negative values, inside of “0” circle) in TrkC-T1 percentage as compared to the siCtrl samples. Error bars were omitted for clarity. Statistically significant changes (siSrsf1 and siElavl1 samples) are represented separately with the corresponding descriptive and analytical statistical information in (D). **D** siRNA-mediated knockdown of *Elavl1* or *Srsf1* changes ratio of TrkC-T1 to TrkC-TK+ significantly. A decrease in *Srsf1* levels led to a decrease in the proportion of TrkC-T1 from total TrkC transcripts, while a decrease in *Elavl1* levels had the opposite effect. *N* = 3. Bars: mean percentage of isoform from total TrkC expression (T1 plus TK+) ± SD. *P* values derived from Brown-Forsythe and Welch ANOVA with Dunnett’s T3 multiple comparison post-hoc test. Overall *p* value: 0.0002.

## 2.7. Srsf1 and Elavl1 alter choice between CFuPN and CPN fate in the developing cortex

Up to this point, we had established that Srsf1 and Elavl1 shift the ratio of the T1 and TK+ transcript variants in opposing ways. Because of this and because our previous work showed that the levels of TrkC-T1 determine the outcome of neuronal fate acquisition (Parthasarathy et al., 2021), we hypothesized that Srsf1 and Elavl1 are also involved in this process and that altering their levels *in vivo* will, in turn, lead to a shift in the ratio of neuronal subtypes similar to T1 level alterations.

To test this hypothesis, we overexpressed Srsf1 or Elavl1 in NPCs of the developing cortex employing *in utero* electroporation of expression plasmids (pCAG-Srsf1-IG, expressing Srsf1-IRES-GFP under the control of the pCAG promoter, and the equivalent for Elavl1). Because we wished to characterize the TrkC-T1-dependent effects of these splicing factors, we chose to perform the electroporation at E 12.5, thus ensuring their overexpression across the time window of strong TrkC-T1 expression in NPCs (in normal development, we found this to be E 12.5 - E 14.5, as shown in Parthasarathy et al., 2021). As an analysis time point, we chose E 16.5, because this leaves sufficient time for the generation of both deeper layer neurons, produced between E 12.5 - E 14.5, and upper layer neurons, produced from E 14.5 up to the day of embryonic brain collection, E 16.5. We interrogated the generation of neuronal identities in the electroporated cortices by using immunofluorescent co-staining of GFP to visualize electroporated NPCs and their progeny, and quantifying the percentage of these GFP-positive cells that also expressed Ctip2 or Satb2 as markers for corticothalamic and cortico-cortical projection neuron identities, respectively (Arlotta et al., 2005; Molyneaux et al., 2005; Britanova et al., 2008; Alcamo et al., 2008). We compared the percentages of Ctip2-positive and Satb2-positive electroporated cells between the cortices electroporated with the Srsf1 or Elavl1 expression plasmids and the cortices of the respective littermates electroporated with the empty vector backbone (pCAGIG) (Figure 2.8 and Figure 2.9).

We found that overexpressing Srsf1 led to an increase in the proportion of Ctip2-positive cells (on average, 1.20-fold more than in pCAGIG-electroporated cells) and a decrease in the proportion of Satb2-positive cells (0.72 of Satb2-positive cells in pCAGIG-electroporated cortices) (Figure 2.8 A). This result is strongly reminiscent of that observed when overexpressing TrkC-T1 in the developing cortex by IUE (Parthasarathy et al., 2021). Conversely, overexpressing Elavl1 led to a decrease in the proportion of Ctip2-positive cells (0.62-fold of that in pCAGIG-electroporated cells) and a

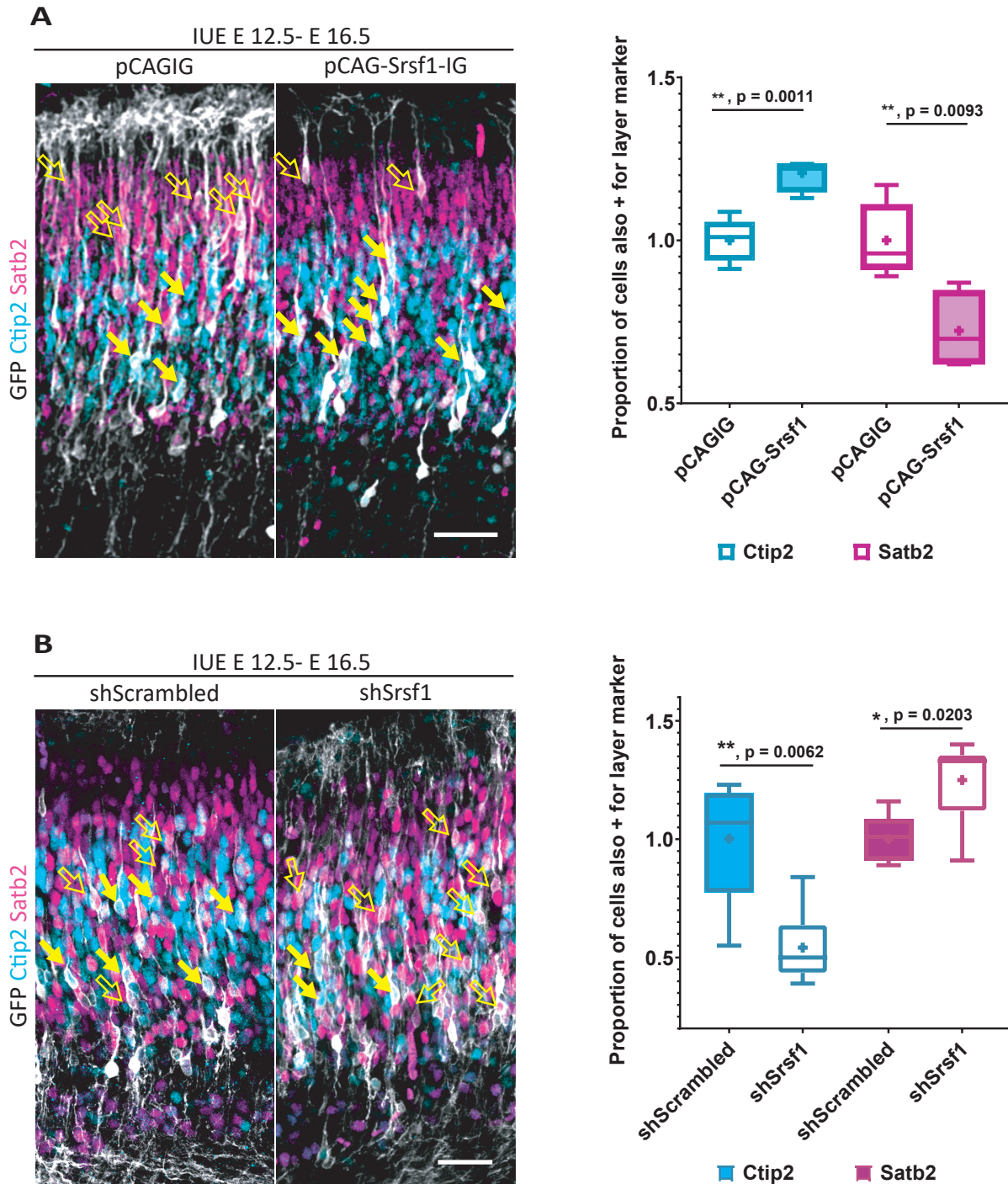


**Figure 2.8 Manipulation of Srsf1 levels *in vivo* in neural progenitor cells (NPCs) of the developing cortex alters CFuPN-CPN fate choice.** **A** Plasmid solutions containing either Srsf1 overexpression constructs (pCAG-Srsf1-IRES-GFP) or empty vector constructs (pCAG-IRES-GFP, abbreviated pCAGIG) were picoinjected into the lateral ventricles of E 12.5 embryos while in utero and then electroporated into the aRGs lining the ventricle. Co-expression of GFP and one of the neuronal fate markers Ctip2 (CFuPN subtype) or Satb2 (CPN subtype) was quantified at E 16.5. N=5 for each condition. P values derived from unpaired, two-tailed Student's t test with Welch's correction. **B** The same experimental setup was employed to quantify the effects of shRNA-based knockdown of Srsf1 on fate decision. N=5 for shScrambled and N=6 for shSrsf1. Box plot whiskers: minima and maxima of the sample. Horizontal line: median. Plus sign: mean of the sample. Empty arrows: GFP+Satb2 double-positive cells. Full arrows: GFP+Ctip2 double-positive cells. Scale bars = 50  $\mu$ m.

comparable increase in Satb2-positive cells (1.34-fold more than in the control brains) (Figure 2.9 A).

The knockdown of Srsf1 or Elavl1 had effects opposite to those of their overexpression. The downregulation of Srsf1 via shRNAs from E 12.5 to E 16.5 led to a decrease in the proportion of Ctip2-positive neurons to approximately 0.6-fold of numbers in

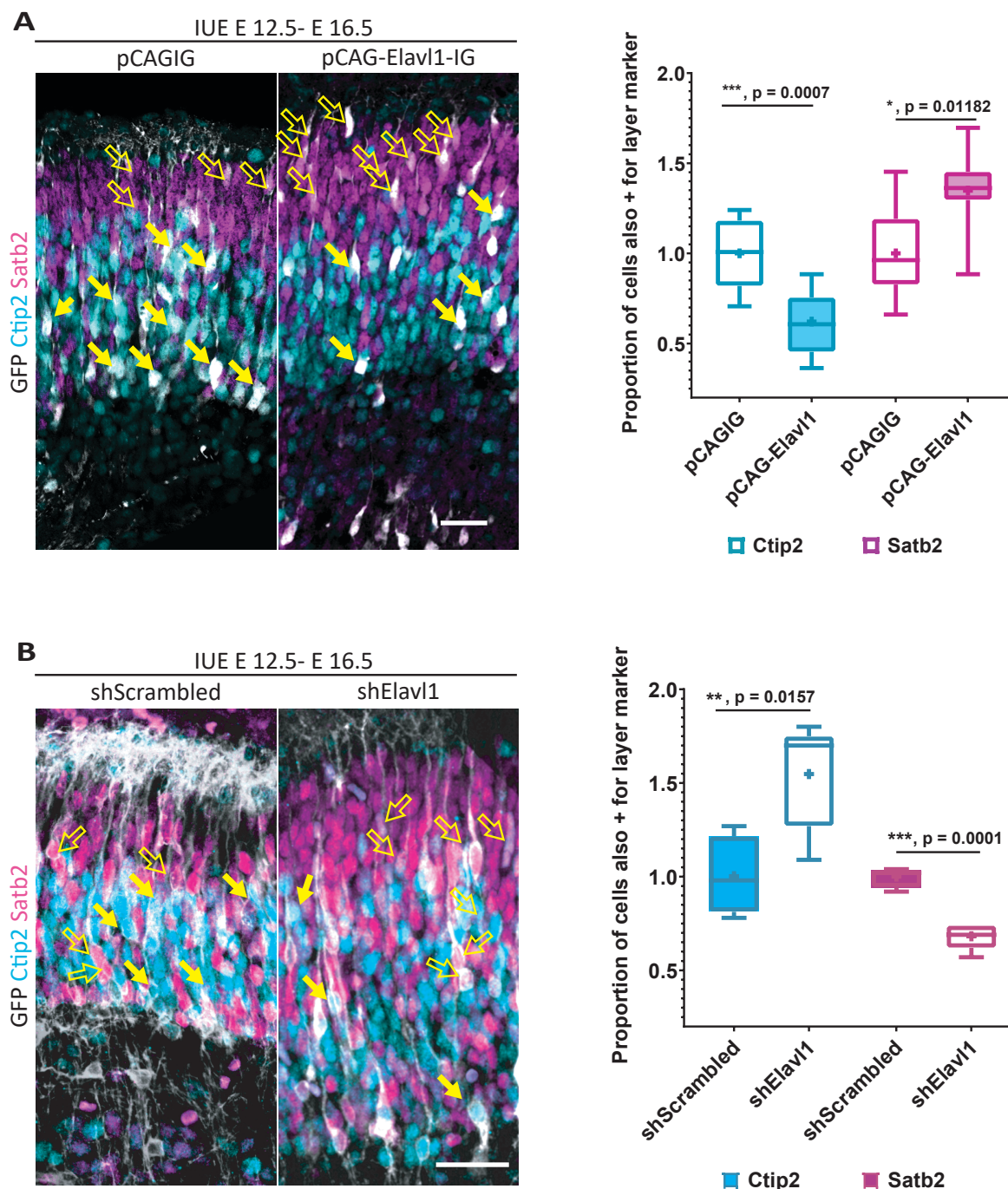


**Figure 2.9 Manipulation of Elavl1 levels *in vivo* in neural progenitor cells (NPCs) of the developing cortex alters CFuPN-CPN fate choice.** The same experimental setup described in Figure 2.8 was employed to alter Elavl1 levels in the NPCs of the developing cortex. **A** Overexpression of Elavl1 and quantification of the CFuPN and CPN fate of electroporated cells and their progeny. Co-expression of (continued on next page)

(continued from previous page) GFP and one of the neuronal fate markers Ctip2 (CFuPN subtype) or Satb2 (CPN subtype) was quantified at E 16.5. pCAGIG: N=10. pCAG-Elavl1: N=7. Box plot whiskers: minima and maxima of the sample. Horizontal line: median. Plus sign: mean of the sample. P values derived from unpaired, two-tailed Student's t test. Empty arrows: GFP+Satb2 double-positive cells. Full arrows: GFP+Ctip2 double-positive cells. Scale bars = 50  $\mu$ m.

control electroporations ( $0.5417 \pm 0.1295$ ), and there was a concomitant increase in Satb2-positive ones up to around 1.3-fold of control (Figure 2.8 B). shRNA expression constructs against Elavl1 (Figure 2.9 B) led to an increase in the proportion of Ctip2-positive neurons (55% more than in control) and vice versa for Satb2-positive ones ( $0.6820 \pm 0.0429$ ).

## **2.8. Srsf1 and Elavl1 directly influence the ratio of TrkC-T1 to TrkC-TK+ on both the transcript and protein levels**

From the results presented so far, we concluded that Srsf1 and Elavl1 influence fate decisions pertaining to neuron subtypes in cortex development, and that, *in vitro*, they significantly alter the ratio of TrkC-T1 to TrkC-TK+ transcript. We were interested in understanding whether these splicing factors enforce their effects on corticogenesis also by altering TrkC alternative splicing. To interrogate a system as close to the *in vivo* conditions as possible, we devised an experimental paradigm in which we isolated and brought in culture primary neurons from the cortices of embryos at E 13.5, in which we overexpressed Srsf1, Elavl1 or the empty vector backbone by nucleofection (Figure 2.10 A). After two days in culture, we analyzed the distribution of TrkC transcript variants and protein isoforms, respectively.

Using the TaqMan probes for TrkC-T1 and TrkC-TK+ described before (Figure 2.2), we quantified the levels of the two transcripts in the primary neurons previously nucleofected with Srsf1 or Elavl1 expression constructs (Figure 2.10 B). When overexpressing Srsf1, we could observe an increase in the proportion of TrkC-T1 transcript and a decrease in that of TrkC-TK+, as compared to the nucleofection of the empty vector backbone (pCAGIG). Furthermore, we saw the reverse effect when nucleofecting the Elavl1 overexpression construct.

Since the final amount of protein depends not just on the transcript levels, but also on various posttranslational regulatory processes, we wanted to test whether the shift in TrkC transcript variant distribution that we observed in qPCR also translated to the protein level. Indeed, by Western blotting protein lysates from the primary neurons nucleofected with Srsf1 or Elavl1 and detecting both TrkC isoforms (Figure 2.10 C), we could observe similar changes to those seen in qPCR: an accumulation of TrkC-T1 at the expense of TrkC-TK+ in the Srsf1-nucleofected neurons, and vice versa for the Elavl1-transfected neurons. These findings are in line with the results we obtained before in terms of transcript variant distribution by knocking down these splicing factors in N2A cells (Figure 2.7), suggesting that Srsf1 and Elavl1 are the main drivers of TrkC splicing in cortical neurons. The effect size on protein level is only about half of that observed on the mRNA level (Figure 2.10 B and Figure 2.7 D), which suggests other potential regulatory mechanisms that fine-tune the changes on the level of mRNA.

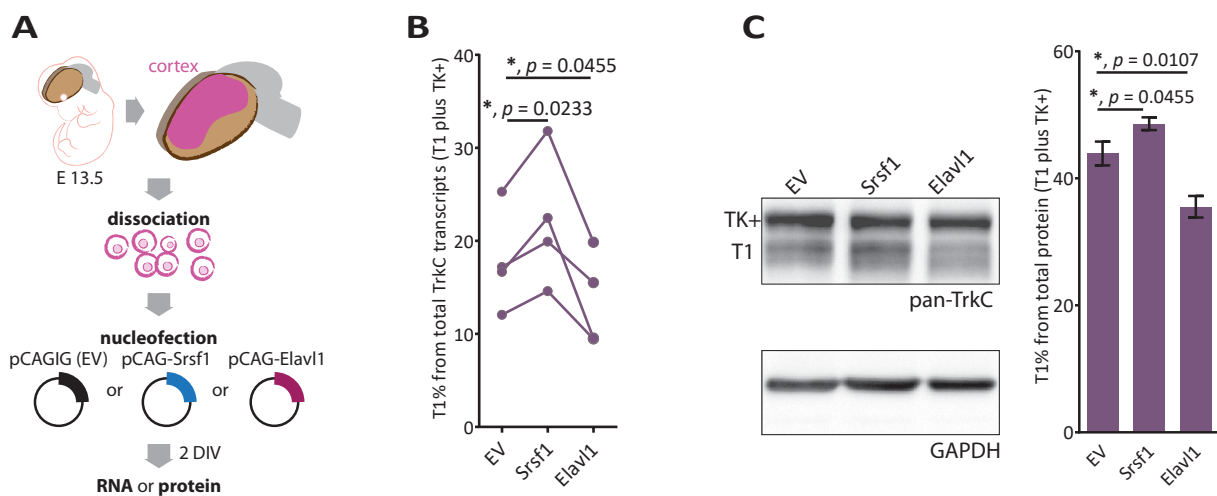


**Figure 2.10 Srsf1 and Elavl1 alter transcript and protein balance of TrkC isoforms T1 and TK+ in primary cortical neurons.** **A Experimental strategy.** Cortices from full litters of E 13.5 embryos were microdissected, dissociated into primary cortical cells and nucleofected with plasmids expressing either Srsf1, Elavl1, or empty expression constructs (pCAGIG = EV). Nucleofected cells were cultured for two days *in vitro* (DIV), after which total RNA or protein were extracted. **B** Srsf1 and Elavl1 alter transcript variant ratio of TrkC-T1 and TrkC-TK+. qPCR on material from the nucleofected, cultured primary cortical cells. Lines represent paired replicates from the same experiment (cortical cells from one full litter split into 3 nucleofection conditions). P values from one-way ANOVA; overall p value: 0.0046. **C** Srsf1 and Elavl1 alter ratio of TrkC-T1 and TrkC-TK+ proteins. Lysate from the nucleofected, cultured primary cortical cells was Western blotted and probed with a pan-TrkC antibody, which detects both TrkC-TK+ (130 kDa) and TrkC-T1 (100 kDa). GAPDH was detected as a loading control. P values from one-way ANOVA; overall p value: 0.0278.

## 2.9. The effects of Srsf1 and Elavl1 on the CFuPN-CPN fate decision are dependent on the levels of TrkC-T1

We wanted to investigate whether the effect of Srsf1 and Elavl1 on neuron subtype fate acquisition (Figure 2.8 and Figure 2.9) is mediated by the balance of TrkC-T1 to TrkC-TK+ *in vivo*. For this purpose, we electroporated either splicing factor together

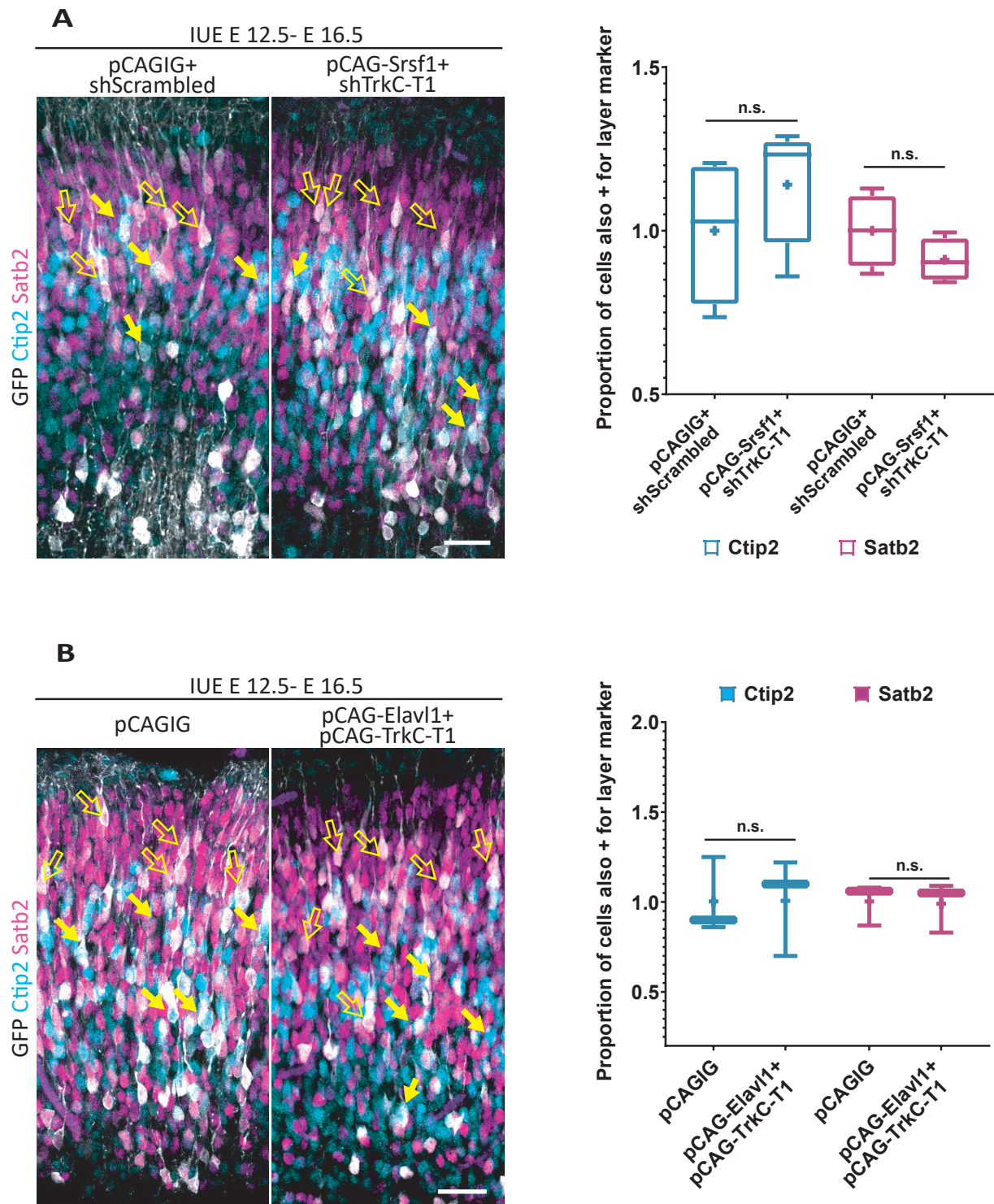


**Figure 2.11 Suppressing the modifications in TrkC-T1 levels induced by Elavl1 and Srsf1 abolishes the effects of these factors on the CFuPN-CPN fate decision.** **A** Knocking down TrkC-T1 while overexpressing Srsf1 does not alter the proportion of Ctip2- or Satb2-positive progeny, compared to control constructs. Constructs were electroporated as shown and the quantification was performed as described in previous figures. N = 4 for pCAGIG+shScrambled, N=5 for pCAG-Srsf1+shTrkC-T1. Mean  $\pm$  SD: Ctip2 =  $1 \pm 0.2237$  in control versus  $1.141 \pm 0.1787$  in pCAG-Srsf1 + shTrkC-T1, Satb2 =  $1 \pm 0.1109$  in control versus  $0.9914 \pm 0.06534$  in pCAG-Srsf1 + shTrkC-T1. **B** The simultaneous overexpression of Elavl1 and TrkC-T1 has no significant effect on the proportion Ctip2 or Satb2 cells, compared to the empty vector control. N = 3 for both pCAGIG and pCAG-Elavl1 + pCAG-TrkC-T1. Mean  $\pm$  SD: Ctip2 =  $1 \pm 0.2146$  in control versus  $1.007 \pm 0.1723$  in pCAG-Elavl1 + pCAG-TrkC-T1, Satb2 =  $1 \pm 0.1159$  in control versus  $0.99 \pm 0.14$  in pCAG-Elavl1 + pCAG-TrkC-T1. P values derived from unpaired two-tailed Student's t test. Box plot whiskers: minima and maxima of the sample. Horizontal line: median. Plus sign: mean of the sample. Empty arrows: GFP+Satb2 double-positive cells. Full arrows: GFP+Ctip2 double-positive cells. Scale bars = 50  $\mu$ m.

with a construct that should compensate for the previously shown effects (Figure 2.7.) of these factors on TrkC AS. We therefore overexpressed Srsf1 while downregulating TrkC-T1 and overexpressed Elavl1 while simultaneously overexpressing TrkC-T1 using the same *in vivo* experimental paradigm as for the other manipulations of gene products.

We overexpressed Srsf1 from E 12.5 to E 16.5 together with the previously published construct expressing an shRNA against TrkC-T1 (Parthasarathy et al., 2021). The fate analysis of the progeny resulting from the electroporation showed that there were no significant changes in neither the proportion of CFuPN nor that of CPN when compared to the control (Figure 2.11 A). Interestingly, in spite of employing the shRNA against TrkC-T1, which we have shown to be highly effective at suppressing this transcript and protein (Parthasarathy et al., 2021), we saw a trend towards an increase in Ctip2-positive cell numbers and a trend towards a decrease in Satb2-positive numbers. In the case of the simultaneous overexpression of Elavl1 and TrkC-T1, we saw no significant changes in the proportions of Ctip2- and Satb2-positive cells (Figure 2.11 B).

We therefore concluded that the effects of Srsf1 and Elavl1 on neuron subtype fate acquisition are, at least partially, dependent on these splicing factors regulating the TrkC AS event that gives rise to TrkC-T1 or TrkC-TK+.

## 2.10. *Srsf1* and *Elavl1* are differentially expressed in the histological compartments of the developing cortex

We previously showed that the production of deeper layer neurons is critically impacted by the regulation of TrkC-TK+ to TrkC-T1 balance in the ventricular zone (VZ) of the developing cortex from E 12.5 to E 13.5 (Parthasarathy et al., 2021). This knowledge, in connection with the results shown above and previous findings indicating that splicing factors often exert combinatorial control on alternative splicing events (reviewed in Fu and Ares, 2014), led us to wonder if the expression patterns

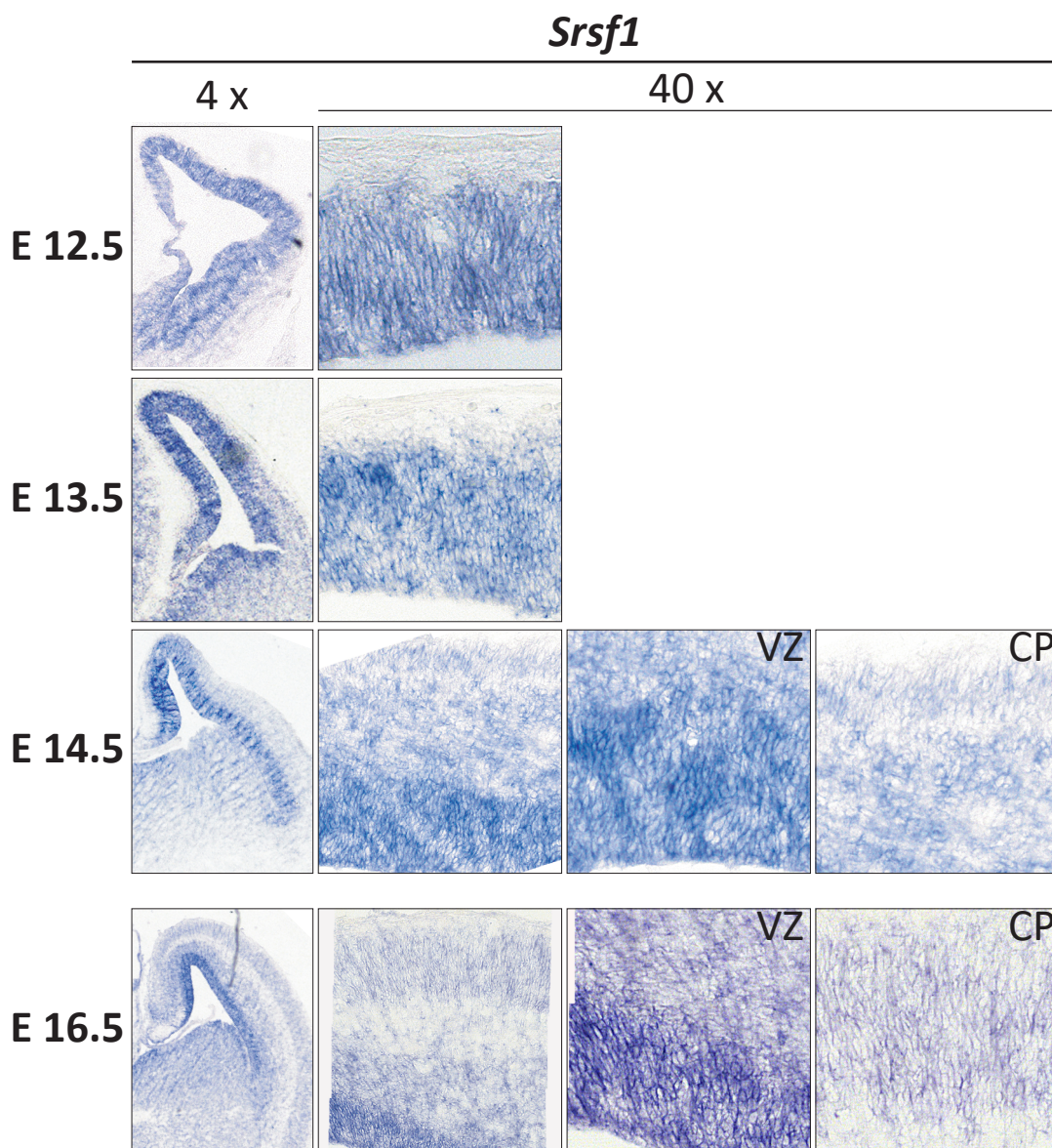


**Figure 2.12 Expression of *Srsf1* mRNA concentrates in the VZ of the developing cortex.** Left-hand column of panels show overviews of the brain sections at the indicated stage, with the signal for *Srsf1* in dark blue. Panels on the right-hand side show a higher magnification for either the entire thickness of the cortex (E 12.5 and E 13.5) or for representative areas in the VZ or CP. VZ - ventricular zone, CP - cortical plate..

of *Srsf1* and *Elavl1* could explain the observed TrkC AS patterns. To address this, we performed in situ hybridization for the *Srsf1* and *Elavl1* transcripts on brain sections at the embryonic development stages relevant for TrkC AS regulation and deep layer neuron production (E 12.5 – E 14.5) and at the peak of CPN production (E 16.5)(Figure 2.12 and Figure 2.13). At these stages, we found the *Srsf1* transcripts to be strongly represented in the ventricular zone (VZ), in contrast to other cortical compartments, where far weaker expression was detected. The distinction between the *Srsf1* expression compartments was clear even up to E 14.5, where TrkC-T1 expression in NPCs

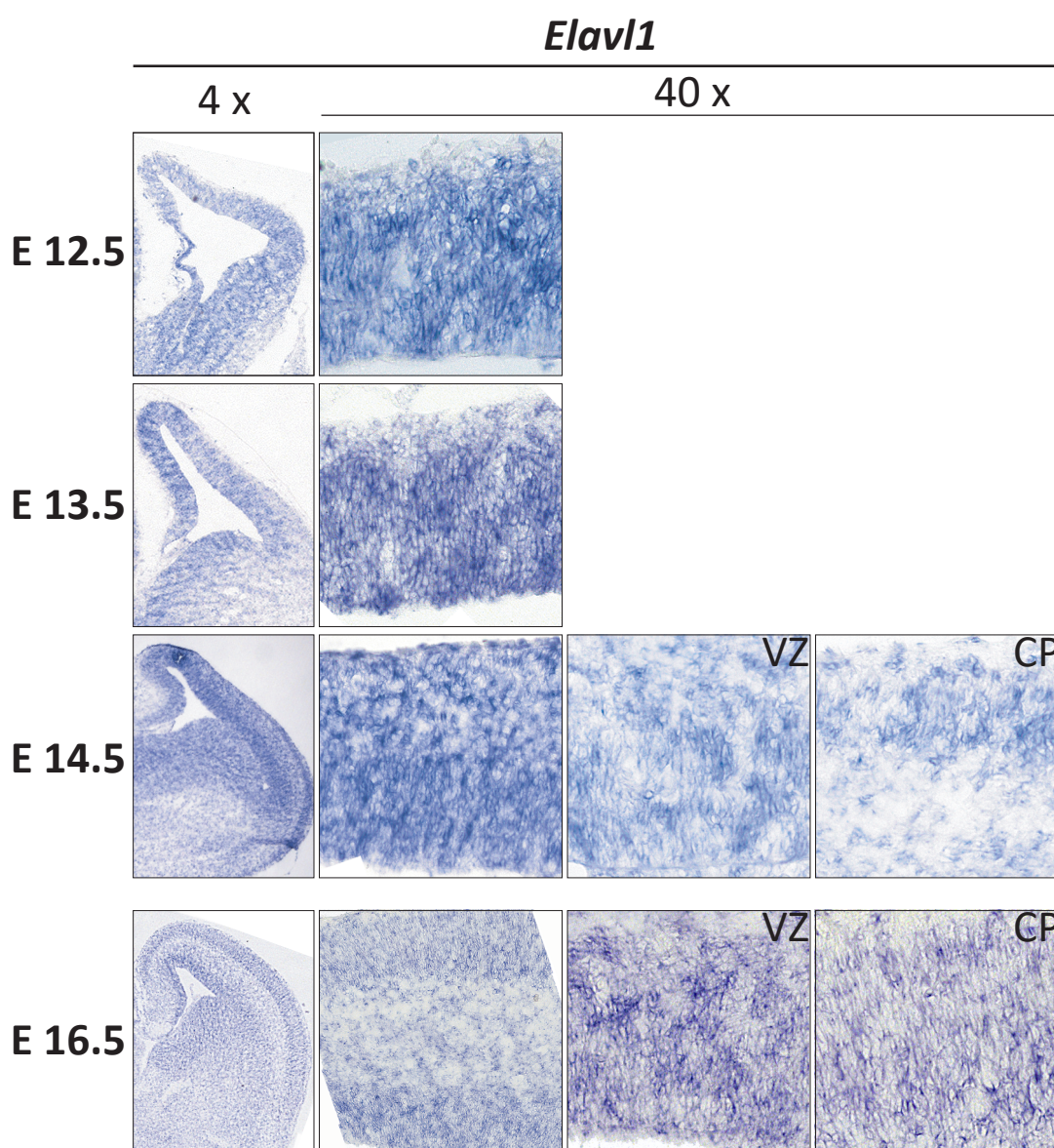


**Figure 2.13 Expression of *Elavl1* mRNA is comparable in the VZ and CP of the developing cortex.** Left-hand column of panels show overviews of the brain sections at the indicated stage, with the signal for *Srsf1* in dark blue. Panels on the right-hand side show a higher magnification for either the entire thickness of the cortex (E 12.5 and E 13.5) or for representative areas in the VZ or CP. VZ - ventricular zone, CP - cortical plate.

fades (Parthasarathy et al., 2021) and deeper layer neurogenesis ceases (Greig et al., 2013). *Elavl1* transcripts were also readily detectable in the developing cortex, but with a far less pronounced preference for the VZ compared to *Srsf1*. Its less distinct expression between compartments also translates to the protein level, as seen in immunofluorescent stainings on E 13.5 brain sections (Figure 2.14).

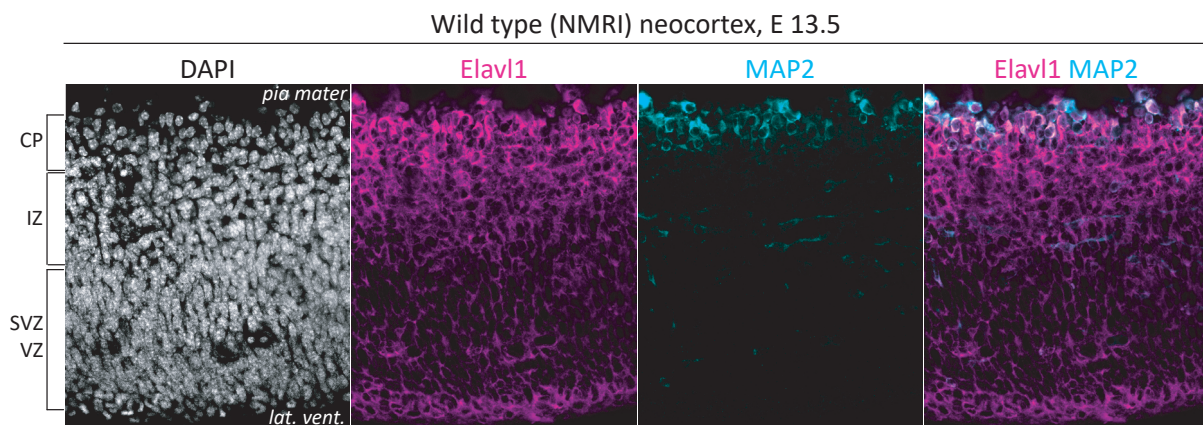


**Figure 2.14 Expression of the *Elavl1* protein in the wild type developing cortex is comparable between VZ and CP at E 13.5.** Immunofluorescent micrographs of cortex sections stained with antibodies against *Elavl1* and the neuronal marker *MAP2* show similar signal intensity in the VZ/nascent SVZ as in the CP. VZ - ventricular zone, SVZ - subventricular zone, IZ - intermediate zone, CP - cortical plate, lat. vent. - lateral ventricle.

## 2.11. *Srsf1* and *Elavl1* are expressed in different NPC- and neuron-specific ratios in the developing cortex

We asked if the observed expression patterns could lead to different splicing-regulatory environments in NPCs and neurons and thus to the observed differences in *TrkC* transcript ratios. As the nature of tissue in situ hybridization does not allow very accurate comparisons between transcript quantities, especially between transcripts of different genes, we employed the prominin-1 experimental setup to FACS sort neurons and apical radial glial NPCs and assess the *Srsf1* and *Elavl1* transcript quantities at E 12.5 (Figure 2.15 A), when *TrkC-T1* is prominent in NPCs (Parthasarathy et al., 2021). In the sorted NPCs and neurons, we could see differences in the amounts of *Srsf1* and *Elavl1*, respectively, that underscored the cell-type specific differences observed using in situ hybridization. *Srsf1* was found to be increased around tenfold in Prom-1-positive cells (NPCs) compared to Prom-1-negative ones (Figure 2.15 B). In contrast, while there was a tendency of an increase in *Elavl1* transcripts in the Prom-1-positive cells, this was not significant (Figure 2.15 C).

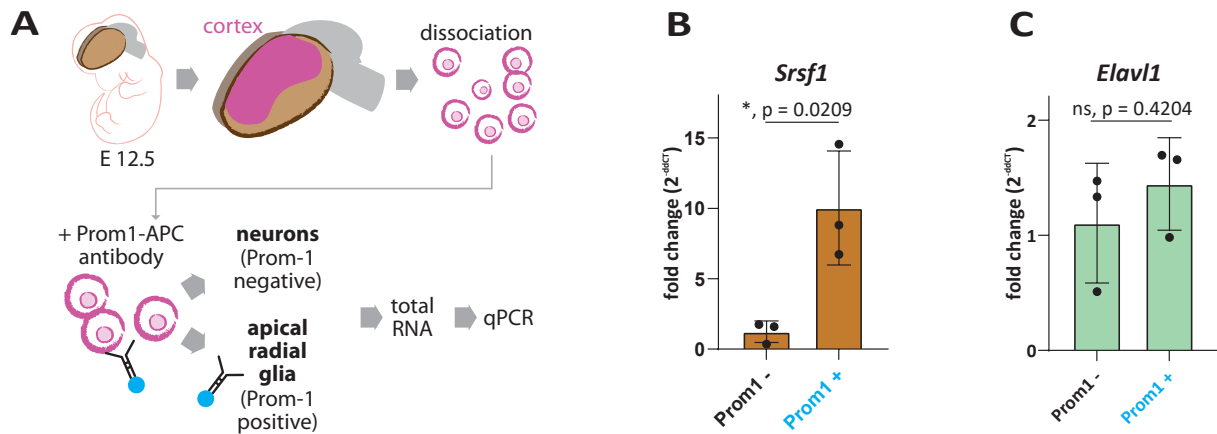


**Figure 2.15 The expression of *Srsf1* and *Elavl1* shows different ratios in NPCs versus neurons. A** Experimental setup **B** Quantification of *Srsf1* mRNA levels by qPCR showed strong expression in prominin-1-positive cells when compared to prominin-1-negative cells. **C** *Elavl1* mRNA levels did not differ significantly between Prom-1-positive and Prom-1-negative cells. Values depicted are fold changes resulting from  $2^{-\Delta\Delta CT}$  analysis using the Prom-1-negative sample as a calibrator sample and *Hprt* or *Oaz1*, respectively, as internal controls.  $N = 3$ . P values derived from unpaired, two-tailed Student's t test. Dots represent fold change values in individual replicates.  $N = 3$  for all. P values derived from two-tailed unpaired Student's t test.

## 2.12 Bioinformatic analysis of the *Ntrk3* primary transcript suggests the presence of an *Srsf1*-dependent exonic splicing enhancer in exon 13A

In order to elucidate whether the effect of *Srsf1* and *Elavl1* splicing is achieved by direct interaction, we sought to find the splicing enhancers and/or silencers that these splicing factors bind. As the alternative exons of the *TrkC* pre-mRNA are flanked by unwieldily large introns (see Figure 2.2 A, 51.6 kb for intron 13 between exons 12 and 13A, 1.5 kb for intron 14 between exons 13A and 14A, and 40 kb between exons 14A and 13), directly generating a splicing minigene reporter was not possible. Additionally, assays seeking to test the binding of a splicing factor to an RNA sequence benefit from using as short a sequence as possible, because a long bait will inevitably contain a high number of potential splicing factor binding sequences and will hence generate a large pool of splicing factors that bind *in vitro*, thus hindering the identification of key splicing factors and splicing regulatory elements controlling the outcome of the splicing event. In order to zone in onto the sequence elements likely to control *TrkC* alternative splicing, we performed bioinformatic analysis of the splice sites flanking exons 12, 13A, 14A and 13.

We analyzed the probability of each intron-exon/exon-intron junction of the aforementioned exons to be recognized by the spliceosome (Figure 2.16). We did so using two previously published algorithms, HBond and MAXENT (Freund et al., 2003,

Yeo & Burge, 2004), both of which analyze the sequence around these junctions in regard to different splicing-relevant parameters. HBond is a prediction tool for the probability of the free end of the spliceosomal component U1 snRNA to bind to the 5' splice site (ss) of an intron, based on a model incorporating how many hydrogen bonds there could be formed between the two RNAs and the positions they could be formed in. MAXENT is a machine-learning based algorithm that quantifies the probability of an exon-intron junction sequence to be a functional splice site, based on the maximum entropy distribution in relation to experimentally supported splice site sequences.

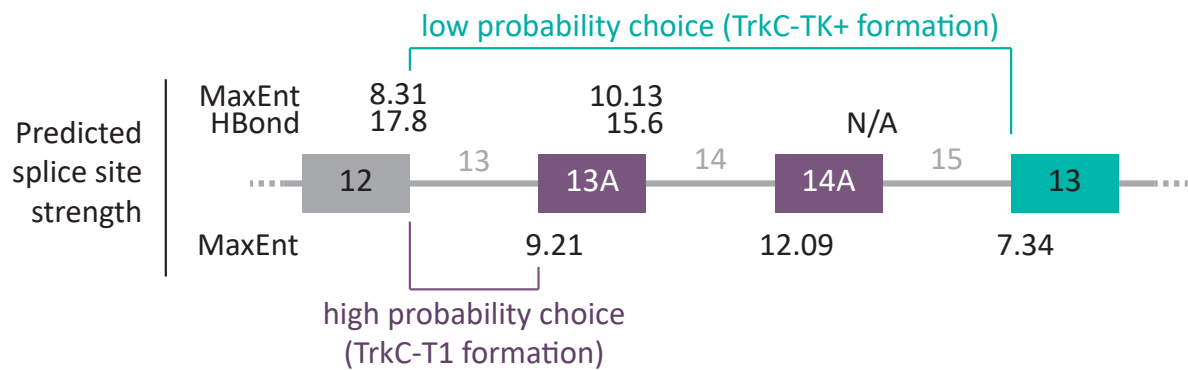


**Figure 2.16 Bioinformatic analysis of the Ntrk3 primary transcript predicts TrkC-T1 as the preferred alternative splicing outcome.** The MaxEnt (Yeo & Burge, 2004) and HBond (Freund et al., 2003) tools were used to predict the probability of intron-exon and exon-intron junctions relevant to TrkC AS being recognized by the spliceosome (splice site strength). The splicing of intron 13, which favors the formation of the TrkC-T1 transcript variant, is predicted to be the preferred outcome, based on the combination of the flanking splice site strengths. This likely hinders the recognition of the far further downstream intron-exon boundary of intron 15/exon 15, which is also weaker than any of the preceding splice sites, and thus makes the formation of the TrkC-TK+ splice variant less likely than that of the T1 variant. This suggests that exon 13A splicing must be suppressed in order to enable formation of the TrkC-TK+ isoform. N/A – intron starting with AG instead of GU; possibly targeted by minor spliceosome and therefore not analyzable with MaxEnt or HBond.

We observed very high predicted recognition probability for the 5' splice site after the last exon shared between the two TrkC variants (intron 13 5'ss) and after exon 13A (intron 14 5'ss) (Figure 2.16). The 5' splice site of exon 14A could not be analyzed because it is not a classic, GT-type 5' splice site. Since splicing occurs co-transcriptionally (Naftelberg et al., 2015) and hence splice sites are recognized in a 5' to 3' direction, the intron 13 5' splice site is recognized first and can then pair during the construction of the spliceosome with any of the downstream 3' splice sites. Of these, the strongest is the 3' splice site before exon 14A. However, in a transcriptomic

dataset from the E 13.5 cortex, we were not able to find any TrkC transcripts that skip exon 13A but include exon 14A (Ingo Bormuth, unpublished data), and such a transcript variant has not been described, as shown in the Ensembl genome browser (Supplementary Figure 2, Yates et al., 2019). The 3' splice site in intron 15, before the TrkC-TK+-specific exon 13, is the weakest. From all of this information, we concluded that the excision of intron 13 and hence the formation of TrkC-T1 is the default outcome of the TrkC alternative splicing event, meaning that this needs to be overridden in order to generate the TrkC-TK+ variant.

### **2.13 Fragment 3 of exon 13A contains a GAR exonic splicing enhancer crucial for the formation of TrkC-T1**

The recognition of a weak splice site, such as the 3' one in intron 15, can be achieved if its stronger upstream counterparts are either masked by splicing factor activity, or if, in the right context, a splicing factor that further promotes the recognition of the strong splice sites is not present anymore, increasing the probability that these splice sites will be skipped (Brillen et al., 2017 (1)). Since the inclusion of exon 13A seems to be the preferred outcome of TrkC splicing, we reasoned that it could harbor the regulatory sequences necessary for controlling this outcome. Therefore, we used the HEXplorer tool (Erkelenz et al., 2014) to analyze the splicing-regulatory potential of exon 13A (Figure 2.17). HEXplorer calculates the probability of each nucleotide in a given sequence to be part of a splicing regulatory region, based on its position in all possible hexameric sequences that overlap it. The resulting profile of a sequence gives insight into a potential role as a splicing enhancer or silencer.

When we analyzed the sequence of exon 13A, we found three main regions (Figure 2.17). The 5' region (fragment 1) seems most likely a splicing silencer, the middle region (fragment 2) an enhancer, and the last one (fragment 3) had both potentially enhancing and potentially silencing regions. To determine whether these predictions translate into functional roles and zone into potential splicing factor binding sites, we tested the splicing-regulatory properties of each of the three fragments using a splice reporter vector (Brillen et al., 2017 (2)).

In the splicing reporter vector described in Brillen et al (Figure 2.18 C), fragments from the gene of interest are cloned into a heterologous three-exon minigene construct, expressed in an *in cellulo* system, after which the splicing pattern is assessed

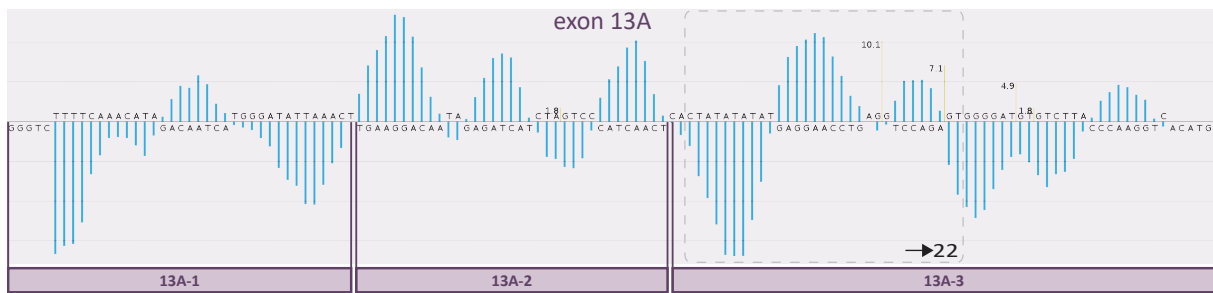


**Figure 2.17 Bioinformatic analysis of exon 13A suggests its subdivision in three major splicing-regulatory regions.** Using the HEXplorer tool (Erkelenz et al., 2014), we found that exon 13A can be subdivided in roughly three regions with different putative splicing-regulatory properties: a 5' one (labelled 13A-1) predicted to act as a splicing inhibitor, a middle one (13A-2) predicted to have enhancer activity, and a 3' one (13A-3) predicted to primarily function as an enhancer.

by RT-PCR. This way, one can elucidate whether the sequence contributes to the inclusion of the exon containing it and providing information on the presence or absence of cis-regulatory elements in the source exon and on their type. We transfected the splicing reporter vectors to N2A cells, given their high degree of similarity to neurons, and analyzed the outcome (Figure 2.18 E). In accord with the predictions, fragment 1 from exon 13A favored exon skipping and fragment 2 exon inclusion. Fragment 3 proved to be an exonic splicing enhancer as well, albeit with incomplete penetrance. We reasoned that this indicates the presence of a cis-regulatory element in this fragment that can be dynamically regulated.

We analyzed the sequence of fragment 3 using the ESEfinder tool (Cartegni et al., 2003). In this sequence, we found several elements likely to be bound by Srsf1, Srsf2, Srsf5 or Srsf6 (Figure 2.18 A), all well above the baseline thresholds established by the authors. However, we had already shown that the knockdown of Srsf2, 5 and 6 does not have a significant effect on the balance of TrkC-T1 to TK+ (Figure 2.7). We therefore focused on the three GA-rich (GAR) elements potentially bound by Srsf1. A HEXplorer-based analysis of nucleotides essential for the maintenance of the splicing-regulatory properties of fragment 3 suggested that a single nucleotide substitution in the sequence area of the first GAR element could severely disrupt the ability of this fragment to act as an enhancer (Figure 2.18 B). Indeed, inducing this mutation in the fragment 3 splicing reporter vector reduced exon inclusion strongly, once more underscoring the importance of this region in exon 13A inclusion (Figure 2.18 E).

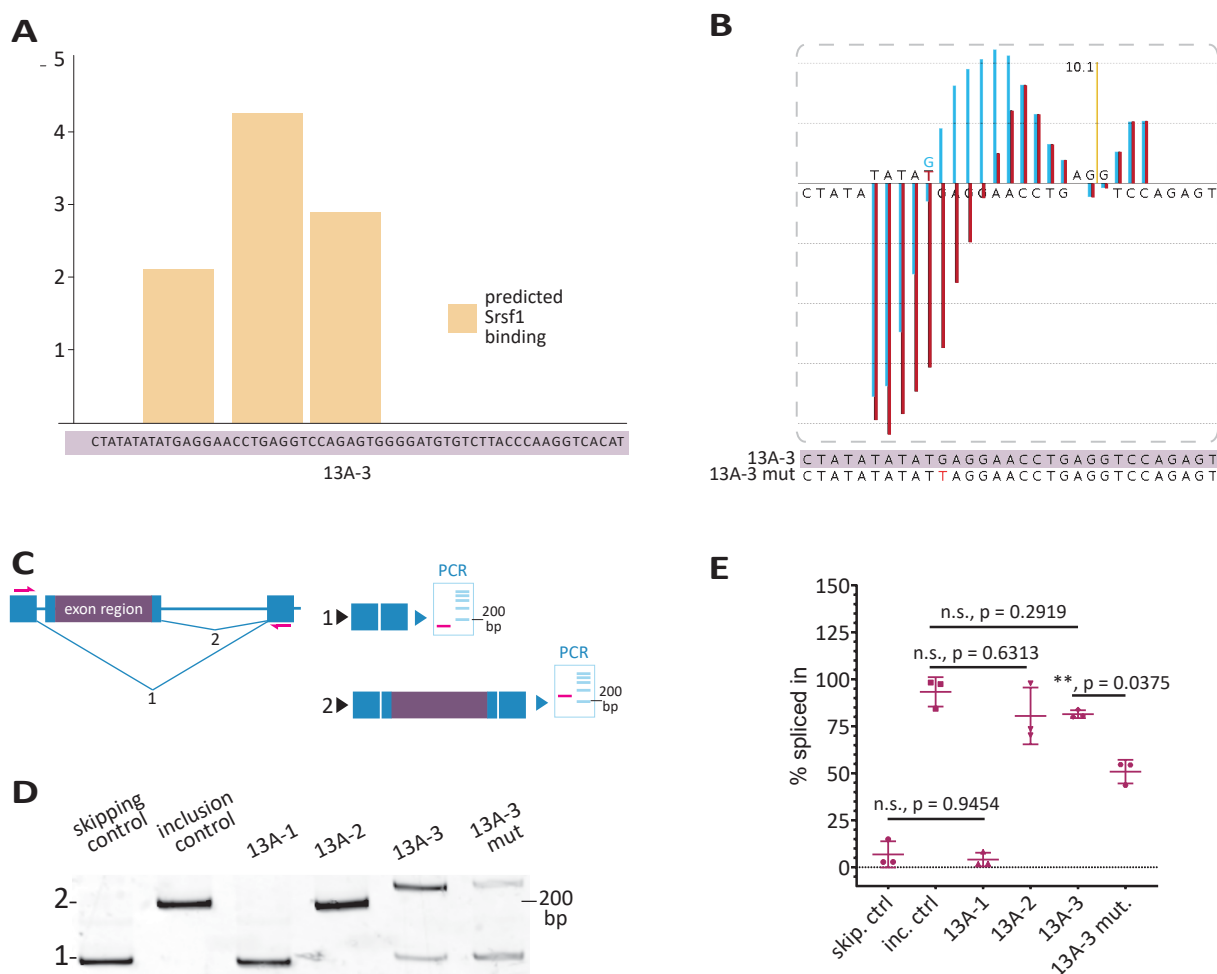


**Figure 2.18** Part 3 of exon 13A (13A-3) acts as a splicing enhancer and contains high probability predicted Srsf1 binding sites overlapping a potential GA-rich exonic splicing enhancer (GAR-ESE) element. **A** The third part of exon 13 (13A-3) was found to contain three high-strength putative Srsf1 binding sites using the ESEfinder tool (Cartegni et al., 2003). **B** The location of the Srsf1 binding sites predicted by ESEfinder coincides with a sequence stretch predicted by HEXplorer to be crucial for the splicing-enhancing properties of this exon part. A mutation at this site (G→T, indicated in red in lower sequence) is predicted to strongly disrupt its splicing-enhancing properties. HEXplorer profile of the wild type 13A-3 sequence is depicted in blue. Profile of 13A-3 with the disruptive mutation (13A-3 mut) depicted in red and shifted to the right of the wild type profile. **C** Splicing reporter vector used to assess enhancing or inhibiting properties of exon 13A fragments, as described in Brillen et al., 2017 (2). The splicing-regulatory properties of an exon region are tested by inserting it in a central exon and assessing its inclusion or skipping by RT-PCR. **D-E** The parts of exon 13A delimited in (Figure 2.17) act as predicted by the HEXplorer algorithm, with 13A-3 acting primarily as an enhancer. The mutation of this exon part predicted to disrupt Srsf1 binding impedes the splicing enhancing ability of this sequence, leading to a significant reduction of exon inclusion, as quantified in E. Skipping and inclusion controls contain TIA-1 and SRSF7 binding sites, respectively, as described in Brillen et al., 2017 (2). N=3 for all conditions. P values derived from Brown-Forsythe and Welch ANOVA test with Dunnett's T3 post-hoc multiple comparisons test. Overall p value: <0.0001.

## 2.14 The splicing-enhancing effect of fragment 3 of the TrkC-T1-specific exon 13A depends on Srsf1

To test whether the splicing enhancer in fragment 3 of exon 13A is indeed dependent on the presence of Srsf1, we transfected the 13A-3 splicing reporter vector into N2A cells together with a control siRNA or an siRNA against Srsf1 (Figure 2.19 A). After 48 hours, we found that, indeed, the knockdown of Srsf1 caused a significant decrease in the splicing-enhancing effects of the 13A-3 sequence (Figure 2.19 B). Interestingly, the loss of splicing enhancing ability was not complete, as we did not see a stochastic distribution of the resulting splicing variants.

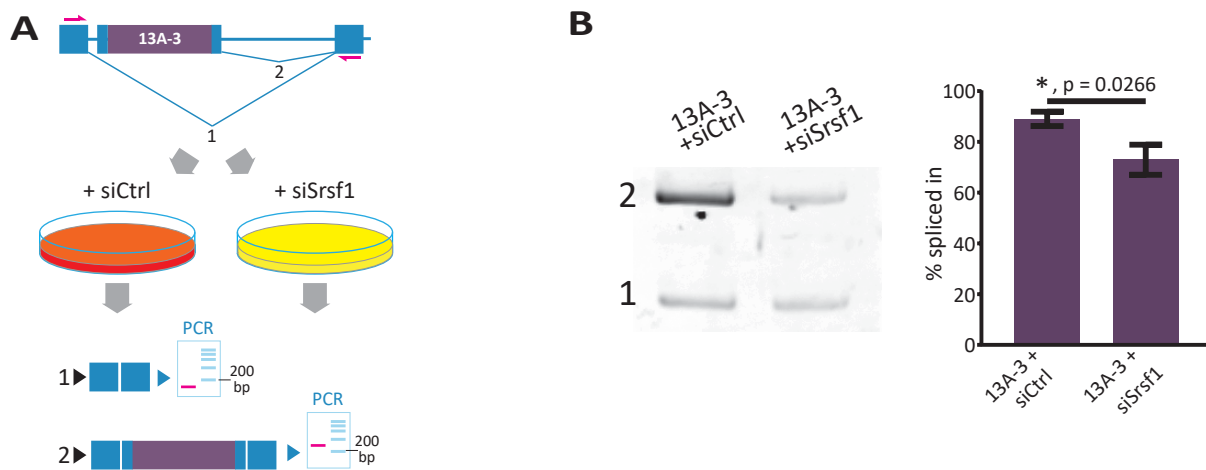


**Figure 2.19** The splicing enhancing properties of fragment 3 of exon 13A depend on Srsf1. **A** Experimental setup. The effects of the siSrsf1 knockdown were assessed using the RT=PCR described in Figure 2.18 C. **B** Knocking down Srsf1 leads to decreased inclusion of the 13A-3-containing exon, but not a complete loss of its splicing-enhancing properties. N=3 for both conditions. P values derived from unpaired, two-tailed Student's t test with Welch's correction.

## 2.15 The SR protein kinases Srpk1 and Srpk2 participate in the CFuPN fate choice, but not by involvement in TrkC alternative splicing

SR protein activity and intracellular localization is known to be regulated through the phosphorylation by SR protein kinases (Srpks) (Aubol et al., 2009; Ghosh and Adams, 2011; Gonçalves and Jordan, 2015; Czubyty and Piekieleko-Witkowska, 2017). Furthermore, Srpk1 and Srpk2 show distinct localization in the histological compartments of the developing cortex (GenePaint dataset MH1491; Visel et al., 2014). We therefore investigated whether these kinases influence fate acquisition in the developing cortex. To this end, we electroporated a combination of Srpk1 and Srpk2 overexpression constructs into the developing cortex at E 12.5, and assessed the fate of the progeny

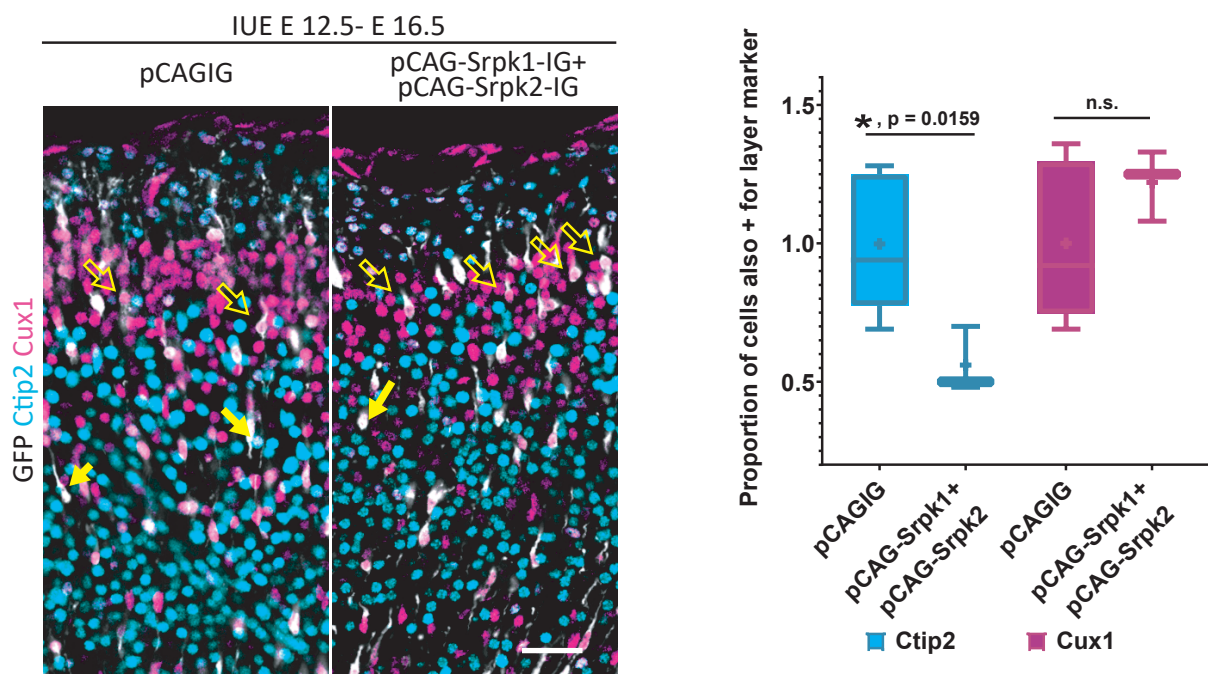


**Figure 2.19 Srpk1 and Srpk2 influence CFuPN fate.** Upregulating the levels of the protein kinases Srpk1 and Srpk2 in the E 12.5 cortex increases the numbers of Ctip2-positive cells, but not that of Cux-1 positive cells (superficial layer cells), compared to control constructs. Constructs were electroporated as shown and the quantification was performed as described in previous figures. N = 5 for pCAGIG, N = 3 for pCAG-Srpk1+pCAG-Srpk2. Mean  $\pm$  SD: Ctip2 =  $1 \pm 0.2480$  in control versus  $0.56 \pm 0.1217$  in pCAG-Srpk1+pCAG-Srpk2; Cux1 =  $1 \pm 0.285$  in control versus  $1.22 \pm 0.1277$  in pCAG-Srpk1+pCAG-Srpk2. P values derived from unpaired two-tailed Student's t test, with Welch's correction for Ctip2. Box plot whiskers: minima and maxima of the sample. Horizontal line: median. Plus sign: mean of the sample. Empty arrows: GFP+Cux1 double-positive cells. Full arrows: GFP+Ctip2 double-positive cells. Scale bar = 50  $\mu$ m.

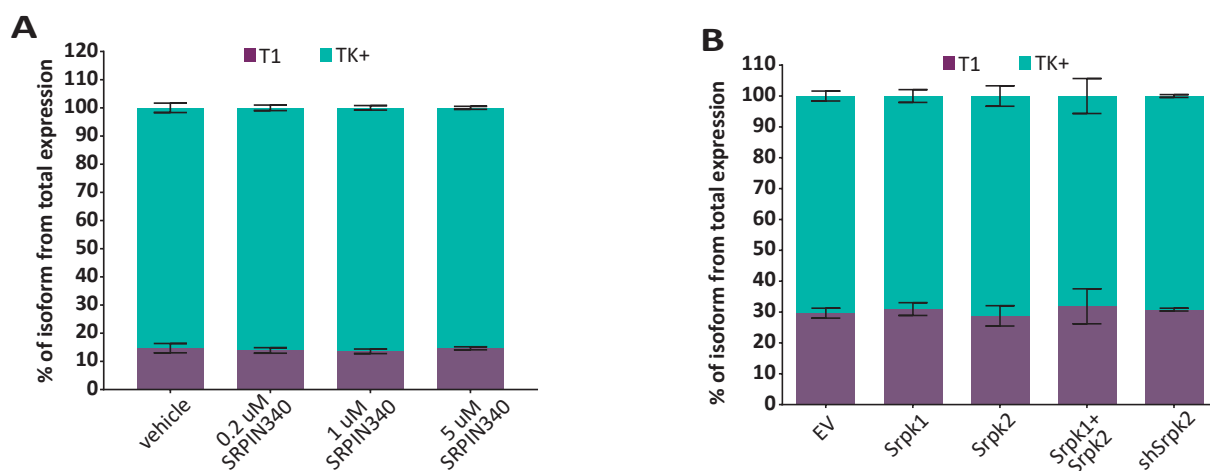


**Figure 2.20 Srpk1 and Srpk2 do not affect TrkC AS.** **A** Treatment of primary cortical cells with the Srpk inhibitor SRPIN340 (Fukuhara et al., 2006) for two days did not alter balance between the T1 and TK+ transcript variants. **B** Neither overexpression nor knockdown of Srpk1 and/or Srpk2 in N2A cells significantly altered the balance between the T1 and TK+ transcript variants. Vehicle - DMSO; EV - empty vector.

at E 16.5. We observed a significant decrease in the proportion of Ctip2-positive neurons, but no change in the proportion of superficial layer progeny (Cux1-positive cells). Next, we wanted to know whether this effect on CFuPN fate is mediated by an involvement of the kinases in TrkC AS. To address this question, we overexpressed or downregulated Srpk1 and Srpk2 in N2A cells or treated primary cortical cells with a selective Srpk 1/2 inhibitor, SRPIN340 (Fukuhara et al., 2006; Nowak et al., 2010; Gammons et al., 2013), and subsequently analyzed the TrkC AS event using qPCR (Figure 2.20). To our surprise, none of the alterations of Srpk levels or activity changed the TrkC-T1 to TrkC-TK+ balance in a significant manner, regardless of the cell type employed.

- this page intentionally left blank -

### 3. DISCUSSION

Generating a suitable balance between projection neuron subtypes in the cerebral cortex is important for the developmental assembly of both local and long-range neuronal circuits that support cognitive function (Molyneaux et al., 2007; Greig et al., 2013). Over the last three decades, we have amassed substantial knowledge about individual factors and transcriptional networks that govern neuron subtype fate decisions in the developing cortex. However, we have far less understanding of the molecular processes that set the stage for the proper deployment of these fate-determining factors, and especially little of the pre-mRNA-centric mechanisms that ensure the necessary dosage for such factors in the temporal and spatial dimensions of cortex development. In this work, we show through *in vivo* gain- and loss-of-function experiments that alternative splicing regulation plays a crucial role in establishing the cell type-specific dosage of TrkC-T1, a determinant of CFuPN fate. To our knowledge, this is the first known instance of alternative splicing permitting and supporting the genesis of this projection neuron subtype and controlling the ratio between CFuPN and CPN numbers.

#### 3.1. THE BALANCE OF TRKC ALTERNATIVE SPLICING ISOFORMS IS CELL-TYPE SPECIFIC IN NPCS AND NEURONS

The increased frequency of AS events in the brain in bulk has been posited to arise from the combination of the numerous neuronal and non-neuronal cell types it contains and their individual AS signatures (Nilsen and Graveley, 2010). Assisted by FACS sorting of unfixed primary cortical cells and TaqMan qPCR, we show that, at E 12.5, the aRGCs and neurons of the murine cerebral cortex exhibit different splicing variant ratios of the neurotrophin-3 receptor, TrkC (Figure 2.5). As also shown by qPCRs on cortical cDNAs from subsequent developmental days (Figure 2.2), the balance between TrkC-TK+, the catalytic, canonical receptor isoform, and TrkC-T1, the truncated, kinase-dead isoform, shifts in favor of TrkC-TK+ from the onset to the endpoint of neurogenic differentiation.

While we could previously not detect TrkC-TK+ in the VZ, the NPC-containing germinal zone of the cortex, by RNA *in situ* hybridization (Parthasarathy et al., 2021), the cell sorting experiment shows that this transcript variant is expressed in the VZ compartment as well. This suggests that the *in situ* hybridization procedure was ei-

ther not sufficiently sensitive or the duration of the chromogenic reaction it relies on was interrupted too soon to allow VZ detection of the transcript, likely due to the near-saturation signal observed for TrkC-TK+ in the cortical plate (Parthasarathy et al., 2021).

In an extension of our previous findings, this finely tuned but significantly different cell-type specific ratio of TrkC AS isoforms suggests that it is not just the level of TrkC-T1 in the NPCs that has functional consequences for the choice between producing CFuPN or CPN (Parthasarathy et al., 2021), but that there is also an interplay between the functions of the two receptors, as seen in other neuronal systems. It has been shown before that, in amyotrophic lateral sclerosis (ALS), motor neuron death is precipitated by an overrepresentation of TrkC-T1 in these neurons. The excess signals triggered or relayed by this receptor led to TNF $\alpha$ -mediated neurotoxicity, an effect that could be counteracted by the overactivation of signaling through the TK+ receptor isoform (Brahimi et al., 2016). Furthermore, Ichinose and Snider showed that the exact ratio of T1 to TK+ in dorsal root ganglia-derived neurons is crucial for regulating the number of primary axonal processes (Ichinose and Snider, 2000), with the two receptors having antagonistic effects. In the developing cortex, we showed in our previous work (Parthasarathy et al., 2021) that TrkC-T1 does not simply act as a dominant-negative isoform that binds the TrkC-TK+ receptor in the fate acquisition process in NPCs, but as a factor that restricts the availability of the scaffolding adapter molecule ShcA, which is essential for downstream MAPK/ERK1/2 pathway activation and fate choice between CFuPN and CPN. In this previous work, we did not identify the other NPC receptors with phospho-tyrosine domains affected by the changes in ShcA levels. Still, there is one striking connection between the preceding work and the results presented in this project that suggests the other main player is TrkC-TK+. In an earlier project (Parthasarathy et al., 2014), our research group found that NT-3 produced by the postmitotic neurons in the cortical plate acts as a negative feedback mediator to the NPCs, switching their neuronal subtype output from deep layer-fated progeny to superficial layer progeny. Furthermore, in Parthasarathy et al., 2021, we established that low-affinity NT-3-binding receptors such as the TrkB isoforms and the Trk-modulating receptor p75 do not participate in the CFuPN-CPN fate switch, and TrkA is not detectable in the E 11.5 - E 13.5 cortex (Allen Brain Atlas ISH database for the developing mouse brain, experiments 100046592 and 100046577), thus further supporting the hypothesis that TrkC-TK+ is the feedback signal receptor. For direct evidence, further work is required that explores the cell fate consequences of a mosaic deletion or knockdown of TrkC-TK+ from E 12.5.

One can envision an extended model of the interaction of TrkC-TK+ and TrkC-T1 signaling in cell fate switching from CFuPN to CPN (Figure 3.1). This interaction could involve TrkC-TK+ being prevented from relaying the fate-switching NT-3 feedback signal into the NPCs during the time frame in which TrkC-T1 is strongly represented in these progenitors (until E 13.5, Parthasarathy et al., 2021) and restricts the pool of available ShcA. As cortex development progresses, two straightforward mechanisms are possible for switching to the production of fates other than CFuPN. First, the balance of the two isoforms in the NPCs could gradually shift past a particular threshold of TrkC-TK+ quantity, which may topple fate-relevant intracellular signaling by activating a sufficient proportion of the ShcA protein not bound by TrkC-T1. The intracellular relaying of the fate switching signal through TK+ may thereby be de-repressed, leading to the previously described increase in the levels of activated Erk1/2 that favor superficial neuron production (Parthasarathy et al., 2021). Alternatively, or in combination with the above, the amount of NT-3 that neurons produce may cross a critical threshold for activating pathways downstream of TrkC-TK+, since the neuron pool itself increases with corticogenesis. Whether either of these alternatives truly reflects the *in vivo* situation could be tested in one instance by quantifying the TrkC protein isoforms in sorted NPCs from cortices at different developmental time points, using a highly sensitive technique such as selective reaction monitoring and mass spectrometry (Schreiner et al., 2015). However, for cortex development stages beyond E 13.5, the sorting strategy would need to be expanded to distinguish between the Prom-1-positive aRGCs and IPs, for which no characteristic extracellular epitopes have been identified so far. Another experiment could involve the positioning of an NT-3-saturated material in different amounts on acute cortical slices from E 12.5 embryos (see Trivino-Paredes et al., 2019 for a description of the technique) and disentangling the connection between TrkC-TK+ and MAPK/Erk1/2 signaling using luciferase-based reporters for the expression of phospho-Erk1/2-regulated genes in combination with overexpression or knockdown constructs for TrkC-TK+. The constructs could be constitutively expressed or electroporated in the NPCs prior to slice preparation.

An important caveat to consider in this model is that TrkC signaling in the NPCs may be further modulated through transactivation by G-protein coupled receptors and EGF receptors, as shown in other systems (Rajagopal et al., 2004; Puehringer et al., 2013). Second, these models assume that the quantity of ShcA in NPCs that is not bound by TrkC-T1 is sufficient for MAPK/Erk pathway activation through increased levels of NT-3 or TrkC-TK+. Further exploration is also needed to understand how

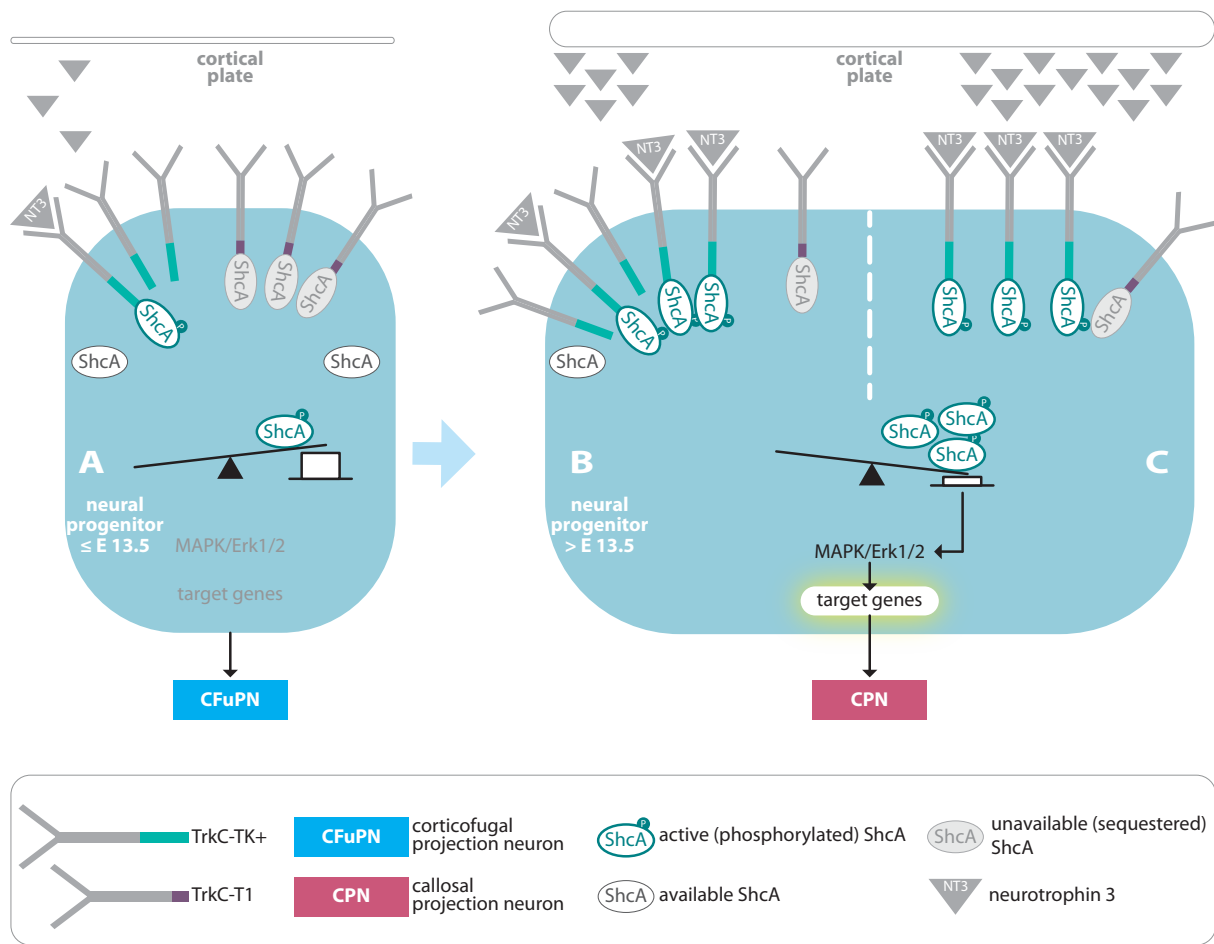


**Figure 3.1 Model for the involvement of the TrkC-T1 to TrkC-TK+ ratio in cortical neuron subtype fate acquisition.** **A** Early neural progenitor cells (NPCs) exhibit low MAPK/Erk1/2 pathway activity due to the sequestration of available ShcA molecules by the elevated numbers of TrkC-T1 receptors. This prevents ShcA phosphorylation by TrkC-TK+, which could otherwise relay extracellular feedback signals from the already produced neurons. In turn, the low levels of active ShcA are not sufficient to activate the MAPK/Erk1/2 pathway and thus trigger the expression of genes relevant to CPN fate acquisition. Therefore, only CFuPN are produced until around E 13.5. **B and C** After E 13.5, MAPK/Erk1/2 signalling may get triggered, leading to CPN production, in two possible scenarios. Either (**B**) the ratio of TrkC-TK+ to TrkC-T1 tips over in favor of TrkC-TK+ enough to use a much higher proportion of the available ShcA than in early NPCs, or (**C**) the concentration of neurotrophin-3 (NT-3) secreted by the neurons already settled in the cortical plate rises enough to activate most of the TrkC-TK+ receptors available in the NPC. Both scenarios lead to an accumulation of phosphorylated ShcA, which tips the scales of MAPK/Erk1/2 pathway activity so that target genes leading to CPN genesis are activated.

the relationships between the TrkC isoforms and the other members of the Shc family, ShcB and ShcC, shape the functional interplay between TrkC-TK+ and TrkC-T1 in neurons. While ShcA is reported to be exclusively expressed in the VZ during development (Conti et al., 1997), ShcB and ShcC were observed to accumulate in neurons upon cell cycle exit (Nakamura et al., 1998; McFarland et al., 2006). ShcC is recruited by TrkC-TK+ (Nakazawa et al., 2002) and could be the mediator of the antagonistic

effects of the TrkC isoforms on axonogenesis (Ichinose and Snider, 2000). In addition to this, ShcC is necessary for long-term potentiation, a key mechanism of learning and memory, and is reported to be neuroprotective, suggesting an involvement in survival signaling pathways along with the Trk receptors (Xie et al., 2007; Miyamoto et al., 2005; Sagi et al., 2015). Interestingly, pyramidal neurons exhibit subtype-specific responsiveness to neurotrophins, with the dendritogenesis of layer VI neurons most strongly affected by NT-3 (McAllister et al., 1995). Therefore, the ratio of TrkC-TK+ to T1 may even serve neuron subtype-specific functions, an avenue yet to be explored through quantifying the TrkC-TK+ to T1 ratio along with the determination of the subtype by staining for identity markers such as Ctip2, Tbr1, or Satb2.

A final aspect that remains to be elucidated is whether the TrkC-T1/TrkC-TK+ balance is uniform across NPCs. There is evidence that some NPCs are biased towards producing neuronal lineages restricted to specific subtypes (Franco et al., 2012), so it may be that the NPC pool is segregated between progenitors that exhibit a CFuPN-favoring T1/TK+ balance and others with a CPN-favoring balance. Here, single-cell proteomics (Kelly, 2020) may provide us with long-sought answers.

We focused our subsequent research efforts on identifying the splicing factors regulating the TrkC-TK+ to TrkC-T1 balance because the data did not support a contribution of different transcript stabilities or miRNA-induced transcript decay to the T1/TK+ ratio in NPCs. Outside of the embryonic NPC context, a SNP in the TrkC-T1 3' UTR is thought to modulate susceptibility to anxiety disorders and major depression (Muiños-Gimeno et al., 2009, de Miranda et al., 2020). This SNP affects a binding site for miR-128, the strictly postmitotic neuronal miRNA that TargetScan predicted, and for miR-509. The TargetScan algorithm did not predict a binding site for miR-509 in the TrkC-T1 UTR, but, since the TargetScan prediction scores are based on cross-species conservation of the miRNA binding sites, regulation through miR-509 may be a novel, possibly human-specific, manner of fine-tuning TrkC receptor levels in the adult brain. Aside from this, the only instance of posttranslational quantity control that is known for TrkC is the cleavage of the receptors upon NT-3 binding (Mateos et al., 2003). However, our previous work showed that the fate-determining effect of TrkC-T1 is independent of this, as a mutant with a deletion of the NT-3-binding domains in the extracellular domain (ECD) steered fate acquisition just as the wild-type receptor did (Parthasarathy et al., 2021). Furthermore, the behavior of the TrkC transcript variant ratio across developmental time, as assessed by qPCR, correlates well with what we had previously observed on the protein level (Parthasarathy et al.,

2021), suggesting that, for TrkC isoforms, the protein quantity is strongly dependent on the transcript quantity and less so on other types of differential posttranslational regulation.

### 3.2. SRSF1 AND ELAVL1 CO-REGULATE THE BALANCE OF TRKC ALTERNATIVE SPLICING

Previous large-scale RNA sequencing projects and bioinformatic analyses showed that alternative last exons are an especially finely regulated class of AS events in developing neural cells, that their splicing often leads to the co-expression of two main protein isoforms with distinct C-termini, and that AS frequently affects protein domains subjected to signaling-relevant phosphorylation (Merkin et al., 2012; Yap et al., 2016). Fittingly, the two TrkC receptor isoforms studied here consist of a shared ECD with two immunoglobulin-like domains for neurotrophin binding, a shared single transmembrane domain, but two different intracellular domains (ICDs), with (TK+) or without (T1) kinase functionality. The ICDs arise from the mutually exclusive utilization of exons 13A-14A or 13-17 during alternative pre-mRNA splicing, which we show to be regulated by the splicing factors Srsf1 and Elavl1 *in vitro* and in primary neurons from developing cortices.

Human and rodent TrkC receptors show the highest degree of homology among the Trk receptors (Shelton et al., 1995). While the ECDs are less conserved and not necessary for the effects on fate acquisition (Parthasarathy et al., 2021), the truncated ICD of TrkC-T1 is highly conserved, with 81 of the 83 amino acids identical between rat, mouse, pig, and human (Shelton et al., 1995). Together with the prominent role of TrkC isoforms in carcinogenesis (reviewed in Amatu et al., 2019) and the involvement of their cellular balance in nervous system genesis and function (Brahimi et al., 2016; Ichinose and Snider, 2000), this high degree of conservation emphasizes that TrkC alternative splicing plays crucial roles in tissue development and homeostasis and underscores the need to uncover the regulatory mechanisms for this splicing event.

Here, we present evidence that the splicing factors Srsf1 and Elavl1 control the formation of TrkC-TK+ and TrkC-T1 (Figure 2.7). While AS cis-regulatory element signatures diverged strongly during recent evolution (Merkin et al., 2012; Barbosa-Morais et al., 2012), most AS-regulating RBPs are thought to have conserved co-expression patterns in different tissues and to form robust, tissue-specific co-regulatory

networks (Mazin, 2018; Furlanis 2018; Weyn-Vanhetenryck, 2018). In spite of this, there are no previous reports presenting direct evidence of Srsf1 and Elavl1 co-regulating a mammalian alternative splicing event. The only previously reported circumstantial evidence is the upregulation of both splicing factors in human papillomavirus 16-positive cell clones, which correlates with an increase in the late mRNA AS variant L1 from the viral genome (Dhanjal et al., 2015).

Srsf1 is a potent proto-oncogene, described first as a splicing factor involved in both constitutive and alternative splicing, but also implicated in a recently emerging array of other mechanisms controlling mRNAs, such as transcription, nonsense-mediated decay, subcellular localization, and translation (Zuo & Manley, 94; Zhang and Krainer, 2004; Sato et al., 2008; Huang et al., 2003; Sanford et al., 2009; and see Das and Krainer, 2014 for an extensive review on Srsf1 functions). It is the founding member of the SR protein family, and CLIP-Seq studies have shown that it preferentially binds exons (Sanford et al., 2009; Pandit et al., 2013), thereby promoting exon definition and the recruitment of spliceosomal components for constitutive splicing. In alternative splicing, Srsf1 binding in the ESEs in cassette exons promotes their inclusion (Pandit et al., 2013; Black, 2003).

The most frequently described counterplayers of Srsf1 are proteins from the heterogeneous nuclear ribonucleoprotein (hnRNP) family, such as PTBP (Mayeda & Krainer, 1992), which oftentimes promote cassette exon skipping (Erkelenz et al., 2013b; Dreyfuss et al., 1993; Fu and Ares, 2014). The exact combinatorial effect of Srsf1 and hnRNPs on AS is not always easily predicted, though, because hnRNP-based regulation also depends on the position of the bound SRE relative to the regulated exons. For instance, the binding of the hnRNP Nova induces exon inclusion when bound in the intron downstream of the regulated exon and vice versa when bound upstream (Taliaferro et al., 2016; Fu and Ares, 2014; Licatalosi et al., 2008). It was therefore surprising that, in the case of TrkC AS, the counterplayer to the Srsf1-promoted inclusion of exons 13A and 14A was Elavl1, in spite of our siRNA-based screening covering hnRNPs known to be developmentally regulated in the cortex (Figures 2.6 and 2.7). Elavl1, also known as HuR, has been shown to act as an AS regulator in a few instances, but is most prominently linked to mRNA stability and translational regulation, as it binds to AU-rich elements in the 3' UTR of mRNAs and thereby stabilizes them (Fan et al., 1997; Fan and Steitz, 1998; Meisner & Filipowicz, 2011; Lebedeva et al., 2011; Mukherjee et al., 2011; Ince-Dunn et al., 2012).

Upon bioinformatic analysis of the splice site strength at the exon/intron junctions relevant for TrkC-T1 formation, we found that there is a high probability for the formation of the TrkC-T1 transcript variant through AS, as opposed to TrkC-T1. This finding prompted our investigation into the potential for splicing regulation of different sequence subsets of exon 13A using the HEXplorer algorithm and ESEfinder (Erkelenz et al., 2015; Cartegni et al., 2003), which revealed a potential GA-rich ESE in the 3' third of the exon. In subsequent reporter experiments, we found that this splicing-regulatory element favors the choice of the downstream splice site over the upstream one (Figure 2.16), thus likely contributing to exon 13A inclusion. We then showed this effect to be dependent on Srsf1 using siRNA-mediated knockdown of this factor (Figure 2.19). Srsf1 is known to promote the inclusion of exons when bound to ESEs contained therein (Pandit et al., 2013), and Srsf1 binding motifs are generally strongly represented towards the 3' ends of exons (Wang et al., 2005), patterns that our findings also follow. The consensus binding sequence for Srsf1 binding has been reported to be GGAGA (Liu et al., 1998; Wang et al., 2005; Tacke & Manley, 1995; Das and Krainer, 2014), with the sequential guanosines being particularly important for the recognition of the binding site through the RRM2 motif of Srsf1 (Cléry et al., 2013). In the case of the Srsf1-dependent ESE in exon 13A, the involved sequence is GAGGA, also GA-rich and containing two sequential guanosines. Surprisingly, however, the nucleotide that was predicted and shown to alter the strength of the enhancer was not within the G pair but the very first guanosine. This may, on the one hand, reflect the complexity of the relationship between sequence composition and SF binding strength (Begg et al., 2020; Jankowsky and Harris, 2015), but may also indicate that this SRE is not solely or directly bound by Srsf1.

The loss of the enhancing ability of the Srsf1-dependent ESE in the absence of Srsf1 is not complete (Figure 2.19). This also suggests that the enhancing effect may not entirely be dependent on Srsf1, but on other SFs as well. A broader search for SR protein binding sites using ESEfinder shows that the GA-rich motif is likely to also be bound by Srsf2, a closely related SR protein with oftentimes overlapping binding sites and functions (Cartegni et al., 2003; Long & Cáceres, 2009). Even if we could not detect a significant impact of Srsf2 by itself on TrkC AS (Figure 2.7), whether only Srsf1, Srsf1 and Srsf2, or combinations of other SFs bind this splicing-regulatory element and influence the splicing outcome must be further explored. This could be achieved by crosslinking RNA probes containing this motif to proteins from nuclear extracts with subsequent identification of the binding partners via mass spectrometry.

Taken together, we believe we have uncovered the first instance of bipartite, antagonistic alternative splicing regulation through *Srsf1* and *Elavl1*, which targets *TrkC* AS. While we found no evidence supporting the regulation of the *TrkC*-T1/TK+ balance downstream of AS, at the level of transcript stability, it has to be said that we can, at this time, not entirely exclude some contribution from AS-regulatory mechanisms other than *Srsf1* and *Elavl1*. Kinetic parameters of RNA polymerase II, such as its elongation speed, are closely linked to splice site selection. An artificially induced slowing of the pre-mRNA elongation alters the coupling between transcription and AS and has been found to perturb neural differentiation (Maslon et al., 2019; Naftelberg et al., 2015). RNA polymerase speed depends, among other factors, on the chromatin state of the CDS, and nucleosome occupancy at exonic sequences is thought to act as a “speed bump” that slows down transcription and favors exon inclusion. Further studies are necessary to understand whether chromatin structure at the alternative exons in the *TrkC* pre-mRNA changes in different cell types or over developmental time, which could be achieved by performing ATAC-Seq (reviewed in Shashikant & Ettenson, 2019).

### 3.3. SRSF1 AND ELAVL1 LEVELS DEFINE CELL-TYPE SPECIFIC SPLICING-REGULATORY ENVIRONMENTS IN THE DEVELOPING CORTEX

In comparison to other mammalian tissues, the increased frequency of AS events in the brain has been ascribed to a particularly high number of expressed genes, among which RBPs, regulators of RNA homeostasis, are strongly represented. This environment is ideally suited to give rise to complex networks of SFs that co-regulate AS and fine-tune transcript and protein diversity (de la Grange et al., 2010; Grosso et al., 2008). The developing brain is not exempt from this, as work from Weyn-Vanheterenryck and colleagues showed the combinatorial involvement of SFs in two neurodevelopmental switches between AS profiles. The described large-scale switches occurred at E 14.5 and P4 to P7 and involved the *Ptbp*, *Nova*, *Rbfox*, and *Mbnl* RBP families (Weyn-Vanheterenryck et al., 2018). In this project, we show that fate-controlling splicing changes occur even earlier in cortex development and are a result of the cell type-specific combinatorial control through *Srsf1* and *Elavl1*. By RNA in situ hybridization at different cortex development stages and qPCR on primary aRG and neurons, we found that the expression of *Srsf1* is in stark contrast between the VZ and the CP, and between aRG and neurons, respectively, whereas that of *Elavl1* is highly similar

between the two cell types (Figure 2.13 and 2.15). As the TrkC locus is active in both cell types (Figure 2.5 and Parthasarathy et al., 2021) and we have shown the direct regulation of TrkC AS by Srsf1 and Elavl1, we believe that the differing abundances of these SFs generate the splicing-regulatory environments that dictate TrkC isoform balance.

Previous findings on the roles of Srsf1 in CNS development are scarce. Due to the pleiotropic nature of Srsf1, its constitutive, ubiquitous deletion in mice is embryonically lethal. The lethality was primarily ascribed to cardiomyopathy caused by mis-splicing of the Ca<sup>2+</sup>/calmodulin kinase delta (Xu et al., 2005). In the adult nervous system, Srsf1 has, so far, been shown to regulate synapse function via ApoER2 splicing and, together with the splicing regulator Quaking/QKI, to act as the effector of a generalized splicing switch that is triggered by neuronal activation (Hinrich et al., 2016; Barry et al., 2014). An indirect indication of an involvement of Srsf1 in brain development was made in the study of Lee and colleagues, who knocked Srsf1 down in zebrafish using morpholino oligonucleotides (Lee et al., 2016). In the wild-type animals, the authors saw strong expression of Srsf1 in the retina and CNS, but in the Srsf1 knockdown animals, the described effects centered on cardiovascular and skeletal system malformations. However, the authors also noted that the animals exhibit microcephaly, but concluded that this is due to cartilage malformation by neural crest cell involvement and did not investigate the CNS and its development. We know, though, that other genes, such as Satb2, affect the development of both the cranium and the cortex (Zarate et al., 2018; Dobрева et al., 2006) due to the shared developmental origins of the CNS and the neural crest cells. Still, thus far, there have been no reports of Srsf1 partaking in neurogenic processes, and there was no known association of this splicing factor with TrkC.

In the adult mammalian brain, the Elavl family of RBPs is reported to participate in alternative splicing that regulates the glutamate synthesis pathway in excitatory neurons (Ince-Dunn et al., 2012). This RBP family has recently been shown to participate in neurogenic AS switches in the fruit fly CNS development, but the cellular and histological consequences of these switches were not explored (Lee et al., 2021). In murine cortex development, the 2014 publication from Kraushar and colleagues showed that Elavl1/HuR controls the stage-specific regulation of mRNA translation. Elavl1 was shown to alter the phosphorylation states of core ribosomal components via association with the eIF2-alpha kinase 4, which impacts the association of transcripts with ribosomal components and the formation of polysomes (see next section for a

more detailed discussion of the phenotype). The group also found that the Elavl1 protein is expressed in progenitors and the CP at E 13.5, a distribution we could confirm on the RNA level by RNA in situ hybridization and by immunofluorescence.

NPCs express Srsf1 more strongly than neurons, while Elavl1 transcript and protein levels are similar between the two cell types. The Srsf1 expression profile we uncovered matches that shown in the 2015 cortex scSeq dataset of Telley and colleagues, but that of Elavl1 does not (Telley et al., 2019). Elavl1 is also shown to be primarily expressed in NPCs in this dataset (see Supplementary Figure 4). However, we know from both our work and that of Kraushar and colleagues (Kraushar et al., 2014) that the Elavl1 protein is represented in neurons. The discrepancy between these findings and the scSeq data may be due to the overall weaker expression of Elavl1, at least as compared to that of Srsf1. The Elavl1 transcript signal did not reach the same degree of chromatic saturation as that of Srsf1 in the VZ even after several cycles of replenishing the chromogenic substrate. In contrast, the Srsf1 signal was readily visible in under an hour of color development time and with only one substrate application. The scSeq study result may therefore be biased in the case of Elavl1 due to sequencing depth that is not sufficient to reliably quantify the levels of this transcript.

While we clearly see the impact of the different splicing environments defined by Srsf1 and Elavl1 on TrkC AS, these findings invite further exploration of whether the activity of Srsf1 and Elavl1 is more finely regulated for other AS events in NPCs and neurons. It is, for instance, well-known that the activity and nuclear localization of Srsf1 are affected by its phosphorylation status (Xiao and Manley, 98; Yeakley et al., 1999). We could not specifically detect endogenous Srsf1 protein in the cortex, as knockdown experiments in cell culture showed that all the tested commercially available antibodies bound unspecifically, which may be due to sequence and structural homology with other SR proteins. We know that the SR protein kinase Srpk1 is expressed in the VZ at E 14.5 (GenePaint dataset MH1491; Visel et al., 2014), and, while we could observe an effect of Srpk1 and Srpk2 overexpression on the CFuPN/CPN fate choice (Figure 2.19), this is likely not achieved via TrkC AS, as changes in Srpk levels or activity had no significant effect on the T1/TK+ balance (Figure 2.20).

The nuclear sequestration of Elavl1, necessary for a function in AS, is also affected by its phosphorylation (Kim et al., 2008) but the micrographs detecting endogenous Elavl1 show a highly similar cytoplasm-to-nucleus distribution in both VZ and CP at E 13.5 in our work and previous work (Figure 2.14, Kraushar et al., 2014). We there-

fore deem it unlikely that Elavl1 splicing activity is differentially regulated in NPCs and neurons by its localization.

Interestingly, we observed that, even when TrkC-T1 is knocked down, the effects of Srsf1 on CFuPN and CPN fate are partially maintained. This result suggests that Srsf1 may also affect fate-controlling transcripts other than those from the TrkC locus. To investigate what other splicing events might be affected by Srsf1, one could generate a mouse line with a knock-in of shRNA-expressing sequences targeting Srsf1, preceded by a loxP-termination codon-loxP cassette (Yu and McMahon, 2006). Thereby, Srsf1 knockdown could be conditionally achieved in the cortex upon breeding with a strain expressing Cre from an Emx1-driven locus, as this transcription factor is specific to cortical NPCs (Gorski et al., 2002). One could then perform RNA-Seq on NPCs sorted from the knockdown and wild-type animals to better understand the broader AS context affected by Srsf1.

An interesting idea to consider is whether the Srsf1/Elavl1 balance may affect aRG and IPs differently, seeing how these two types of progenitors have different degrees of fate plasticity (Oberst et al., 2019), or whether this is true for NPC subpopulations that express fate choice-relevant transcripts such as Cux2, Otx1 or Fezf2 (Nieto et al., 2004; Zimmer et al., 2004; Guo et al., 2013; Gao et al., 2014). Since it is not possible to unequivocally distinguish between aRGs and IPs in a chromogenic in situ hybridization that already detects Srsf1 or Elavl1 transcripts, further research could involve assessing the co-expression of Srsf1 and Elavl1 with Pax6 or Tbr1, or with the aforementioned identity-related transcripts, for instance, via RNA FISH methods.

In summary, our findings from the in situ hybridization and the qPCR on sorted NPCs and neurons show that the balance between Srsf1 and Elavl1 is likely very different in NPCs and neurons. Together with the antagonistic effects of these factors on TrkC AS, which we showed on mRNA and protein level (Figures 2.7 and 2.10), we conclude that Srsf1 and Elavl1 shape cell-type-specific splicing regulatory environments. This result is in line with previous findings that showed differential splicing between these cell types is essential for proper neurogenic differentiation (Zhang et al., 2016; Begg et al., 2020; Makeyev et al., 2007; Boutz et al., 2007; Su et al., 2018).

### 3.4. SRSF1 AND ELAVL1 REGULATE PROJECTION NEURON IDENTITY ACQUISITION BY CONTROLLING TRKC ALTERNATIVE SPLICING

There are few previous pieces of evidence documenting the involvement of transcript variant ratios or splicing factor-regulated AS events in cell subtype fate decisions, and even fewer regarding neuron subtype decisions. Pfurr and colleagues (Pfurr et al., 2017) showed that two splicing variants of the basic helix-loop-helix TF E2A control the production of Tbr1- and Satb2-positive neurons, but this is not a fate switch, as one of the isoforms leads to an increase in the numbers of both neuron subtypes. The only known case of a splicing factor being involved in a neuron subtype decision in corticogenesis is that of SRRM4. SRRM4 was shown to impact the numbers of, again, Tbr1- and Satb2-positive neurons (Quesnel-Vallières, 2015). However, this was not a definitive regulation of the overarching CFuPN fate. Tbr1-positive (CThPNs) and Satb2-positive (CPNs) neurons only show minor overlap in their generation time frames and minimal shared layer occupancy (Greig et al., 2013), so the ultimate impact magnitude of this fate control mechanism is unknown. Furthermore, the alternatively spliced transcripts mediating this function of SRRM4 were not described (Quesnel-Vallières, 2015). In our work presented in this dissertation, we show, for the first time, that the splicing factors Srsf1 and Elavl1 drive significant changes in the fate acquisition process for CFuPN and CPN in the developing cortex, an effect mediated by their antagonistic effects of TrkC alternative splicing and the resulting balance between the receptor isoforms TrkC-T1 and TrkC-TK+ (Figures 2.7 and 2.10).

To our knowledge, Srsf1 had never been brought in connection with neuronal fate decisions before. Interestingly, in hepatocellular carcinoma, Srsf1 has been found to promote Erk activation without changing its protein levels (Zhao et al., 2015). We previously showed that the activation of Erk by phosphorylation in cortical NPCs triggers the acquisition of superficial layer fate in the resulting progeny. In the work presented here, we show that Srsf1 promotes the generation of TrkC-T1, which induces a preference for deep layer neuron formation. These results can be brought into agreement under two considerations. First, we could confirm *in vivo* that the CFuPN-inducing effect of Srsf1 is mediated by TrkC-T1 by knocking down TrkC-T1 concomitant to Srsf1 overexpression (Figure 2.11), which diminished the increase in Ctip2-positive neurons observed with solely the Srsf1 upregulation. Second, we see that the strong expression of Srsf1 in the cortical VZ is maintained outside of the time frame in which TrkC-T1 exerts its CFuPN-promoting effects, so after E 14.5. This expression pattern might mean that the presence of Srsf1 in NPCs has a dual function in fate acquisition, depending on the developmental stage, acting as a general consolidator of

the neuron subtype fate that must be produced at that particular stage (Figure 3.2). In early NPCs, Srsf1 may promote the formation of TrkC-T1 through AS, which antagonizes the activation of Erk via Srsf1 and ensures proper deep layer neuron generation. Later in development, once TrkC expression in NPCs ceases or decreases, Srsf1 may promote superficial layer genesis by heightening MAPK/ERK pathway activity. However, we see that Srsf1 overexpression at E 12.5 with concomitant downregulation of TrkC-T1 does not automatically lead to an overproduction of CPN. Combined, the evidence suggests that Srsf1 might act as a background enforcer of distinct fates in NPCs whose ultimate effect may depend on factors such as TrkC but likely also further fate determinants. Whether this is truly the case remains to be elucidated through further genetic studies.

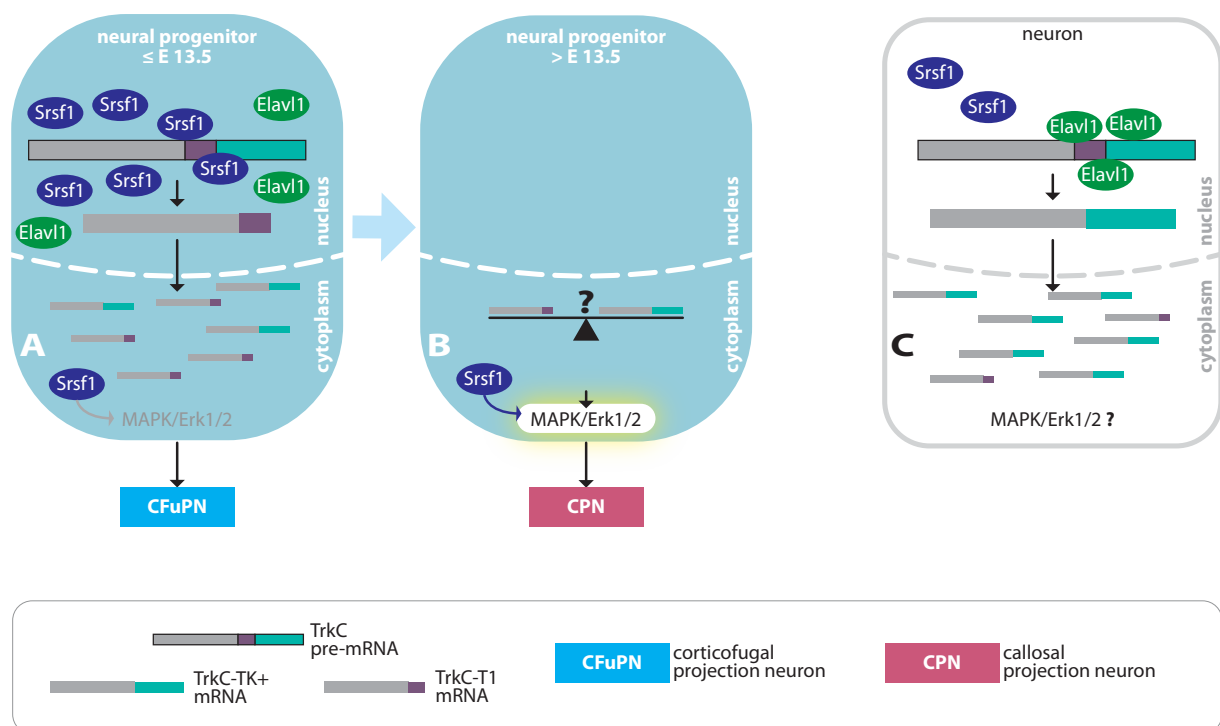


**Figure 3.2 Model for the cell type-specific effect of Elavl1 and Srsf1 on TrkC alternative splicing.** **A** Early neural progenitor cells (NPCs, 13.5 or younger) express the TrkC gene and higher quantities of Srsf1 compared to neurons (C), thus shifting the splicing environment towards one that favors the production of TrkC-T1 and hence CFuPN. Srsf1 can activate MAPK/Erk1/2 signaling, but this may not be sufficient to override the CFuPN fate determination by TrkC-T1. **B** As the NPCs mature, the TrkC locus becomes in general less active or other factors lead to an unknown balance between TrkC-T1 and TrkC-TK+ (question mark), which permits MAPK/Erk1/2 activation by Srsf1 and possibly receptor tyrosine kinases such as TrkC-TK+ or others. Consequently, NPCs switch to the production of CPN. **C** In postmitotic neurons, the lower levels of Srsf1 allow Elavl1 to exert its splicing-regulatory effects on the TrkC pre-mRNAs, leading to a higher proportion of TrkC-TK+ transcripts, which are needed to produce the neurotrophin-3 receptor. MAPK/Erk1/2 activity levels and their roles in neurons are not yet known.

Kraushar and colleagues found that *Elavl1* controls translational changes in the developing cortex. Among the transcripts associated with specific projection neuron subtypes, the distribution of *Bcl11b* (*Ctip2*) mRNA in the unbound versus 40S-60S and polysomal fractions was shifted towards the latter, suggesting that a lack of *Elavl1* leads to more *Ctip2* being bound by ribosomes and possibly translated, and, by corollary, that *Elavl1* could normally contribute to lowering *Ctip2* protein levels. In contrast, *Satb2* mRNAs were not found to significantly shift from one fraction to another. Even though the authors suggest that *Elavl1* may be involved in fate decisions, they do not rigorously quantify this and solely analyze the distribution of neurons positive for *Ctip2* and *Satb2* across the radial (inside-out) axis of the cortex, where they find *Ctip2* neurons to be mispositioned, but not *Satb2* ones. Intriguingly, though, the authors report that the *Foxg1*-driven *Elavl1* cKO brains lack a *corpus callosum*, a fiber tract for the formation of which *Satb2* is unequivocally necessary (Britanova et al., 2008; Alcamo et al., 2008). The brains of *Satb2*-null mice show a misrouting of the axons that would normally cross the midline into the contralateral hemisphere via the *corpus callosum*, projecting instead through the anterior commissure. The later *Elavl1* cKO brains (*Emx1*-driven) possess a *corpus callosum*, but the authors neither assess its thickness nor study the ratio of axonal projections in the *corpus callosum* versus the anterior commissure.

Our results show both directly and indirectly that *Elavl1* participates in the CFuPN/CPN fate decision. The knockdown of *Elavl1* leads to a decrease of TrkC-TK+ with a concomitant increase in TrkC-T1, a change we previously found to cause a surge in *Ctip2*-positive neuron numbers at the expense of *Satb2*-positive ones (Parthasarathy et al., 2021). The *in vivo* overexpression and knockdown of *Elavl1* support this connection, with *Elavl1* overexpression leading to a decrease in *Ctip2*-positive neurons and an increase in *Satb2*-positive ones and vice versa in the knockdown. It is, therefore, interesting to consider whether *Elavl1* may have a dual role in establishing the CFuPN fate, both via the AS of TrkC in NPCs and after cell cycle exit in deep layer neurons. We do not know yet whether the CFuPN/CPN-producing identity of the NPC has an immutable effect on the identity of the progeny. For instance, newborn deeper layer neurons have been reported to briefly co-express *Ctip2* and *Satb2* at E 13.5 and then resolve into separate CFuPN and CPN populations (Srinivasan et al., 2012; Greig et al., 2013). This may occur because of the quantities of *Ctip2* and *Satb2* relative to one another, which may be already set via factors inherited from the NPC lineage or could still be plastic in the neuron. Here, we present evidence that *Elavl1* can influence the final number of *Ctip2*-positive neurons that are produced via TrkC

AS in the NPC. It remains to be explored through the postmitotic, Dcx-promoter-driven overexpression and knockdown of Elavl1 whether this RBP continues to consolidate CFuPN fate at the expense of CPN after cell cycle exit or whether its effect on Ctip2 in the neurons is strictly in ensuring proper terminal differentiation.

In conclusion, we show direct *in vivo* evidence that Elavl1 and Srsf1 contribute to the fate switch between CFuPN and CPN in the developing cortex, acting at the level of TrkC AS. What was unexpected was that the sole overexpression and downregulation of Srsf1 were sufficient to achieve these effects, as observed in the siRNA experiments. Hence, the phosphorylation of Srsf1 by the Srpk family or Clk does not seem to be limiting for the fate choice process, which also matches our observation that the Srpks had no effect on the TrkC-T1/TK+ balance.

One challenge with studying the roles of RBPs and, by extension, splicing factors is that they often have pleiotropic involvement at different stages of a process (DeBoer et al., 2013). As discussed previously, cortex development is rife with examples of the same splicing factors acting at different levels (Hamada et al., 2015; Kim et al., 2013; Begg et al., 2020; Makeyev et al., 2007; Boutz et al., 2007; Su et al., 2018). Seeing as the cell type-specific distribution of Srsf1 and Elavl1 is maintained outside of the time window in which CFuPN and CPN fate acquisition overlap, their balance may participate in other NPC- or neuron-specific splicing events that are independent of TrkC AS but of import to later developmental processes. Since we observe that the expression pattern of these factors is maintained up to E 16.5, they may participate in the fate shift from neurogenesis to gliogenesis. This could be tested by IUE of overexpression and knockdown constructs for Srsf1 or Elavl1 at later stages of corticogenesis. Furthermore, Srsf1 and Elavl1 are not just involved in AS regulation. Performing a brief GO term analysis in the BioGRID database (Oughtred et al., 2020; Stark et al., 2006) for known interaction partners of Srsf1 and Elavl1, one can find that both factors also control gene expression. For Srsf1, this is supported by studies such as that of Lee and colleagues in zebrafish (Lee et al., 2016) or by its effect on the transcription of the HIV-1 genome (Paz et al., 2014), and, for Elavl1, by its involvement in the transcription of the gonadotropin receptor (Terasaka et al., 2019). Therefore, the global implications of the Srsf1-Elavl1 regulatory tandem may extend well beyond alternative splicing regulation and call for interactomic studies that cover gene expression, alternative splicing, and protein composition.

## 4. MATERIALS AND METHODS

### 4.1. CELL CULTURE AND TREATMENT

N2A and HEK293T cells were, unless otherwise specified, cultured in uncoated plastic dishes at 37°C and 5% CO<sub>2</sub> in a medium consisting of DMEM (4.5 g glucose/L, supplied with GlutaMAX L-glutamine, Gibco, 10566) supplemented with 10% fetal bovine serum (Biochrom) and penicillin-streptomycin (1:100 from a stock of 10.000 U/mL, Gibco, 15140122). At around 80% coverage from confluency, cells were split using a 0.25% trypsin solution (1:10 dilution of 2.5% stock, Gibco, 15090046) in phosphate-buffered saline (PBS).

For EGF stimulation, we used recombinant murine EGF purchased from ImmunoTools (200 µg/mL, 12343406). Briefly, cells to be stimulated were plated in 12-well dishes,  $3 \times 10^5$  cells per well. The following day, the medium was exchanged the day before stimulation to 1 mL fresh medium. On the day of the stimulation, 150 µL of the medium from each well was transferred to sterile 1.5 mL Eppendorf tubes, supplied with 0.5 uL EGF, and rapidly re-applied to the cells. Cells were kept in the EGF-enriched medium for a total of 60 minutes, then harvested by resuspension in PBS.

For the actinomycin D time course treatment for inhibiting transcription, cells were seeded in the wells of individual well plates, one plate per time point tested. Actinomycin D was applied for the indicated length of time (final concentration: 20 µg/mL from 5 mg/mL stock, Sigma-Aldrich, A9415). Treated cells were washed once with PBS and the pellets were snap-frozen in liquid nitrogen.

SR protein kinase inhibition was performed using the selective Srpk inhibitor SRPIN340 purchased from Cayman Chemicals (16284, enzyme kinetic properties described in Fukuhara et al., 2006), dissolved in sterile ethanol at a final concentration of 20 µM, for 24 hours. Sterile ethanol was used for the mock/vehicle samples.

Primary cortical neurons were cultured in dishes priorly coated overnight at room temperature with poly-L-lysine (final concentration 10 µg/mL, from 0.1 mg/mL stock, Sigma-Aldrich, A-005-M) and laminin (final concentration 0.2 µg/mL, from Engelbreth-Holm-Swarm murine sarcoma basement membrane, L2020, Sigma-Aldrich) in sterile PBS. On the day of neuron preparation, the PLL/laminin solution was re-

moved, the wells washed twice with sterile PBS and dried, after which half of the final volume of neuron culture medium was added per well. For the neuron preparation, pregnant dams were sacrificed at the indicated pregnancy day. The uterine horns were excised and transferred to PBS on ice, after which embryos were swiftly decapitated and the heads transferred to HBSS++ (no phenol red, Gibco, 14025092). Cephalic skin, muscle and skull were removed to expose the brain, after which the cortical hemispheres were cut parallel to the anteroposterior midline at two positions, once centrally to remove the hippocampal anlage and once laterally to detach them from the ganglionic eminences. Olfactory bulbs and the meninges were removed, and the cortical tissue pieces were transferred to an ice-chilled tube with HBSS-- (no phenol red, Gibco, 14175095). After collecting the cortices from a whole litter of embryos, the HBSS-- was discarded and the tissue pieces washed twice with fresh HBSS--. Tissue dissociation was performed by adding a trypsin solution (final concentration of 0.3125% in HBSS--, made from 500  $\mu$ L 2.5% trypsin stock, Gibco, 15090046, plus 3.5 mL HBSS--) pre-warmed to 37°C to the tissue and incubating the tubes at 37°C for 15 to 30 minutes, mixing occasionally and checking the dissociation progress. To stop the digestion, 10 mL of DMEM with 10% FBS was added and tubes were gently flicked to homogenize. The tubes were then centrifuged at 170 rcf and 4°C for 5 minutes. The supernatant was removed and a DNase I solution in DMEM culture medium (final concentration of 0.05 mg/mL, made from 500  $\mu$ L DNase I stock at 0.5 mg/mL, Roche, 10104159001, plus 4.5 mL DMEM with 10% FBS) was added to the trypsin solution/tissue mixture and the tubes gently flicked to homogenize the solution. DNase I digestion was performed for 2 minutes at room temperature. The tubes were then centrifuged at 170 rcf and 4°C for 5 minutes, the supernatant was removed and the cells washed twice with 5 mL DMEM culture medium while gently triturating the cell agglutinates. The cortical cells were resuspended in embryonic neuron culture medium as required for the downstream application. For nucleofection (see section 4.2.), the cells were first resuspended in DMEM culture medium, split to the needed number of conditions, nucleofected, then cultured in BrainPhys-based culture medium (1 mL SM1 supplement, provided with BrainPhys medium, 500  $\mu$ L GlutaMAX supplement, Gibco, 35050061, in 48 mL BrainPhys medium, STEMCell Technologies, 05792). When cortical cells were not nucleofected, they were directly resuspended in Neurobasal-based culture medium (1 mL 50x B27 supplement without vitamin A, Gibco, 12587010, 500  $\mu$ L GlutaMAX supplement, 500  $\mu$ L of penicillin-streptomycin stock, all in 48 mL Neurobasal medium, Gibco, 12348017). All wells for all conditions of an experiment were seeded at the same density, ranging from 3 to 6  $\times 10^5$  cortical cells per  $\text{cm}^2$ .

## 4.2. DELIVERING EXPRESSION CONSTRUCTS INTO CULTURED CELLS

### Transfection of immortalized cells

For transfecting N2A or HEK293T cells with expression constructs, we employed the TurboFect reagent (Thermo Scientific, R0533), according to the instructions of the producer.

### Nucleofection of primary cortical neurons

To increase uptake efficiency, expression constructs were delivered into primary cortical neurons by nucleofection. We used the Mouse Neuron Nucleofector Kit according to the producer-supplied protocol (Lonza, VPG-1001) together with the Amaxa Nucleofector device (Nucleofector 2b, Lonza, AAB-1001). We nucleofected 1  $\mu\text{g}$  of plasmid for every  $10^6$  cortical cells, washed cells once with DMEM culture medium, and then plated them in BrainPhys medium (see previous section).

## 4.3. TISSUE PROCESSING

For staining procedures, embryonic brains were fixated in 4% PFA in PBS according to the embryonic stage (E 12.5 for 2 hours, E 13.5 for 3, and so on), briefly rinsed and then subjected to dehydration by increased sucrose concentration (first 15% w/v and then 30% w/v). After this, brains were either embedded in O.C.T. compound (Sakura, 4583) for in situ hybridization or snap frozen in a bath of 2-methylbutane (Carl Roth, 3926.2) at  $-30$  to  $-20^\circ\text{C}$  for free-floating sectioning.

Using a Leica cryostat, brains were either cut in 15  $\mu\text{m}$  sections for in situ hybridization and then captured on SuperFrost Plus slides (Thermo Scientific/Menzel, J1800AMNZ), or cut free-floating at 50  $\mu\text{m}$  thickness and then stored in PBS with 0.3% sodium azide at  $4^\circ\text{C}$ .

Antigen retrieval was performed once, according to the producer's instructions (Vector citrate-based antigen retrieval solution, Vector Laboratories, H-3300-250).

#### 4.4. CELL AND TISSUE STAINING PROCEDURES

##### Chromogenic RNA *in situ* hybridization

The primers used to generate the sequences to be used as *in situ* hybridization probes were:

Primer	Sequence
Srsf1 fw	GGCTACGACTACGACGGCTACCGG
Srsf1 rv	ATTATTTAGGTGACACTATAGGATTGTACTGAGTAAAGGAAAAGTGT
Elavl1 fw	GTTAGACAGATGGGGAGTGTGTT
Elavl1 rv	ATTATTTAGGTGACACTATAGTGCTCACAAGAAGGGATGCG

Digoxigenin (DIG)-labeled RNA probes against the target genes were synthesized by transcribing for 2 hours at 37°C from linearized pJET1.2 plasmids (CloneJET PCR Cloning Kit, cat. no. K1231) in the presence of DIG-labelled nucleotides (1 µg linearized plasmid, 2 µL 10x transcription buffer, 2 µL of 100 mM DTT, 0.5 µL RNase inhibitor, 2 µL of 10x DIG labeling mix, Roche, 11277073910, 20 U RNA polymerase, to 20 µL with RNase-free MilliQ water). Probes were then purified using the RNeasy Mini Kit (Qiagen, 74104). 50 µL of the eluted RNA solution were mixed with 100 µL formamide to obtain the probe solution. Probe quality (RNA integrity) was checked on an agarose gel after 5 minutes of denaturation at 95°C.

Slides with brain sections were dried in a vacuum dryer for 10-15 minutes prior to the *in situ* hybridization procedure. All recipients and solutions used prior to the RNA probe hybridization were treated against RNase contamination. 1 mL of hybridization solution was applied per slide (50% deionised formamide pro analysi, 0.1 mg/mL yeast tRNA, 10% dextran sulphate, 1:50 dilution of Denhardt's solution, Thermo Fisher, 750018, and a 1:10 dilution of a salt solution containing 2M NaCl, 50mM EDTA, 100mM Tris-HCl pH.7.5, 50mM NaH<sub>2</sub>PO<sub>4</sub>·2H<sub>2</sub>O, 50mM Na<sub>2</sub>HPO<sub>4</sub>). The slides were covered with coverslips and incubated at 65°C for an hour in a humid chamber. In the meanwhile, RNA probes were mixed with 1 mL hybridization buffer and denatured for 5 minutes at 70°C. 200 µL of the probe mixture were applied per slide and slides were incubated as before over night.

On the second day, unbound probe was removed by incubating the slides three times for an hour each at 65°C in a stringent washing solution (50% formamide, 1x SSC, 0.1%

Tween-20). For preparing the incubation with anti-DIG antibodies, slides were then washed twice with MABT buffer (100 mM maleic acid, 150 mM NaCl, 0.1% Tween-20, pH 7.5) at room temperature. Blocking was performed for one hour with 1 mL of blocking solution per slide (2% blocking reagent, Roche, 11 096 176 001, 10% sheep serum in 1x MABT), after which a solution of 1:1500 alkaline phosphatase-coupled anti-DIG antibody fragments was applied overnight at 4°C (anti-DIG AP-labelled Fab fragments, Roche, 11093274910).

On the third day, unbound antibody was washed at room temperature 3 x 15 minutes in 1x MABT buffer, then 2x 5 minutes in pre-staining solution (4 mL of 5M NaCl, 10 mL of 1M MgCl<sub>2</sub>, 20 mL of 1M Tris pH 9.5, 0.2 mL of Tween 20 in 166 mL of MilliQ water). Slides were then incubated at 37°C in staining solution with chromogenic AP substrate until the colored precipitate could be observed. Staining solution: 0.8 mL of 5M NaCl, 2 mL of 1M MgCl<sub>2</sub>, 4 mL of 1M Tris pH 9.5, 13.2 mL H<sub>2</sub>O, 40 µL Tween 20, 40 µL of NBT (1000x = 100 mg/mL in 70% DMSO), 40 µL of BCIP (1000x = 50 mg/mL in 100% DMSO), supplemented up to 40 mL with 10% PVA in H<sub>2</sub>O. After signal generation, the slides were dehydrated in a series of baths in ascending ethanol concentration (50% - 100%), each for 2 minutes, then twice in 100% xylene. Coverslips were mounted with Entellan (Sigma-Aldrich, 107960).

### **Immunofluorescent staining**

Cells were cultured on coverslips coated with 0.1% gelatin. The coverslips with cells were then washed 3x in PBS, fixated for 15 minutes at 4°C with 4% PFA in PBS, then washed two more times for 10 minutes in PBS. Coverslips were placed cell side up on cling film-topped glass slides in a humid chamber and epitopes were blocked for 30 minutes in blocking solution (10% horse serum, 0.1% Triton X-100 in PBS). 50 µL primary antibody in blocking solution:PBS 1:1 was used per 13 mm coverslip overnight at 4°C. On the second day, coverslips were washed 4x 10 minutes in washing solution (0.05% T-X100 in PBS). Fluorophore-conjugated secondary antibodies (Dianova) were applied in 30 µL blocking solution:PBS for 1h30 at room temperature. Coverslips were then counterstained 5 minutes with Hoechst stain, washed once in washing solution, three times in PBS, and then mounted with ImmuMount (Fisher Scientific, 10622689).

In the wells of a 24-well-plate, several 50 µm brain sections per well were first

blocked for 30 minutes in blocking solution (10% horse serum, 0.1% Triton X-100 in PBS), then incubated overnight with primary antibody in blocking solution. On the second day, sections were washed 4x 10 minutes in an excess of PBS, then fluorophore-coupled secondary antibodies were applied for 4 h at room temperature. Sections were then pulled onto SuperFrost Plus glass slides, left to briefly dry and mounted with ImmuMount and #1.5 cover glasses.

#### 4.5. LIST OF ANTIBODIES USED IN THIS STUDY

Antibody against...	Antibody source	Concentration
goat anti-GFP	Rockland, 600-101-215	1:1000 in IF
rat anti-Ctip2	Abcam, 18465	1:300 in IF
rabbit anti-Satb2	custom preparation for Tarabykin research group	1:300 in IF
rabbit anti-Cux1	Santa Cruz (discontinued)	1:100 in IF
mouse anti-Elavl1	Santa Cruz, sc-5261	1:300 in IF
mouse anti-hnRNP L	Santa Cruz, 4D11	1:10000 in WB
rabbit anti-pan-TrkC	Cell Signaling, 3376	1:2000 in WB, 1:100 in IF
rabbit anti-Myc tag	Cell Signaling, 2278	1:500 in IF
rabbit anti-HA tag	Cell Signaling, 3724	1:500 in IF
mouse anti-GAPDH	HyTest, 5G4cc	1:100000 in WB
mouse anti-GM130	BD Biosciences, 610822	1:1000 in IF
rat anti-Prominin-1, clone 13A4	eBioscience, 17-1331-81	1:200 for FACS
rat IgG1 isotype control	eBioscience, 17-4301-81	1:200 for FACS

Fluorophore-coupled donkey secondary antibodies were purchased from Dianova and used 1:300-1:1000. HRP-coupled secondary antibodies for Western blotting were from Jackson Immunoresearch and used 1:5000.

#### 4.6. IMAGE ACQUISITION, PROCESSING AND QUANTIFICATION

##### Image acquisition for *in situ* hybridization

Slides were imaged on a Zeiss BX60 system. Linear modifications of brightness were performed using ImageJ software.

## **Image acquisition for immunofluorescence**

Slides were imaged on a Leica Sp8 confocal laser scanning system with a DMI6000C-SB microscope (BioSupraMol facility at Freie Universität Berlin).

## **Analysis of fluorescence micrographs**

For fate acquisition assessment, around 100 to 300 GFP-positive cells per analyzed electroporation site were interrogated for *Ctip2* and *Satb2* or *Cux1* co-expression. Counting was performed blinded using the Cell Counter plugin in ImageJ. For each electroporated litter, brain sections were matched for anteroposterior and lateromedial position of the electroporation site. To quantify the fold change in fate, individual brains were compared to the average percentage of double positive cells of that fate in the littermate controls.

For subcellular localization using ImageJ, we used ROIs of the same size, one over the accumulation of TrkC-T1 signal and one for the cytoplasm. We then calculated the ratio between the mean fluorescence intensities in these ROIs in the Shc channel for each of the analyzed cells.

## **4.7. FLUORESCENCE-ASSISTED CELL SORTING (FACS)**

A suspension of primary cortical cells was prepared as described in section 4.1. Instead of plating the resulting cells, they were resuspended in PBS, stained with the APC-coupled anti-prominin-1 or isotype control antibody plus propidium iodide in PBS on ice for 30 minutes, and then sorted for PI and APC signal using a BD FACS-Canto sorter. PI-positive cells were collected in two separate tubes, depending on the presence or absence of APC signal. The collection medium was based on the Neurobasal culture medium (see section 4.1.) but supplemented with recombinant murine EGF (final concentration: 40 ng/mL, ImmunoTools, 12343406 ) and FGF2 (final concentration: 40 ng/mL, ImmunoTools, 12343623). Cells were then pelleted by centrifugation at 500 rpm and 4°C, the supernatant was removed, cells washed once with PBS and the pellets snap-frozen in liquid nitrogen for downstream applications.

#### 4.8. RNA EXTRACTION

For downstream use in TaqMan qPCR, cortex pieces were collected in the LB+TG buffer of the Promega ReliaPrep RNA extraction kit (Z6212) and minced using an UltraTurrax homogenizer (IKA, 0003737000). RNA was extracted using this kit according to the manufacturer's protocol. Prior to reverse transcription, RNA quality and integrity were assessed on an Agilent BioAnalyzer 2100 system (BIH Core Facility Genomics). Only samples with a RINe value higher than 8.5 out of 10 were used further.

For RNA extraction from cultured cells, the culture medium was removed and TRIzol reagent (Ambion/Invitrogen, 15596018) was added directly to the wells, with subsequent cell scraping and uptake in RNase-free tubes. All further steps were performed at 4°C unless otherwise specified. Chloroform was added in a 1:5 ratio and the mixture homogenized by vortexing. Subsequently, nucleic acids were extracted by phase separation through centrifugation, precipitated with isopropanol, resuspended in RNase-free H<sub>2</sub>O and digested with RNase-free DNase I (Lucigen, D9905K). RNAs were subjected to a second phenol-chloroform-isoamyl alcohol extraction (PCI from Carl Roth, X985.1) and subsequently precipitated with an equal volume of 100% ethanol with sodium acetate (final concentration: 150 mM). Finally, the RNA pellets were washed with 70% ethanol, left to air-dry, and then resuspended in nuclease-free H<sub>2</sub>O.

#### 4.9. cDNA FIRST-STRAND SYNTHESIS

For downstream use in TaqMan qPCR, cDNA first strand synthesis was performed using an oligo(dT) primer (Promega, C1101) and the Promega GoScript reverse transcription system (A5000).

For all other applications, cDNA was reverse-transcribed using MMuLV reverse transcriptase (Enzymatics/Qiagen, P7040L) using either oligo(dT) primers or gene-specific reverse primers (see section 4.11.), according to the producer's protocol.

#### 4.10. QUANTITATIVE REAL-TIME PCR

## TaqMan qPCR

TaqMan qPCR for TrkC-T1 and TK+ was performed in multiplex reactions using the FastAdvanced Master Mix (Thermo Fisher, 4444557) on a StepOne Plus qPCR cycler (Thermo Fisher/Applied Biosystems, 4376600). Reactions were set up according to the master mix protocol using the equivalent of 25 ng reverse transcribed RNA per 10  $\mu$ L reaction. Reactions were performed in technical quadruplicates and the number of biological replicates indicated in the figures. The TaqMan probes used were: for TrkC-T1, VIC-tagged Mm01317842\_m1, and for TrkC-TK+, a custom-designed exon-junction spanning FAM-tagged probe (AR47VWU). Both probes were from Thermo Fisher. Cq values of the two transcripts were used to calculate the fold difference between TrkC-T1 and TrkC-TK+ input quantities, and these values used to calculate the percentage each transcript variant occupied in the total TrkC transcript quantity (TrkC-T1+TrkC-TK+).

## SYBR Green qPCR

SYBR Green qPCR was performed on the same device, using the Promega GoTaq qPCR system (A6001), according to the producer's protocol. The primers used in qPCR were first tested for coupling efficiency between 90 and 110% over an input range of reverse transcribed RNA (cDNA first strand) quantities from 0.1 to 30 ng.

Primer	Sequence
Srsf1 fw	CCCTTCGCCTTCGTTGAGTTCG
Srsf1 rv	GAAACTCTACCCGCAGCCGG
Elavl1 fw	TCGGGATAAAGTAGCAGGACACAG
Elavl1 rv	CTGGAGTCTCAAGCCGTTTCAGT
Hprt fw	CAACGGGGGACATAAAAGTTATTGGTGGA
Hprt rv	TGCAACCTTAACCATTTTGGGGCTGT
Oaz1 fw	AAGGACAGTTTTCAGCTCTCC
Oaz1 rv	TCTGTCCTCACGGTTCTTGGG

Results were quantified using the  $2^{-\Delta\Delta CT}$  method.

## 4.11. SPLICING-SENSITIVE PCR

Splicing-sensitive PCRs were performed with transcript variant-discriminating primers either with radioactive labeling of primers or without.

For the radioactive splicing-sensitive PCRs, 2  $\mu\text{L}$  of the shared primer (100 ng/ $\mu\text{L}$ ) were mixed with 10 units T4 PNK (Molox), 10  $\mu\text{L}$  PNK buffer (70 mM Tris-HCl pH 7.6, 10mM MgCl<sub>2</sub>, 5mM DTT), 84.5  $\mu\text{L}$  H<sub>2</sub>O and 2.5  $\mu\text{L}$  <sup>32</sup>P- $\gamma$ -ATP (Hartmann Analytic, SRP-501). The mixture was incubated for one hour at 37°C, then purified by phenol-chloroform extraction. Primer pellets were resuspended in 80  $\mu\text{L}$  H<sub>2</sub>O, and 1  $\mu\text{L}$  of this labeled primer was used per 20  $\mu\text{L}$  PCR reaction. The marker, pBR322-Mspl Digest (NEB, N3032S), was labeled in the same way, and the pellet was resuspended in 40  $\mu\text{L}$  H<sub>2</sub>O plus 40  $\mu\text{L}$  formamide loading dye (formamide with 21 mM EDTA, 0.02 w/v bromphenol blue, 0.02 w/v xylene cyanol). 5  $\mu\text{L}$  RT-PCR mix, 1.5  $\mu\text{L}$  10x Taq reaction buffer (0.5 M KCl, 0.1 M Tris, pH 8.3, 15 mM MgCl<sub>2</sub>, 0.01% gelatine), 1  $\mu\text{L}$  non-labeled forward primer (2.5 ng/ $\mu\text{L}$ ), 1  $\mu\text{L}$  reverse primer (5 ng/ $\mu\text{L}$ ), 1  $\mu\text{L}$  radioactively labeled forward primer ( 2.5 ng/ $\mu\text{L}$ ) and 0.5  $\mu\text{L}$  Taq polymerase (purified in the research group) in a 20  $\mu\text{L}$  reaction. Reactions were topped with mineral oil to prevent evaporation. After the run, the PCR products were mixed 1:1 with formamide loading dye, denatured alongside the marker for 5 min at 95°C, and 5  $\mu\text{L}$  were applied to a denaturing polyacrylamide-urea gel (7 M urea, 8% polyacrylamide in 0.5x TBE) that was pre-run unloaded for 15 minutes to ensure optimal product denaturation. Once the desired degree of resolution was reached, gels were transferred to Whatman paper, vacuum-dried and finally assembled together with a photostimulable phosphor plate in photographic cassettes. Exposure was performed for two hours or overnight, depending on the strength of the luminous signal. Imaging was performed with a GE Healthcare Typhoon 7000 FLA imager and the result quantified using the BioRad ImageLab 6.0 software.

Primer	Sequence
T1/TK+ common fw	AGCCCACTGCATCACATCAA
T1-specific rv	GGGTAAGACACATCCCCACTC
TK+-specific rv	GGCTCCCTCACCCAATTCTC

Non-radioactive splicing-sensitive PCRs were performed using the GoTaq G2 polymerase (Promega, M7845) with the equivalent of 10 ng reverse-transcribed RNA as cDNA first strand per 20  $\mu\text{L}$  reaction and 40 amplification cycles. 3  $\mu\text{L}$  of the PCR product was mixed with 3  $\mu\text{L}$  formamide loading dye and denatured for 5 min at 95°C prior to application on an 8% polyacrylamide-urea gel that was pre-run unloaded for 15 minutes. The primer sequences were optimized by the research group of Prof.

Heiner Schaal at U Düsseldorf, who also kindly provided the reporter vector SVSD1 (published in Brillen et al., 2017). Analysis was performed as described above.

Primer	Sequence
Splicing reporter vector fw	TGAGGAGGCTTTTTGGAGG
Splicing reporter vector rv	TTCACTAATCGAATGGATCTGTC

## 4.12. MOLECULAR CLONING OF EXPRESSION AND REPORTER CONSTRUCTS

### Subcloning of ORFs for expression constructs

The pCAGIG backbone was a kind gift from Dr. Kuo Yan. ORFs of Srsf1, Elavl1, Srpk1 and Srpk2 were incorporated in this backbone using the NEBuilder HiFi DNA Assembly Cloning Kit (NEB, E2621S) as recommended by the kit protocol. Primers were designed using the NEBuilder online tool (<https://nebuilder.neb.com>).

Primer	Sequence
Srsf1 fw	aattcaccgggtagcgatATGTCGGGAGGTGGTGTG
Srsf1 rv	gtagcggccgcaccggtgatTTATGTACGAGAGCGAGATCTG
Elavl1 fw	aattcaccgggtagcgatATGTCTAATGGTTATGAAGAC
Elavl1 rv	gtagcggccgcaccggtgatTTATTTGTGGGACTTGTTG
Srpk1 fw	aattcaccgggtagcgatATGGAGCGGAAAGTGCTC
Srpk1 rv	gtagcggccgcaccggtgatTTAGGAGTTTAGCCAAGGATG
Srpk2 fw	aattcaccgggtagcgatATGTCAGTAACTCTGAGAAG
Srpk2 rv	gtagcggccgcaccggtgatCTAAGAATTCAACCAAGGATG

### Generation of splicing reporter vectors

The SVSD1 reporter backbone was a gift from Prof. Heiner Schaal at U Düsseldorf (published in Brillen et al., 2017). 5 µL of forward and of reverse oligonucleotides containing the regions of interest of exon 13A and SacI and EcoRI overhangs were annealed in 90 µL annealing buffer (final concentrations: 10 mM Tris, pH 7.5, 50 mM NaCl, 1 mM EDTA, pH 8, 10 mM MgCl<sub>2</sub>, all dissolved in water). Annealed oligonucleotides were phosphorylated using T4 PNK as described for radioactive primer labeling. The oligonucleotide duplexes were ligated with the SacI- and EcoRI-digested

SVSD1 backbone to generate the reporter vectors.

Oligonucleotide	Sequence
13A-1 fw	aattGGGTCTTTTCAAACATAGACAATCATGGGATATTAACtagct
13A-1 rv	AGTTTAATATCCCATGATTGTCTATGTTTGAAAAGACCC
13A-2 fw	aattTGAAGGACAATAGAGATCATCTAGTCCCATCAACTCagct
13A-2 rv	GAGTTGATGGGACTAGATGATCTCTATTGTCCTTCA
13A-3 fw	aattCTATATATATGAGGAACCTGAGGTCCAGAGTGGGGATGTGTCTTACCCAAGGTCACATGagct
13A-3 rv	CATGTGACCTTGGGTAAGACACATCCCCACTCTGGACCTCAGGTTCCCTCATATATATAG

Insert-positive vectors were selected by transformation into *E. coli* XL-10 Gold and subsequent colony PCR using the primers fw TGAGGAGGCTTTTTTGGAGG and rv GGTTGCTTCCTCCACACAG. Constructs were then purified and sequenced to confirm correct insertion.

#### 4.13. KNOCKDOWN CONSTRUCTS

The shScrambled vector (pLKO.1-Venus-shScrambled) was a kind gift from Dr. Mateusz Ambrozkiwicz. The shRNA against TrkC-T1 is published in Parthasarathy et al., 2021. The other knockdown constructs were Mission shRNA in pLKO.1 backbone (Srsf1: TRCN0000287199 and TRCN0000294703; Elavl1: TRCN0000112087 and TRCN0000308991, all from Sigma Aldrich and all with a certified knockdown efficiency of over 90%).

siRNA constructs were a part of an ON-TARGETplus siRNA library from Dharmacon/Horizon Discovery. For Srsf1 knockdown, we used a pool of four siRNAs (Horizon Discovery, L-040886-01-0005). The control siRNA was siAllstar (Eurofins genomics, fw (UUC UCC GAA CGU GUC ACG U)TT, rv (ACG UGA CAC GUU CGG AGA A)TT).

#### 4.14. siRNA-BASED KNOCKDOWN

For the simple siRNA-based knockdown,  $5 \times 10^4$  N2A cells were seeded per well of a 24-well plate. The following day, cells were transfected with the siRNA pools at a

final concentration of 0.02 pmol/ $\mu$ L using OptiMEM (Thermo Fisher/Gibco, 31985062) and the RotiFect reagent (Carl Roth, P001.4) according to the producer's protocol. The knockdown duration was 48 hours, after which the medium was removed, the cells directly collected in TRIzol reagent and snap frozen in liquid nitrogen.

For the siRNA-based knockdown of Srsf1 together with the transfection of splicing reporter vectors, we used the same number of cells but performed reverse transfection instead. Using the same reagents, we allowed the siRNA-/plasmid-RotiFect complexes to form in OptiMEM in the empty wells of 24-well plates and then seeded the indicated number of freshly dissociated cells into the wells in 0.5 mL DMEM culture medium. siRNAs were used in the same concentration as above, together with a total of 1  $\mu$ g of plasmid per well. Cells were collected in the same manner described above.

#### 4.15. PROTEIN EXTRACT PREPARATION AND WESTERN BLOTTING

We collected both cells and tissue directly in RIPA buffer (50mM Tris pH 8, 150mM NaCl, 0.1% SDS, 1% NP40 (Tergitol), 0.5% Na deoxycholate) freshly mixed with protease and phosphatase inhibitors (PhosStop from Roche, equivalent of 1 tablet per 10 mL, protease inhibitor cocktail from Sigma, 1 $\times$ , 5  $\mu$ g/mL pepstatin, 2.5 mM sodium orthovanadate, 10 mM benzaminidine, 10  $\mu$ g/mL leupeptin, 1 mM  $\beta$ -glycerophosphate and 5 mM NaF). 150  $\mu$ L RIPA with inhibitors was used per well of a 6-well plate. The tissue was first minced as described under "RNA extraction". The tissue homogenate or cell suspension were briefly sonicated on ice (three pulses at 70% amplitude), then centrifuged at maximal speed and 4°C for 20 minutes. The cleared lysate was transferred to a fresh tube and stored at -80°C.

For protein concentration measurement, we used the Pierce BCA Protein Assay Kit (Thermo Fisher, 23225) and a BioTEK Synergy HT plate photometer. Samples for Western blotting were adjusted with RIPA buffer to achieve the same protein concentration. The same amount of total protein was applied on all lanes of the polyacrylamide gel.

For gel electrophoresis, protein lysates were first mixed with loading buffer (312.5 mM Tris, pH 6.8, 50% glycerol, 20% SDS, 20%  $\beta$ -mercaptoethanol and 2% bromophenol blue) and then denatured for 5 minutes at 95°C. Samples were run on 8-10% polyacrylamide gels with stacking and running phases in Laemmli buffer, alongside the

PageRuler Plus Pre-Stained protein ladder (Thermo Fisher, 26620).

For blotting, gels were transferred onto a PVDF membrane (Immobilon-P, pore size 0.45  $\mu\text{m}$ , Millipore, IPVH000010) in a composite of Whatman paper flanked by sponges. The transfer was performed in transfer buffer (1:5 methanol, 1:5 transfer buffer stock - 144.2 g glycine, 30.3 g Tris base, 1 g SDS in total of 2L water - and 3:5 water) while cooling the transfer system on ice to prevent protein denaturation.

After blotting, membranes were washed twice with TBS-T on a rotating platform, then blocked for 30 minutes with blocking solution (5% BSA in TBS-T). Primary antibodies were diluted in blocking solution and applied to the blots overnight at 4°C with gentle agitation. On the following day, antibodies were recovered, the membranes washed thrice in TBS-T, then incubated with secondary, HRP-coupled antibodies for two hours. This was followed by three more washes in TBS-T and signal development using a luminol-based HRP substrate (Lightning ECL Plus reagent, Perkin Elmer, NEL104001EA) in a Bio-Rad Gel Doc XR imager.

Blots were quantified using the ImageLab 6.0 software (BioRad).

#### 4.16. ANIMAL CARE AND HUSBANDRY

Wild-type mice of the NMRI strain were housed, bred, operated on and sacrificed in the animal facility of Charité Universitätsmedizin, in accordance to animal experimentation licenses granted to the research group Tarabykin by the Landesamt für Gesundheit und Soziales, Berlin (T102/11, G206/16 and G54/19). In the breedings, the day of vaginal plug detection was considered E 0.5.

#### 4.17. *IN UTERO* ELECTROPORATION

Endotoxin-free plasmid DNA was prepared using the NucleoBond Xtra Midi Prep Kit (Macherey-Nagel, 740410.100). Prior to IUE, DNA concentration was adjusted to 500 ng/ $\mu\text{L}$  and mixed with FastGreen dye (final concentration: 0.1%, Sigma-Aldrich). For the IUE, micropipettes were created by heating and extending borosilicate glass capillaries (1.5 - 1.8 mm  $\times$  10 cm, Kimble and Chase) in a HEKA PIP5 temperature

controlled pipette puller. The IUE procedure was performed on deeply anesthetized pregnant mice, in accordance to animal experiment permits. A pneumatic pump (PicoPump PV820, World Precision Instruments) was used to deliver the plasmid DNA solution through the micropipettes into the embryonic ventricles. Electroporation was performed with paddle electrodes connected to an electroporator device (CUY21 from Bex Co. Ltd.) in 5 pulses of 34 V. After the surgery, the animals were allowed to recover under application of analgesic and regular observation. At the indicated embryonic dates, the pregnant dams were killed and the embryonic brains were collected as described under “Tissue processing”.

#### 4.18. STATISTICAL ANALYSIS

All statistical analysis was performed using the Prism software (GraphPad), employing the tests indicated in the respective experiments.

- this page intentionally left blank -

## BIBLIOGRAPHY

- » Agarwal, Vikram, George W. Bell, Jin-Wu Nam, and David P. Bartel. 2015. “Predicting Effective MicroRNA Target Sites in Mammalian MRNAs.” *ELife* 4 (August). <https://doi.org/10.7554/eLife.05005>.
- » Alcamo, Elizabeth A., Laura Chirivella, Marcel Dautzenberg, Gergana Dobрева, Isabel Fariñas, Rudolf Grosschedl, and Susan K. McConnell. 2008. “Satb2 Regulates Callosal Projection Neuron Identity in the Developing Cerebral Cortex.” *Neuron* 57 (3): 364–77. <https://doi.org/10.1016/j.neuron.2007.12.012>.
- » Allodi, Ilary, and Eva Hedlund. 2014. “Directed Midbrain and Spinal Cord Neurogenesis from Pluripotent Stem Cells to Model Development and Disease in a Dish.” *Frontiers in Neuroscience* 8. <https://doi.org/10.3389/fnins.2014.00109>.
- » Alt, F. W., A. L. Bothwell, M. Knapp, E. Siden, E. Mather, M. Koshland, and D. Baltimore. 1980. “Synthesis of Secreted and Membrane-Bound Immunoglobulin Mu Heavy Chains Is Directed by MRNAs That Differ at Their 3’ Ends.” *Cell* 20 (2): 293–301. [https://doi.org/10.1016/0092-8674\(80\)90615-7](https://doi.org/10.1016/0092-8674(80)90615-7).
- » Amatu, A, A Sartore-Bianchi, K Bencardino, E G Pizzutilo, F Tosi, and S Siena. 2019. “Tropomyosin Receptor Kinase (TRK) Biology and the Role of NTRK Gene Fusions in Cancer.” *Annals of Oncology* 30 (Suppl 8): viii5–15. <https://doi.org/10.1093/annonc/mdz383>.
- » Anderson, Jeffrey S., T. Jason Druzgal, Alyson Froehlich, Molly B. DuBray, Nicholas Lange, Andrew L. Alexander, Tracy Abildskov, et al. 2011. “Decreased Interhemispheric Functional Connectivity in Autism.” *Cerebral Cortex* 21 (5): 1134–46. <https://doi.org/10.1093/cercor/bhq190>.
- » Anderson, S. A., D. D. Eisenstat, L. Shi, and J. L. R. Rubenstein. 1997. “Interneuron Migration from Basal Forebrain to Neocortex: Dependence on Dlx Genes.” *Science* 278 (5337): 474–76. <https://doi.org/10.1126/science.278.5337.474>.
- » Andriamananjara, Andry, Rayan Muntari, and Alessandro Crimi. 2019. “Overlaps in Brain Dynamic Functional Connectivity between Schizophrenia and Autism Spectrum Disorder.” *Scientific African* 2 (March): e00019. <https://doi.org/10.1016/j.sciaf.2018.e00019>.
- » Angevine, J. B., and R. L. Sidman. 1961. “Autoradiographic Study of Cell Migration during Histogenesis of Cerebral Cortex in the Mouse.” *Nature* 192 (November): 766–68. <https://doi.org/10.1038/192766b0>.
- » Arai, Yoko, and Alessandra Pierani. 2014. “Development and Evolution of Cortical Fields.” *Neuroscience Research* 86 (September): 66–76. <https://doi.org/10.1016/j.neures.2014.06.005>.
- » Arlotta, Paola, Bradley J. Molyneaux, Jinhui Chen, Jun Inoue, Ryo Kominami, and Jeffrey D. Macklis. 2005. “Neuronal Subtype-Specific Genes That Control Corticospinal Motor Neuron Development *in Vivo*.” *Neuron* 45 (2): 207–21. <https://doi.org/10.1016/j.neuron.2004.12.036>.
- » Assimacopoulos, Stavroula, Elizabeth A. Grove, and Clifton W. Ragsdale. 2003. “Identification of a Pax6-Dependent Epidermal Growth Factor Family Signaling Source at the Lateral Edge of the Embryonic Cerebral Cortex.” *Journal of Neuroscience* 23 (16): 6399–6403. <https://doi.org/10.1523/JNEUROSCI.23-16-06399.2003>.

- » Aubol, Brandon E., Sutapa Chakrabarti, Jacky Ngo, Jennifer Shaffer, Brad Nolen, Xiang-Dong Fu, Gourisankar Ghosh, and Joseph A. Adams. 2003. "Processive Phosphorylation of Alternative Splicing Factor/Splicing Factor 2." *Proceedings of the National Academy of Sciences* 100 (22): 12601–6. <https://doi.org/10.1073/pnas.1635129100>.
- » Azevedo, Frederico A. C., Ludmila R. B. Carvalho, Lea T. Grinberg, José Marcelo Farfel, Renata E. L. Ferretti, Renata E. P. Leite, Wilson Jacob Filho, Roberto Lent, and Suzana Herculano-Houzel. 2009. "Equal Numbers of Neuronal and Nonneuronal Cells Make the Human Brain an Isometrically Scaled-up Primate Brain." *Journal of Comparative Neurology* 513 (5): 532–41. <https://doi.org/10.1002/cne.21974>.
- » Barash, Yoseph, John A. Calarco, Weijun Gao, Qun Pan, Xinchun Wang, Ofer Shai, Benjamin J. Blencowe, and Brendan J. Frey. 2010. "Deciphering the Splicing Code." *Nature* 465 (7294): 53–59. <https://doi.org/10.1038/nature09000>.
- » Barbosa-Morais, Nuno L., Manuel Irimia, Qun Pan, Hui Y. Xiong, Serge Gueroussov, Leo J. Lee, Valentina Slobodeniuc, et al. 2012. "The Evolutionary Landscape of Alternative Splicing in Vertebrate Species." *Science (New York, N.Y.)* 338 (6114): 1587–93. <https://doi.org/10.1126/science.1230612>.
- » Barnabé-Heider, Fanie, Julie A. Wasylnka, Karl J. L. Fernandes, Christian Porsche, Michael Sendtner, David R. Kaplan, and Freda D. Miller. 2005. "Evidence That Embryonic Neurons Regulate the Onset of Cortical Gliogenesis via Cardiotrophin-1." *Neuron* 48 (2): 253–65. <https://doi.org/10.1016/j.neuron.2005.08.037>.
- » Barry, G., J. A. Briggs, D. P. Vanichkina, E. M. Poth, N. J. Beveridge, V. S. Ratnu, S. P. Nayler, et al. 2014. "The Long Non-Coding RNA Gomafu Is Acutely Regulated in Response to Neuronal Activation and Involved in Schizophrenia-Associated Alternative Splicing." *Molecular Psychiatry* 19 (4): 486–94. <https://doi.org/10.1038/mp.2013.45>.
- » Bartheld, Christopher S. von, and Bernd Fritschsch. 2006. "Comparative Analysis of Neurotrophin Receptors and Ligands in Vertebrate Neurons: Tools for Evolutionary Stability or Changes in Neural Circuits?" *Brain, Behavior and Evolution* 68 (3): 157–72. <https://doi.org/10.1159/000094085>.
- » Bartkowska, Katarzyna, Annie Paquin, Andrée S. Gauthier, David R. Kaplan, and Freda D. Miller. 2007. "Trk Signaling Regulates Neural Precursor Cell Proliferation and Differentiation during Cortical Development." *Development* 134 (24): 4369–80. <https://doi.org/10.1242/dev.008227>.
- » Bear, Mark F., Barry W. Connors, and Michael A. Paradiso. 2016. *Neuroscience: Exploring The Brain*. 4th ed. Wolters Kluwer.
- » Bedogni, Francesco, Clementina Cobolli Gigli, Davide Pozzi, Riccardo Lorenzo Rossi, Linda Scaramuzza, Grazisa Rossetti, Massimiliano Pagani, Charlotte Kilstrup-Nielsen, Michela Matteoli, and Nicoletta Landsberger. 2016. "Defects During Mecp2 Null Embryonic Cortex Development Precede the Onset of Overt Neurological Symptoms." *Cerebral Cortex (New York, N.Y.: 1991)* 26 (6): 2517–29. <https://doi.org/10.1093/cercor/bhv078>.
- » Bedogni, Francesco, Rebecca D. Hodge, Gina E. Elsen, Branden R. Nelson, Ray A. M. Daza, Richard P. Beyer, Theo K. Bammler, John L. R. Rubenstein, and Robert F. Hevner. 2010. "Tbr1 Regulates Regional and Laminar Identity of Postmitotic Neurons in Developing Neocortex." *Proceedings of the National Academy of Sciences of the United States of America* 107 (29): 13129–34. <https://doi.org/10.1073/>

pnas.1002285107.

- » Begg, Bridget E., Marvin Jens, Peter Y. Wang, Christine M. Minor, and Christopher B. Burge. 2020. “Concentration-Dependent Splicing Is Enabled by Rbfox Motifs of Intermediate Affinity.” *Nature Structural & Molecular Biology* 27 (10): 901–12. <https://doi.org/10.1038/s41594-020-0475-8>.
- » Berget, S. M., C. Moore, and P. A. Sharp. 1977. “Spliced Segments at the 5’ Terminus of Adenovirus 2 Late MRNA.” *Proceedings of the National Academy of Sciences of the United States of America* 74 (8): 3171–75. <https://doi.org/10.1073/pnas.74.8.3171>.
- » Berry, M, and A W Rogers. 1965. “The Migration of Neuroblasts in the Developing Cerebral Cortex.” *Journal of Anatomy* 99 (Pt 4): 691–709.
- » Bian, Shan, Janet Hong, Qingsong Li, Laura Schebelle, Andrew Pollock, Jennifer L. Knauss, Vidur Garg, and Tao Sun. 2013. “MicroRNA Cluster MiR-17-92 Regulates Neural Stem Cell Expansion and Transition to Intermediate Progenitors in the Developing Mouse Neocortex.” *Cell Reports* 3 (5): 1398–1406. <https://doi.org/10.1016/j.celrep.2013.03.037>.
- » Bibel, Miriam, and Yves-Alain Barde. 2000. “Neurotrophins: Key Regulators of Cell Fate and Cell Shape in the Vertebrate Nervous System.” *Genes & Development* 14 (23): 2919–37. <https://doi.org/10.1101/gad.841400>.
- » Black, Douglas L. 2003. “Mechanisms of Alternative Pre-Messenger RNA Splicing.” *Annual Review of Biochemistry* 72 (1): 291–336. <https://doi.org/10.1146/annurev.biochem.72.121801.161720>.
- » Blencowe, Benjamin J. 2006. “Alternative Splicing: New Insights from Global Analyses.” *Cell* 126 (1): 37–47. <https://doi.org/10.1016/j.cell.2006.06.023>.
- » Boutz, Paul L., Peter Stoilov, Qin Li, Chia-Ho Lin, Geetanjali Chawla, Kristin Ostrow, Lily Shiue, Manuel Ares, and Douglas L. Black. 2007. “A Post-Transcriptional Regulatory Switch in Polypyrimidine Tract-Binding Proteins Reprograms Alternative Splicing in Developing Neurons.” *Genes & Development* 21 (13): 1636–52. <https://doi.org/10.1101/gad.1558107>.
- » Brahim, Fouad, Alba Galan, and Sean Jmaeff. 2020. “Alternative Splicing of a Receptor Intracellular Domain Yields Different Ectodomain Conformations, Enabling Isoform-Selective Functional Ligands.” <https://doi.org/10.1016/j.isci.2020.101447>.
- » Brahim, Fouad, Mario Maira, Pablo F. Barcelona, Alba Galan, Tahar Aboukassim, Katrina Teske, Mary-Louise Rogers, et al. 2016. “The Paradoxical Signals of Two TrkC Receptor Isoforms Supports a Rationale for Novel Therapeutic Strategies in ALS.” Edited by Renping Zhou. *PLOS ONE* 11 (10): e0162307. <https://doi.org/10.1371/journal.pone.0162307>.
- » Brillen, Anna-Lena, Katrin Schöneweis, Lara Walotka, Linda Hartmann, Lisa Müller, Johannes Ptok, Wolfgang Kaisers, et al. 2017. “Succession of Splicing Regulatory Elements Determines Cryptic 5’ss Functionality.” *Nucleic Acids Research* 45 (7): 4202–16. <https://doi.org/10.1093/nar/gkw1317>.
- » Brillen, Anna-Lena, Lara Walotka, Frank Hillebrand, Lisa Müller, Marek Widera, Stephan Theiss, and Heiner Schaal. 2017. “Analysis of Competing HIV-1 Splice Donor Sites Uncovers a Tight Cluster of Splicing Regulatory Elements within Exon 2/2b.” *Journal of Virology* 91 (14): e00389-17. <https://doi.org/10.1128/JVI.00389-17>.

- » Britanova, Olga, Camino de Juan Romero, Amanda Cheung, Kenneth Y. Kwan, Manuela Schwark, Andrea Gyorgy, Tanja Vogel, et al. 2008. “Satb2 Is a Postmitotic Determinant for Upper-Layer Neuron Specification in the Neocortex.” *Neuron* 57 (3): 378–92. <https://doi.org/10.1016/j.neuron.2007.12.028>.
- » Buée, Luc, Thierry Bussière, Valérie Buée-Scherrer, André Delacourte, and Patrick R. Hof. 2000. “Tau Protein Isoforms, Phosphorylation and Role in Neurodegenerative Disorders” These Authors Contributed Equally to This Work.” *Brain Research Reviews* 33 (1): 95–130. [https://doi.org/10.1016/S0165-0173\(00\)00019-9](https://doi.org/10.1016/S0165-0173(00)00019-9).
- » Bulfone, Alessandro, Pietro Carotenuto, Andrea Faedo, Veruska Aglio, Livia Garzia, Anna Maria Bello, Andrea Basile, et al. 2005. “Telencephalic Embryonic Subtractive Sequences: A Unique Collection of Neurodevelopmental Genes.” *The Journal of Neuroscience: The Official Journal of the Society for Neuroscience* 25 (33): 7586–7600. <https://doi.org/10.1523/JNEUROSCI.0522-05.2005>.
- » Bush, Stephen J., Lu Chen, Jaime M. Tovar-Corona, and Araxi O. Urrutia. 2017. “Alternative Splicing and the Evolution of Phenotypic Novelty.” *Phil. Trans. R. Soc. B* 372 (1713): 20150474. <https://doi.org/10.1098/rstb.2015.0474>.
- » Calarco, John A., Simone Superina, Dave O’Hanlon, Mathieu Gabut, Bushra Raj, Qun Pan, Ursula Skalska, et al. 2009. “Regulation of Vertebrate Nervous System Alternative Splicing and Development by an SR-Related Protein.” *Cell* 138 (5): 898–910. <https://doi.org/10.1016/j.cell.2009.06.012>.
- » Calarco, John A., Mei Zhen, and Benjamin J. Blencowe. 2011. “Networking in a Global World: Establishing Functional Connections between Neural Splicing Regulators and Their Target Transcripts.” *RNA* 17 (5): 775–91. <https://doi.org/10.1261/rna.2603911>.
- » Calegari, Federico, Wulf Haubensak, Christiane Haffner, and Wieland B. Huttner. 2005. “Selective Lengthening of the Cell Cycle in the Neurogenic Subpopulation of Neural Progenitor Cells during Mouse Brain Development.” *The Journal of Neuroscience: The Official Journal of the Society for Neuroscience* 25 (28): 6533–38. <https://doi.org/10.1523/JNEUROSCI.0778-05.2005>.
- » Camp, J. Gray, Farhath Badsha, Marta Florio, Sabina Kanton, Tobias Gerber, Michaela Wilsch-Bräuninger, Eric Lewitus, et al. 2015. “Human Cerebral Organoids Recapitulate Gene Expression Programs of Fetal Neocortex Development.” *Proceedings of the National Academy of Sciences of the United States of America* 112 (51): 15672–77. <https://doi.org/10.1073/pnas.1520760112>.
- » Cárdenas, Adrián, and Víctor Borrell. 2020. “Molecular and Cellular Evolution of Corticogenesis in Amniotes.” *Cellular and Molecular Life Sciences: CMLS* 77 (8): 1435–60. <https://doi.org/10.1007/s00018-019-03315-x>.
- » Cartegni, Luca, Jinhua Wang, Zhengwei Zhu, Michael Q. Zhang, and Adrian R. Krainer. 2003. “ESEfinder: A Web Resource to Identify Exonic Splicing Enhancers.” *Nucleic Acids Research* 31 (13): 3568–71. <https://doi.org/10.1093/nar/gkg616>.
- » Caviness, V. S., T. Goto, T. Tarui, T. Takahashi, P. G. Bhide, and R. S. Nowakowski. 2003. “Cell Output, Cell Cycle Duration and Neuronal Specification: A Model of Integrated Mechanisms of the Neocortical Proliferative Process.” *Cerebral Cortex (New York, N.Y.: 1991)* 13 (6): 592–98. <https://doi.org/10.1093/cercor/13.6.592>.
- » Caviness, V. S., and T. Takahashi. 1995. “Proliferative Events in the Cerebral Ventricular Zone.”

Brain & Development 17 (3): 159–63. [https://doi.org/10.1016/0387-7604\(95\)00029-b](https://doi.org/10.1016/0387-7604(95)00029-b).

- » Chakrabarti, Lina, Bi-Dar Wang, Norman H. Lee, and Anthony D. Sandler. 2013. “A Mechanism Linking Id2-TGF $\beta$  Crosstalk to Reversible Adaptive Plasticity in Neuroblastoma.” *PloS One* 8 (12): e83521. <https://doi.org/10.1371/journal.pone.0083521>.
- » Chao, Moses V. 2003. “Neurotrophins and Their Receptors: A Convergence Point for Many Signaling Pathways.” *Nature Reviews Neuroscience* 4 (4): 299–309. <https://doi.org/10.1038/nrn1078>.
- » Chen, Bin, Laura R. Schaevitz, and Susan K. McConnell. 2005. “Fezl Regulates the Differentiation and Axon Targeting of Layer 5 Subcortical Projection Neurons in Cerebral Cortex.” *Proceedings of the National Academy of Sciences of the United States of America* 102 (47): 17184–89. <https://doi.org/10.1073/pnas.0508732102>.
- » Chen, Lu, Stephen J. Bush, Jaime M. Tovar-Corona, Atahualpa Castillo-Morales, and Araxi O. Urrutia. 2014. “Correcting for Differential Transcript Coverage Reveals a Strong Relationship between Alternative Splicing and Organism Complexity.” *Molecular Biology and Evolution* 31 (6): 1402–13. <https://doi.org/10.1093/molbev/msu083>.
- » Chen, Zhe, Bryan B. Gore, Hua Long, Le Ma, and Marc Tessier-Lavigne. 2008. “Alternative Splicing of the Robo3 Axon Guidance Receptor Governs the Midline Switch from Attraction to Repulsion.” *Neuron* 58 (3): 325–32. <https://doi.org/10.1016/j.neuron.2008.02.016>.
- » Chenn, A., and S. K. McConnell. 1995. “Cleavage Orientation and the Asymmetric Inheritance of Notch1 Immunoreactivity in Mammalian Neurogenesis.” *Cell* 82 (4): 631–41. [https://doi.org/10.1016/0092-8674\(95\)90035-7](https://doi.org/10.1016/0092-8674(95)90035-7).
- » Chow, L. T., R. E. Gelinas, T. R. Broker, and R. J. Roberts. 1977. “An Amazing Sequence Arrangement at the 5’ Ends of Adenovirus 2 Messenger RNA.” *Cell* 12 (1): 1–8. [https://doi.org/10.1016/0092-8674\(77\)90180-5](https://doi.org/10.1016/0092-8674(77)90180-5).
- » Chowdhury, Rebecca, Yue Wang, Melissa Campbell, Susan Goderie, Francis Doyle, Scott A. Tenenbaum, Gretchen Kusek, et al. 2021. “STAU2 Binds a Complex RNA Cargo That Changes Temporally with Production of Diverse Intermediate Progenitor Cells during Mouse Corticogenesis.” *Development*. <https://doi.org/10.1242/dev.199376>.
- » Cléry, Antoine, Rahul Sinha, Olga Anczuków, Anna Corrionero, Ahmed Moursy, Gerrit M. Daubner, Juan Valcárcel, Adrian R. Krainer, and Frédéric H.-T. Allain. 2013. “Isolated Pseudo-RNA-Recognition Motifs of SR Proteins Can Regulate Splicing Using a Noncanonical Mode of RNA Recognition.” *Proceedings of the National Academy of Sciences* 110 (30): E2802–11. <https://doi.org/10.1073/pnas.1303445110>.
- » Cobolli Gigli, Clementina, Linda Scaramuzza, Marco De Simone, Riccardo L. Rossi, Davide Pozzi, Massimiliano Pagani, Nicoletta Landsberger, and Francesco Bedogni. 2018. “Lack of Methyl-CpG Binding Protein 2 (MeCP2) Affects Cell Fate Refinement During Embryonic Cortical Development.” *Cerebral Cortex* 28 (5): 1846–56. <https://doi.org/10.1093/cercor/bhx360>.
- » Cohen, Michael, James Briscoe, and Robert Blassberg. 2013. “Morphogen Interpretation: The Transcriptional Logic of Neural Tube Patterning.” *Current Opinion in Genetics & Development* 23 (4): 423–28. <https://doi.org/10.1016/j.gde.2013.04.003>.

- » Conti, Luciano, Claudio De Fraja, Massimo Gulisano, Enrica Migliaccio, Stefano Govoni, and Elena Cattaneo. 1997. "Expression and Activation of SH2/PTB-Containing ShcA Adaptor Protein Reflects the Pattern of Neurogenesis in the Mammalian Brain." *Proceedings of the National Academy of Sciences* 94 (15): 8185–90. <https://doi.org/10.1073/pnas.94.15.8185>.
- » Cook, Kate B., Hilal Kazan, Khalid Zuberi, Quaid Morris, and Timothy R. Hughes. 2011. "RBPDB: A Database of RNA-Binding Specificities." *Nucleic Acids Research* 39 (Database issue): D301–8. <https://doi.org/10.1093/nar/gkq1069>.
- » Cronk, Katharine M., George A. Wilkinson, Rachel Grimes, Esther F. Wheeler, Sonal Jhaveri, Bengt T. Fundin, Immaculada Silos-Santiago, Lino Tessarollo, Louis F. Reichardt, and Frank L. Rice. 2002. "Diverse Dependencies of Developing Merkel Innervation on the TrkA and Both Full-Length and Truncated Isoforms of TrkC." *Development* 129 (15): 3739–50. <https://doi.org/10.1242/dev.129.15.3739>.
- » Cubelos, Beatriz, Carlos G. Briz, Gemma María Esteban-Ortega, and Marta Nieto. 2015. "Cux1 and Cux2 Selectively Target Basal and Apical Dendritic Compartments of Layer II-III Cortical Neurons." *Developmental Neurobiology* 75 (2): 163–72. <https://doi.org/10.1002/dneu.22215>.
- » Czuby, Alicja, and Agnieszka Piekietko-Witkowska. 2017. "Protein Kinases That Phosphorylate Splicing Factors: Roles in Cancer Development, Progression and Possible Therapeutic Options." *The International Journal of Biochemistry & Cell Biology, Splicing*, 91 (October): 102–15. <https://doi.org/10.1016/j.biocel.2017.05.024>.
- » Da Cruz, Sandrine, and Don W Cleveland. 2011. "Understanding the Role of TDP-43 and FUS/TLS in ALS and Beyond." *Current Opinion in Neurobiology, Neurobiology of disease*, 21 (6): 904–19. <https://doi.org/10.1016/j.conb.2011.05.029>.
- » Dang, Lan, and Vincent Tropepe. 2006. "Neural Induction and Neural Stem Cell Development." *Regenerative Medicine* 1 (5): 635–52. <https://doi.org/10.2217/17460751.1.5.635>.
- » Das, Shipra, and Adrian R. Krainer. 2014. "Emerging Functions of SRSF1, Splicing Factor and Oncoprotein, in RNA Metabolism and Cancer." *Molecular Cancer Research* 12 (9): 1195–1204. <https://doi.org/10.1158/1541-7786.MCR-14-0131>.
- » De Crescenzo, Franco, Valentina Postorino, Martina Siracusano, Assia Riccioni, Marco Armando, Paolo Curatolo, and Luigi Mazzone. 2019. "Autistic Symptoms in Schizophrenia Spectrum Disorders: A Systematic Review and Meta-Analysis." *Frontiers in Psychiatry* 10 (February): 78. <https://doi.org/10.3389/fpsy.2019.00078>.
- » DeBoer, E. M., M. L. Kraushar, R. P. Hart, and M. -R. Rasin. 2013. "Post-Transcriptional Regulatory Elements and Spatiotemporal Specification of Neocortical Stem Cells and Projection Neurons." *Neuroscience* 248 (September): 499–528. <https://doi.org/10.1016/j.neuroscience.2013.05.042>.
- » Desai, A. R., and S. K. McConnell. 2000. "Progressive Restriction in Fate Potential by Neural Progenitors during Cerebral Cortical Development." *Development (Cambridge, England)* 127 (13): 2863–72.
- » Dhananjaya, D, H Kuan-Yang, and Tarn Woan-Yuh. 2018. "RBM4 Modulates Radial Migration via Alternative Splicing of Dab1 during Cortex Development." *Molecular and Cellular Biology* 38 (12). <https://doi.org/10.1128/MCB.00007-18>.

- » Dhanjal, Soniya, Naoko Kajitani, Jacob Glahder, Ann-Kristin Mossberg, Cecilia Johansson, and Stefan Schwartz. 2015. “Heterogeneous Nuclear Ribonucleoprotein C Proteins Interact with the Human Papillomavirus Type 16 (HPV16) Early 3'-Untranslated Region and Alleviate Suppression of HPV16 Late L1 mRNA Splicing.” *The Journal of Biological Chemistry* 290 (21): 13354–71. <https://doi.org/10.1074/jbc.M115.638098>.
- » Dillman, Allissa A., David N. Hauser, J. Raphael Gibbs, Michael A. Nalls, Melissa K. McCoy, Iakov N. Rudenko, Dagmar Galter, and Mark R. Cookson. 2013. “Messenger RNA Expression, Splicing and Editing in the Embryonic and Adult Mouse Cerebral Cortex.” *Nature Neuroscience* 16 (4): 499–506. <https://doi.org/10.1038/nn.3332>.
- » Ding, Xinlu, Sanxiong Liu, Miaomiao Tian, Wenhao Zhang, Tao Zhu, Dongdong Li, Jiawei Wu, et al. 2017. “Activity-Induced Histone Modifications Govern Neurexin-1 mRNA Splicing and Memory Preservation.” *Nature Neuroscience* 20 (5): 690–99. <https://doi.org/10.1038/nn.4536>.
- » Dobрева, Gergana, Maria Chahrour, Marcel Dautzenberg, Laura Chirivella, Benoit Kanzler, Isabel Fariñas, Gerard Karsenty, and Rudolf Grosschedl. 2006. “SATB2 Is a Multifunctional Determinant of Craniofacial Patterning and Osteoblast Differentiation.” *Cell* 125 (5): 971–86. <https://doi.org/10.1016/j.cell.2006.05.012>.
- » Dominguez, Martin H., Albert E. Ayoub, and Pasko Rakic. 2013. “POU-III Transcription Factors (Brn1, Brn2, and Oct6) Influence Neurogenesis, Molecular Identity, and Migratory Destination of Upper-Layer Cells of the Cerebral Cortex.” *Cerebral Cortex (New York, N.Y.: 1991)* 23 (11): 2632–43. <https://doi.org/10.1093/cercor/bhs252>.
- » Dreyfuss, Gideon, Michael J. Matunis, Serafin Pinol-Roma, and Christopher G. Burd. 1993. “HnRNP PROTEINS AND THE BIOGENESIS OF MRNA.” *Annual Review of Biochemistry* 62 (1): 289–321. <https://doi.org/10.1146/annurev.bi.62.070193.001445>.
- » Duan, Weicheng, Kang Wang, Yijie Duan, Xufeng Chu, Ruoyun Ma, Ping Hu, and Bo Xiong. 2020. “Integrated Transcriptome Analyses Revealed Key Target Genes in Mouse Models of Autism.” *Autism Research: Official Journal of the International Society for Autism Research* 13 (3): 352–68. <https://doi.org/10.1002/aur.2240>.
- » Early, P., J. Rogers, M. Davis, K. Calame, M. Bond, R. Wall, and L. Hood. 1980. “Two MRNAs Can Be Produced from a Single Immunoglobulin Mu Gene by Alternative RNA Processing Pathways.” *Cell* 20 (2): 313–19. [https://doi.org/10.1016/0092-8674\(80\)90617-0](https://doi.org/10.1016/0092-8674(80)90617-0).
- » Ehrmann, Ingrid, Caroline Dalglish, Yilei Liu, Marina Danilenko, Moira Crosier, Lynn Overman, Helen M. Arthur, et al. 2013. “The Tissue-Specific RNA Binding Protein T-STAR Controls Regional Splicing Patterns of Neurexin Pre-MRNAs in the Brain.” *PLOS Genetics* 9 (4): e1003474. <https://doi.org/10.1371/journal.pgen.1003474>.
- » Englund, Chris, Andy Fink, Charmaine Lau, Diane Pham, Ray A. M. Daza, Alessandro Bulfone, Tom Kowalczyk, and Robert F. Hevner. 2005. “Pax6, Tbr2, and Tbr1 Are Expressed Sequentially by Radial Glia, Intermediate Progenitor Cells, and Postmitotic Neurons in Developing Neocortex.” *Journal of Neuroscience* 25 (1): 247–51. <https://doi.org/10.1523/JNEUROSCI.2899-04.2005>.
- » Erkelenz, Steffen, Frank Hillebrand, Marek Widera, Stephan Theiss, Anaam Fayyaz, Daniel Degrandi, Klaus Pfeffer, and Heiner Schaal. 2015. “Balanced Splicing at the Tat-Specific HIV-1 3' ss A3 Is

Critical for HIV-1 Replication.” *Retrovirology* 12 (March). <https://doi.org/10.1186/s12977-015-0154-8>.

» Erkelenz, Steffen, William F. Mueller, Melanie S. Evans, Anke Busch, Katrin Schöneweis, Klemens J. Hertel, and Heiner Schaal. 2013. “Position-Dependent Splicing Activation and Repression by SR and HnRNP Proteins Rely on Common Mechanisms.” *RNA* 19 (1): 96–102. <https://doi.org/10.1261/rna.037044.112>.

» Erkelenz, Steffen, Stephan Theiss, Marianne Otte, Marek Widera, Jan Otto Peter, and Heiner Schaal. 2013. “HEXploring of the HIV-1 Genome Allows Landscaping of New Potential Splicing Regulatory Elements.” *Retrovirology* 10 (S1): P78. <https://doi.org/10.1186/1742-4690-10-S1-P78>.

» Erkelenz, Steffen, Stephan Theiss, Marianne Otte, Marek Widera, Jan Otto Peter, and Heiner Schaal. 2014. “Genomic HEXploring Allows Landscaping of Novel Potential Splicing Regulatory Elements.” *Nucleic Acids Research* 42 (16): 10681–97. <https://doi.org/10.1093/nar/gku736>.

» Esteban, Pedro F., Hye-Young Yoon, Jodi Becker, Susan G. Dorsey, Paola Caprari, Mary Ellen Palko, Vincenzo Coppola, H. Uri Saragovi, Paul A. Randazzo, and Lino Tessarollo. 2006. “A Kinase-Deficient TrkC Receptor Isoform Activates Arf6–Rac1 Signaling through the Scaffold Protein Tamalin.” *The Journal of Cell Biology* 173 (2): 291. <https://doi.org/10.1083/jcb.200512013>.

» Falcone, Carmen, Natalie-Ya Mevises, Tiffany Hong, Brett Dufour, Xiaohui Chen, Stephen C. Nottor, and Verónica Martínez Cerdeño. 2021. “Neuronal and Glial Cell Number Is Altered in a Cortical Layer-Specific Manner in Autism.” *Autism: The International Journal of Research and Practice*, June, 13623613211014408. <https://doi.org/10.1177/13623613211014408>.

» Fame, Ryann M., Jessica L. MacDonald, Sally L. Dunwoodie, Emi Takahashi, and Jeffrey D. Macklis. 2016. “Cited2 Regulates Neocortical Layer II/III Generation and Somatosensory Callosal Projection Neuron Development and Connectivity.” *The Journal of Neuroscience: The Official Journal of the Society for Neuroscience* 36 (24): 6403–19. <https://doi.org/10.1523/JNEUROSCI.4067-15.2016>.

» Fame, Ryann M., Jessica L. MacDonald, and Jeffrey D. Macklis. 2011. “Development, Specification, and Diversity of Callosal Projection Neurons.” *Trends in Neurosciences* 34 (1): 41–50. <https://doi.org/10.1016/j.tins.2010.10.002>.

» Fan, Xiaoying, Ji Dong, Suijuan Zhong, Yuan Wei, Qian Wu, Liying Yan, Jun Yong, et al. 2018. “Spatial Transcriptomic Survey of Human Embryonic Cerebral Cortex by Single-Cell RNA-Seq Analysis.” *Cell Research* 28 (7): 730–45. <https://doi.org/10.1038/s41422-018-0053-3>.

» Fang, Wei-Qun, Wei-Wei Chen, Liwen Jiang, Kai Liu, Wing-Ho Yung, Amy K.Y. Fu, and Nancy Y. Ip. 2014. “Overproduction of Upper-Layer Neurons in the Neocortex Leads to Autism-like Features in Mice.” *Cell Reports* 9 (5): 1635–43. <https://doi.org/10.1016/j.celrep.2014.11.003>.

» Faravelli, Irene, Monica Bucchia, Paola Rinchetti, Monica Nizzardo, Chiara Simone, Emanuele Frattini, and Stefania Corti. 2014. “Motor Neuron Derivation from Human Embryonic and Induced Pluripotent Stem Cells: Experimental Approaches and Clinical Perspectives.” *Stem Cell Research & Therapy* 5 (4): 87. <https://doi.org/10.1186/scrt476>.

» Fededa, Juan Pablo, Christopher Esk, Beata Mierzwa, Rugile Stanyte, Shuiqiao Yuan, Huili Zheng, Klaus Ebnet, Wei Yan, Juergen A. Knoblich, and Daniel W. Gerlich. 2016. “MicroRNA-34/449 Controls Mitotic Spindle Orientation during Mammalian Cortex Development.” *The EMBO Journal* 35 (22):

2386–98. <https://doi.org/10.15252/emj.201694056>.

- » Fenner, Barbara M. 2012. “Truncated TrkB: Beyond a Dominant Negative Receptor.” *Cytokine & Growth Factor Reviews* 23 (1): 15–24. <https://doi.org/10.1016/j.cytogfr.2012.01.002>.
- » Fietz, Simone A, and Wieland B Huttner. 2011. “Cortical Progenitor Expansion, Self-Renewal and Neurogenesis—a Polarized Perspective.” *Current Opinion in Neurobiology, Developmental neuroscience*, 21 (1): 23–35. <https://doi.org/10.1016/j.conb.2010.10.002>.
- » Fietz, Simone A., Iva Kelava, Johannes Vogt, Michaela Wilsch-Bräuninger, Denise Stenzel, Jennifer L. Fish, Denis Corbeil, et al. 2010. “OSVZ Progenitors of Human and Ferret Neocortex Are Epithelial-like and Expand by Integrin Signaling.” *Nature Neuroscience* 13 (6): 690–99. <https://doi.org/10.1038/nn.2553>.
- » Fietz, Simone A., Robert Lachmann, Holger Brandl, Martin Kircher, Nikolay Samusik, Roland Schröder, Naharajan Lakshmanaperumal, et al. 2012. “Transcriptomes of Germinal Zones of Human and Mouse Fetal Neocortex Suggest a Role of Extracellular Matrix in Progenitor Self-Renewal.” *Proceedings of the National Academy of Sciences* 109 (29): 11836–41. <https://doi.org/10.1073/pnas.1209647109>.
- » Florio, Marta, Mareike Albert, Elena Taverna, Takashi Namba, Holger Brandl, Eric Lewitus, Christiane Haffner, et al. 2015. “Human-Specific Gene ARHGAP11B Promotes Basal Progenitor Amplification and Neocortex Expansion.” *Science (New York, N.Y.)* 347 (6229): 1465–70. <https://doi.org/10.1126/science.aaa1975>.
- » Florio, Marta, and Wieland B. Huttner. 2014. “Neural Progenitors, Neurogenesis and the Evolution of the Neocortex.” *Development (Cambridge, England)* 141 (11): 2182–94. <https://doi.org/10.1242/dev.090571>.
- » Franco, Santos J., Cristina Gil-Sanz, Isabel Martinez-Garay, Ana Espinosa, Sarah R. Harkins-Perry, Cynthia Ramos, and Ulrich Müller. 2012. “Fate-Restricted Neural Progenitors in the Mammalian Cerebral Cortex.” *Science (New York, N.Y.)* 337 (6095): 746–49. <https://doi.org/10.1126/science.1223616>.
- » Frantz, G. D., and S. K. McConnell. 1996. “Restriction of Late Cerebral Cortical Progenitors to an Upper-Layer Fate.” *Neuron* 17 (1): 55–61. [https://doi.org/10.1016/s0896-6273\(00\)80280-9](https://doi.org/10.1016/s0896-6273(00)80280-9).
- » Freund, Marcel, Corinna Asang, Susanne Kammler, Carolin Konermann, Jörg Krummheuer, Marianne Hipp, Imke Meyer, et al. 2003. “A Novel Approach to Describe a U1 SnRNA Binding Site.” *Nucleic Acids Research* 31 (23): 6963–75. <https://doi.org/10.1093/nar/gkg901>.
- » Friedman, Robin C., Kyle Kai-How Farh, Christopher B. Burge, and David P. Bartel. 2009. “Most Mammalian MRNAs Are Conserved Targets of MicroRNAs.” *Genome Research* 19 (1): 92–105. <https://doi.org/10.1101/gr.082701.108>.
- » Fu, Xiang-Dong, and Manuel Ares. 2014. “Context-Dependent Control of Alternative Splicing by RNA-Binding Proteins.” *Nature Reviews Genetics* 15 (10): 689–701. <https://doi.org/10.1038/nrg3778>.
- » Fukuhara, Takeshi, Takamitsu Hosoya, Saki Shimizu, Kengo Sumi, Takako Oshiro, Yoshiyuki Yoshinaka, Masaaki Suzuki, et al. 2006. “Utilization of Host SR Protein Kinases and RNA-Splicing Machinery during Viral Replication.” *Proceedings of the National Academy of Sciences of the United*

States of America 103 (30): 11329–33. <https://doi.org/10.1073/pnas.0604616103>.

- » Furlanis, Elisabetta, Lisa Traunmüller, Geoffrey Fucile, and Peter Scheiffele. 2019. “Landscape of Ribosome-Engaged Transcript Isoforms Reveals Extensive Neuronal-Cell-Class-Specific Alternative Splicing Programs.” *Nature Neuroscience* 22 (10): 1709–17. <https://doi.org/10.1038/s41593-019-0465-5>.
- » Gallego-Paez, L. M., M. C. Bordone, A. C. Leote, N. Saraiva-Agostinho, M. Ascensão-Ferreira, and N. L. Barbosa-Morais. 2017. “Alternative Splicing: The Pledge, the Turn, and the Prestige: The Key Role of Alternative Splicing in Human Biological Systems.” *Human Genetics*, April. <https://doi.org/10.1007/s00439-017-1790-y>.
- » Gammons, Melissa V., Oleg Fedorov, David Ivison, Chunyun Du, Tamsyn Clark, Claire Hopkins, Masatoshi Hagiwara, et al. 2013. “Topical Antiangiogenic SRPK1 Inhibitors Reduce Choroidal Neovascularization in Rodent Models of Exudative AMD.” *Investigative Ophthalmology & Visual Science* 54 (9): 6052–62. <https://doi.org/10.1167/iovs.13-12422>.
- » Gandal, Michael J., Jillian R. Haney, Neelroop N. Parikshak, Virpi Leppa, Gokul Ramaswami, Chris Hartl, Andrew J. Schork, et al. 2018. “Shared Molecular Neuropathology across Major Psychiatric Disorders Parallels Polygenic Overlap.” *Science (New York, N.Y.)* 359 (6376): 693–97. <https://doi.org/10.1126/science.aad6469>.
- » Gao, Peng, Maria Pia Postiglione, Teresa G. Krieger, Luisirene Hernandez, Chao Wang, Zhi Han, Carmen Streicher, et al. 2014. “Deterministic Progenitor Behavior and Unitary Production of Neurons in the Neocortex.” *Cell* 159 (4): 775–88. <https://doi.org/10.1016/j.cell.2014.10.027>.
- » Gao, Zhihua, and Roseline Godbout. 2013. “Reelin-Disabled-1 Signaling in Neuronal Migration: Splicing Takes the Stage.” *Cellular and Molecular Life Sciences: CMLS* 70 (13): 2319–29. <https://doi.org/10.1007/s00018-012-1171-6>.
- » Gao, Zhihua, Ho Yin Poon, Lei Li, Xiaodong Li, Elena Palmesino, Darryl D. Glubrecht, Karen Colwill, et al. 2012. “Splice-Mediated Motif Switching Regulates Disabled-1 Phosphorylation and SH2 Domain Interactions.” *Molecular and Cellular Biology* 32 (14): 2794–2808. <https://doi.org/10.1128/MCB.00570-12>.
- » Geschwind, Daniel H., and Pasko Rakic. 2013. “Cortical Evolution: Judge the Brain by Its Cover.” *Neuron* 80 (3): 633–47. <https://doi.org/10.1016/j.neuron.2013.10.045>.
- » Ghosh, Gourisankar, and Joseph A. Adams. 2011. “Phosphorylation Mechanism and Structure of Serine-Arginine Protein Kinases.” *The FEBS Journal* 278 (4): 587–97. <https://doi.org/10.1111/j.1742-4658.2010.07992.x>.
- » Giudice, Girolamo, Fátima Sánchez-Cabo, Carlos Torroja, and Enrique Lara-Pezzi. 2016. “AT-TRACT—a Database of RNA-Binding Proteins and Associated Motifs.” *Database: The Journal of Biological Databases and Curation* 2016 (April). <https://doi.org/10.1093/database/baw035>.
- » Gorski, Jessica A., Tiffany Talley, Mengsheng Qiu, Luis Puelles, John L. R. Rubenstein, and Kevin R. Jones. 2002. “Cortical Excitatory Neurons and Glia, But Not GABAergic Neurons, Are Produced in the Emx1-Expressing Lineage.” *Journal of Neuroscience* 22 (15): 6309–14. <https://doi.org/10.1523/JNEUROSCI.22-15-06309.2002>.

- » Götz, Magdalena, and Wieland B. Huttner. 2005. "The Cell Biology of Neurogenesis." *Nature Reviews. Molecular Cell Biology* 6 (10): 777–88. <https://doi.org/10.1038/nrm1739>.
- » Grange, Pierre de la, Lise Gratadou, Marc Delord, Martin Dutertre, and Didier Auboeuf. 2010. "Splicing Factor and Exon Profiling across Human Tissues." *Nucleic Acids Research* 38 (9): 2825–38. <https://doi.org/10.1093/nar/gkq008>.
- » Greig, Luciano Custo, Mollie B. Woodworth, Maria J. Galazo, Hari Padmanabhan, and Jeffrey D. Macklis. 2013. "Molecular Logic of Neocortical Projection Neuron Specification, Development and Diversity." *Nature Reviews Neuroscience* 14 (11): 755–69. <https://doi.org/10.1038/nrn3586>.
- » Grosso, Ana Rita, Anita Q. Gomes, Nuno L. Barbosa-Morais, Sandra Caldeira, Natalie P. Thorne, Godfrey Grech, Marieke von Lindern, and Maria Carmo-Fonseca. 2008. "Tissue-Specific Splicing Factor Gene Expression Signatures." *Nucleic Acids Research* 36 (15): 4823–32. <https://doi.org/10.1093/nar/gkn463>.
- » Grove, E. A., S. Tole, J. Limon, L. Yip, and C. W. Ragsdale. 1998. "The Hem of the Embryonic Cerebral Cortex Is Defined by the Expression of Multiple Wnt Genes and Is Compromised in Gli3-Deficient Mice." *Development* 125 (12): 2315–25.
- » Guo, Chao, Matthew J. Eckler, William L. McKenna, Gabriel L. McKinsey, John L. R. Rubenstein, and Bin Chen. 2013. "Fezf2 Expression Identifies a Multipotent Progenitor for Neocortical Projection Neurons, Astrocytes, and Oligodendrocytes." *Neuron* 80 (5): 1167–74. <https://doi.org/10.1016/j.neuron.2013.09.037>.
- » Ha, Minju, and V. Narry Kim. 2014. "Regulation of MicroRNA Biogenesis." *Nature Reviews Molecular Cell Biology* 15 (8): 509–24. <https://doi.org/10.1038/nrm3838>.
- » Hamada, Nanako, Hidenori Ito, Ikuko Iwamoto, Rika Morishita, Hidenori Tabata, and Koh-ichi Nagata. 2015. "Role of the Cytoplasmic Isoform of RBFOX1/A2BP1 in Establishing the Architecture of the Developing Cerebral Cortex." *Molecular Autism* 6 (1): 56. <https://doi.org/10.1186/s13229-015-0049-5>.
- » Han, Hong, Manuel Irimia, P. Joel Ross, Hoon-Ki Sung, Babak Alipanahi, Laurent David, Azadeh Golipour, et al. 2013. "MBNL Proteins Repress Embryonic Stem Cell-Specific Alternative Splicing and Reprogramming." *Nature* 498 (7453): 241–45. <https://doi.org/10.1038/nature12270>.
- » Hanashima, Carina, Suzanne C. Li, Lijian Shen, Eseng Lai, and Gord Fishell. 2004. "Foxg1 Suppresses Early Cortical Cell Fate." *Science* 303 (5654): 56–59. <https://doi.org/10.1126/science.1090674>.
- » Haubensak, Wulf, Alessio Attardo, Winfried Denk, and Wieland B. Huttner. 2004. "Neurons Arise in the Basal Neuroepithelium of the Early Mammalian Telencephalon: A Major Site of Neurogenesis." *Proceedings of the National Academy of Sciences of the United States of America* 101 (9): 3196–3201. <https://doi.org/10.1073/pnas.0308600100>.
- » Heavner, Whitney E., Shaoyi Ji, James H. Notwell, Ethan S. Dyer, Alex M. Tseng, Johannes Birgmeier, Boyoung Yoo, Gill Bejerano, and Susan K. McConnell. 2020. "Transcription Factor Expression Defines Subclasses of Developing Projection Neurons Highly Similar to Single-Cell RNA-Seq Subtypes." *Proceedings of the National Academy of Sciences of the United States of America*, September. <https://doi.org/10.1073/pnas.2008013117>.

- » Hébert, Jean M., and Gord Fishell. 2008. “The Genetics of Early Telencephalon Patterning: Some Assembly Required.” *Nature Reviews. Neuroscience* 9 (9): 678–85. <https://doi.org/10.1038/nrn2463>.
- » Hevner, Robert F., Ray A. M. Daza, John L. R. Rubenstein, Henk Stunnenberg, Jaime F. Olavarria, and Chris Englund. 2003. “Beyond Laminar Fate: Toward a Molecular Classification of Cortical Projection/Pyramidal Neurons.” *Developmental Neuroscience* 25 (2–4): 139–51. <https://doi.org/10.1159/000072263>.
- » Heyd, Florian, and Kristen W. Lynch. 2011. “DEGRADE, MOVE, REGROUP: Signaling Control of Splicing Proteins.” *Trends in Biochemical Sciences* 36 (8): 397–404. <https://doi.org/10.1016/j.tibs.2011.04.003>.
- » Hinrich, Anthony J., Francine M. Jodelka, Jennifer L. Chang, Daniella Brutman, Angela M. Bruno, Clark A. Briggs, Bryan D. James, et al. 2016. “Therapeutic Correction of ApoER2 Splicing in Alzheimer’s Disease Mice Using Antisense Oligonucleotides.” *EMBO Molecular Medicine* 8 (4): 328–45. <https://doi.org/10.15252/emmm.201505846>.
- » Howe, Kevin L, Premanand Achuthan, James Allen, Jamie Allen, Jorge Alvarez-Jarreta, M Ridwan Amode, Irina M Armean, et al. 2021. “Ensembl 2021.” *Nucleic Acids Research* 49 (D1): D884–91. <https://doi.org/10.1093/nar/gkaa942>.
- » Hu, Wen F., Maria H. Chahrour, and Christopher A. Walsh. 2014. “The Diverse Genetic Landscape of Neurodevelopmental Disorders.” *Annual Review of Genomics and Human Genetics* 15: 195–213. <https://doi.org/10.1146/annurev-genom-090413-025600>.
- » Huang, August Yue, Pengpeng Li, Rachel E. Rodin, Sonia N. Kim, Yanmei Dou, Connor J. Kenny, Shyam K. Akula, et al. 2020. “Parallel RNA and DNA Analysis after Deep Sequencing (PRDD-Seq) Reveals Cell Type-Specific Lineage Patterns in Human Brain.” *Proceedings of the National Academy of Sciences of the United States of America* 117 (25): 13886–95. <https://doi.org/10.1073/pnas.2006163117>.
- » Huang, Eric J., and Louis F. Reichardt. 2001. “Neurotrophins: Roles in Neuronal Development and Function.” *Annual Review of Neuroscience* 24: 677. <https://doi.org/10.1146/annurev.neuro.24.1.677>.
- » Huang, Eric J., and Louis F. Reichardt. 2003. “Trk Receptors: Roles in Neuronal Signal Transduction.” *Annual Review of Biochemistry* 72: 609–42. <https://doi.org/10.1146/annurev.biochem.72.121801.161629>.
- » Huang, Yingqun, Renata Gattoni, James Stévenin, and Joan A. Steitz. 2003. “SR Splicing Factors Serve as Adapter Proteins for TAP-Dependent mRNA Export.” *Molecular Cell* 11 (3): 837–43. [https://doi.org/10.1016/S1097-2765\(03\)00089-3](https://doi.org/10.1016/S1097-2765(03)00089-3).
- » Ichinose, T., and W. D. Snider. 2000. “Differential Effects of TrkC Isoforms on Sensory Axon Outgrowth.” *Journal of Neuroscience Research* 59 (3): 365–71. [https://doi.org/10.1002/\(sici\)1097-4547\(20000201\)59:3<365::aid-jnr10>3.0.co;2-i](https://doi.org/10.1002/(sici)1097-4547(20000201)59:3<365::aid-jnr10>3.0.co;2-i).
- » Iijima, Takatoshi, Karen Wu, Harald Witte, Yoko Hanno-Iijima, Timo Glatter, Stéphane Richard, and Peter Scheiffele. 2011. “SAM68 Regulates Neuronal Activity-Dependent Alternative Splicing of Neurexin-1.” *Cell* 147 (7): 1601–14.
- » Ince-Dunn, Gulayse, Hirotaka James Okano, Kirk Jensen, Woong-Yang Park, Zhong Ru, Jernej Ule,

Aldo Mele, et al. 2012. "Neuronal Elav-like (Hu) Proteins Regulate RNA Splicing and Abundance to Control Glutamate Levels and Neuronal Excitability." *Neuron* 75 (6): 1067–80. <https://doi.org/10.1016/j.neuron.2012.07.009>.

» Irimia, Manuel, and Benjamin J Blencowe. 2012. "Alternative Splicing: Decoding an Expansive Regulatory Layer." *Current Opinion in Cell Biology, Nucleus and gene expression*, 24 (3): 323–32. <https://doi.org/10.1016/j.ceb.2012.03.005>.

» Irimia, Manuel, Robert J. Weatheritt, Jonathan D. Ellis, Neelroop N. Parikshak, Thomas Gonatopoulos-Pournatzis, Mariana Babor, Mathieu Quesnel-Vallières, et al. 2014. "A Highly Conserved Program of Neuronal Microexons Is Misregulated in Autistic Brains." *Cell* 159 (7): 1511–23. <https://doi.org/10.1016/j.cell.2014.11.035>.

» Jabaudon, Denis. 2017. "Fate and Freedom in Developing Neocortical Circuits." *Nature Communications* 8 (July). <https://doi.org/10.1038/ncomms16042>.

» Jaffe, Andrew E., Richard E. Straub, Joo Heon Shin, Ran Tao, Yuan Gao, Leonardo Collado-Torres, Tony Kam-Thong, et al. 2018. "Developmental and Genetic Regulation of the Human Cortex Transcriptome Illuminate Schizophrenia Pathogenesis." *Nature Neuroscience* 21 (8): 1117–25. <https://doi.org/10.1038/s41593-018-0197-y>.

» Jankowsky, Eckhard, and Michael E. Harris. 2015. "Specificity and Non-Specificity in RNA-Protein Interactions." *Nature Reviews. Molecular Cell Biology* 16 (9): 533–44. <https://doi.org/10.1038/nrm4032>.

» Johnson, Jason M., John Castle, Philip Garrett-Engele, Zhengyan Kan, Patrick M. Loerch, Christopher D. Armour, Ralph Santos, Eric E. Schadt, Roland Stoughton, and Daniel D. Shoemaker. 2003. "Genome-Wide Survey of Human Alternative Pre-mRNA Splicing with Exon Junction Microarrays." *Science* 302 (5653): 2141–44. <https://doi.org/10.1126/science.1090100>.

» Kageyama, Jorge, Damian Wollny, Barbara Treutlein, and J. Gray Camp. 2018. "ShinyCortex: Exploring Single-Cell Transcriptome Data From the Developing Human Cortex." *Frontiers in Neuroscience* 12: 315. <https://doi.org/10.3389/fnins.2018.00315>.

» Kalsotra, Auinash, and Thomas A. Cooper. 2011. "Functional Consequences of Developmentally Regulated Alternative Splicing." *Nature Reviews Genetics* 12 (10): 715–29. <https://doi.org/10.1038/nrg3052>.

» Kang, Hyo Jung, Yuka Imamura Kawasawa, Feng Cheng, Ying Zhu, Xuming Xu, Mingfeng Li, André M. M. Sousa, et al. 2011. "Spatiotemporal Transcriptome of the Human Brain." *Nature* 478 (7370): 483–89. <https://doi.org/10.1038/nature10523>.

» Kelly, Ryan T. 2020. "Single-Cell Proteomics: Progress and Prospects." *Molecular & Cellular Proteomics: MCP* 19 (11): 1739–48. <https://doi.org/10.1074/mcp.R120.002234>.

» Kim, Kee K., Joseph Nam, Yoh-suke Mukoyama, and Sachiyo Kawamoto. 2013. "Rbfox3-Regulated Alternative Splicing of Numb Promotes Neuronal Differentiation during Development." *The Journal of Cell Biology* 200 (4): 443–58. <https://doi.org/10.1083/jcb.201206146>.

» Klein, R., D. Conway, L. F. Parada, and M. Barbacid. 1990. "The TrkB Tyrosine Protein Kinase Gene

Codes for a Second Neurogenic Receptor That Lacks the Catalytic Kinase Domain.” *Cell* 61 (4): 647–56. [https://doi.org/10.1016/0092-8674\(90\)90476-u](https://doi.org/10.1016/0092-8674(90)90476-u).

» Klein, Rüdiger, Inmaculada Silos-Santiago, Richard J. Smeyne, Sergio A. Lira, Riccardo Brambilla, Sherri Bryant, Li Zhang, William D. Snider, and Mariano Barbacid. 1994. “Disruption of the Neurotrophin-3 Receptor Gene *TrkC* Eliminates La Muscle Afferents and Results in Abnormal Movements.” *Nature* 368 (6468): 249–51. <https://doi.org/10.1038/368249a0>.

» Koester, S. E., and D. D. O’Leary. 1993. “Connectional Distinction between Callosal and Subcortically Projecting Cortical Neurons Is Determined Prior to Axon Extension.” *Developmental Biology* 160 (1): 1–14. <https://doi.org/10.1006/dbio.1993.1281>.

» Kowalczyk, Tom, Adria Pontious, Chris Englund, Ray A. M. Daza, Francesco Bedogni, Rebecca Hodge, Alessio Attardo, Chris Bell, Wieland B. Huttner, and Robert F. Hevner. 2009. “Intermediate Neuronal Progenitors (Basal Progenitors) Produce Pyramidal-Projection Neurons for All Layers of Cerebral Cortex.” *Cerebral Cortex* (New York, N.Y.: 1991) 19 (10): 2439–50. <https://doi.org/10.1093/cercor/bhn260>.

» Kraushar, Matthew L., Kevin Thompson, H. R. Sagara Wijeratne, Barbara Viljetic, Kristina Sakers, Justin W. Marson, Dimitris L. Kontoyiannis, Steven Buyske, Ronald P. Hart, and Mladen-Roko Rasin. 2014. “Temporally Defined Neocortical Translation and Polysome Assembly Are Determined by the RNA-Binding Protein Hu Antigen R.” *Proceedings of the National Academy of Sciences* 111 (36): E3815–24. <https://doi.org/10.1073/pnas.1408305111>.

» Lamballe, Fabienne, Rüdiger Klein, and Mariano Barbacid. 1991. “*TrkC*, a New Member of the *Trk* Family of Tyrosine Protein Kinases, Is a Receptor for Neurotrophin-3.” *Cell* 66 (5): 967–79. [https://doi.org/10.1016/0092-8674\(91\)90442-2](https://doi.org/10.1016/0092-8674(91)90442-2).

» Lareau, Liana F., Maki Inada, Richard E. Green, Jordan C. Wengrod, and Steven E. Brenner. 2007. “Unproductive Splicing of SR Genes Associated with Highly Conserved and Ultraconserved DNA Elements.” *Nature* 446 (7138): 926–29. <https://doi.org/10.1038/nature05676>.

» Lebedeva, Svetlana, Marvin Jens, Kathrin Theil, Björn Schwanhäusser, Matthias Selbach, Markus Landthaler, and Nikolaus Rajewsky. 2011. “Transcriptome-Wide Analysis of Regulatory Interactions of the RNA-Binding Protein HuR.” *Molecular Cell* 43 (3): 340–52. <https://doi.org/10.1016/j.molcel.2011.06.008>.

» Lee, Seungjae, Lu Wei, Binglong Zhang, Raeann Goering, Sonali Majumdar, Jiayu Wen, J. Matthew Taliaferro, and Eric C. Lai. 2021. “ELAV/Hu RNA Binding Proteins Determine Multiple Programs of Neural Alternative Splicing.” *PLOS Genetics* 17 (4): e1009439. <https://doi.org/10.1371/journal.pgen.1009439>.

» Lee, Soo-Ho, Hyun-Kyung Lee, Chowon Kim, Yoo-Kyung Kim, Tayaba Ismail, Youngeun Jeong, Kyeongyeon Park, et al. 2016. “The Splicing Factor SRSF1 Modulates Pattern Formation by Inhibiting Transcription of Tissue Specific Genes during Embryogenesis.” *Biochemical and Biophysical Research Communications* 477 (4): 1011–16. <https://doi.org/10.1016/j.bbrc.2016.07.021>.

» Lee, Yeon, and Donald C. Rio. 2015. “Mechanisms and Regulation of Alternative Pre-mRNA Splicing.” *Annual Review of Biochemistry* 84: 291–323. <https://doi.org/10.1146/annurev-biochem-060614-034316>.

- » Leggere, Janelle C., Yuhki Saito, Robert B. Darnell, Marc Tessier-Lavigne, Harald J. Junge, and Zhe Chen. 2016. “NOVA Regulates Dcc Alternative Splicing during Neuronal Migration and Axon Guidance in the Spinal Cord.” *ELife* 5 (May): e14264. <https://doi.org/10.7554/eLife.14264>.
- » Li, Qin, Ji-Ann Lee, and Douglas L. Black. 2007. “Neuronal Regulation of Alternative Pre-mRNA Splicing.” *Nature Reviews Neuroscience* 8 (11): 819–31. <https://doi.org/10.1038/nrn2237>.
- » Licatalosi, Donny D., Aldo Mele, John J. Fak, Jernej Ule, Melis Kayikci, Sung Wook Chi, Tyson A. Clark, et al. 2008. “HITS-CLIP Yields Genome-Wide Insights into Brain Alternative RNA Processing.” *Nature* 456 (7221): 464–69. <https://doi.org/10.1038/nature07488>.
- » Liu, Hong-Xiang, Michael Zhang, and Adrian R. Krainer. 1998. “Identification of Functional Exonic Splicing Enhancer Motifs Recognized by Individual SR Proteins.” *Genes & Development* 12 (13): 1998–2012. <https://doi.org/10.1101/gad.12.13.1998>.
- » Lodato, Simona, Ashwin S. Shetty, and Paola Arlotta. 2015. “Cerebral Cortex Assembly: Generating and Reprogramming Projection Neuron Diversity.” *Trends in Neurosciences* 38 (2): 117–25. <https://doi.org/10.1016/j.tins.2014.11.003>.
- » Long, Jennifer C., and Javier F. Cáceres. 2009. “The SR Protein Family of Splicing Factors: Master Regulators of Gene Expression.” *The Biochemical Journal* 417 (1): 15–27. <https://doi.org/10.1042/BJ20081501>.
- » Loo, Lipin, Jeremy M. Simon, Lei Xing, Eric S. McCoy, Jesse K. Niehaus, Jiami Guo, E. S. Anton, and Mark J. Zylka. 2019. “Single-Cell Transcriptomic Analysis of Mouse Neocortical Development.” *Nature Communications* 10 (1): 134. <https://doi.org/10.1038/s41467-018-08079-9>.
- » Lukaszewicz, Agnès, Pierre Savatier, Véronique Cortay, Henry Kennedy, and Colette Dehay. 2002. “Contrasting Effects of Basic Fibroblast Growth Factor and Neurotrophin 3 on Cell Cycle Kinetics of Mouse Cortical Stem Cells.” *The Journal of Neuroscience: The Official Journal of the Society for Neuroscience* 22 (15): 6610–22. <https://doi.org/20026666>.
- » Makeyev, Eugene V., Jiangwen Zhang, Monica A. Carrasco, and Tom Maniatis. 2007. “The MicroRNA MiR-124 Promotes Neuronal Differentiation by Triggering Brain-Specific Alternative Pre-mRNA Splicing.” *Molecular Cell* 27 (3): 435–48. <https://doi.org/10.1016/j.molcel.2007.07.015>.
- » Mao, Susu, Hanqin Li, Qi Sun, Ke Zen, Chen-Yu Zhang, and Liang Li. 2014. “MiR-17 Regulates the Proliferation and Differentiation of the Neural Precursor Cells during Mouse Corticogenesis.” *The FEBS Journal* 281 (4): 1144–58. <https://doi.org/10.1111/febs.12680>.
- » Marín, O., and J. L. Rubenstein. 2001. “A Long, Remarkable Journey: Tangential Migration in the Telencephalon.” *Nature Reviews. Neuroscience* 2 (11): 780–90. <https://doi.org/10.1038/35097509>.
- » Martins, Manuella, Silvia Galfrè, Marco Terrigno, Luca Pandolfini, Irene Appolloni, Keagan Dunville, Andrea Marranci, et al. 2021. “A Eutherian-Specific MicroRNA Controls the Translation of *Satb2* in a Model of Cortical Differentiation.” *Stem Cell Reports* 16 (6): 1496–1509. <https://doi.org/10.1016/j.stemcr.2021.04.020>.
- » Maslon, Magdalena M, Ulrich Braunschweig, Stuart Aitken, Abigail R Mann, and Fiona Kilanowski. 2019. “A Slow Transcription Rate Causes Embryonic Lethality and Perturbs Kinetic Coupling of

Neuronal Genes.” *The EMBO Journal* 38 (9): e101244. <https://doi.org/10.15252/embj.2018101244>.

» Mastrovito, Dana, Catherine Hanson, and Stephen Jose Hanson. 2018. “Differences in Atypical Resting-State Effective Connectivity Distinguish Autism from Schizophrenia.” *NeuroImage: Clinical* 18 (January): 367–76. <https://doi.org/10.1016/j.nicl.2018.01.014>.

» Mateos, Stéphanie, Georges Calothy, and Fabienne Lamballe. 2003. “The Noncatalytic TrkCNC2 Receptor Is Cleaved by Metalloproteases upon Neurotrophin-3 Stimulation.” *Oncogene* 22 (5): 740–45. <https://doi.org/10.1038/sj.onc.1206213>.

» Matlin, Arianne J., Francis Clark, and Christopher W. J. Smith. 2005. “Understanding Alternative Splicing: Towards a Cellular Code.” *Nature Reviews. Molecular Cell Biology* 6 (5): 386–98. <https://doi.org/10.1038/nrm1645>.

» Mayeda, Akila, and Adrian R. Krainer. 1992. “Regulation of Alternative Pre-mRNA Splicing by HnRNP A1 and Splicing Factor SF2.” *Cell* 68 (2): 365–75. [https://doi.org/10.1016/0092-8674\(92\)90477-T](https://doi.org/10.1016/0092-8674(92)90477-T).

» Mazin, Pavel V., Xi Jiang, Ning Fu, Dingding Han, Meng Guo, Mikhail S. Gelfand, and Philipp Khaitovich. 2018. “Conservation, Evolution, and Regulation of Splicing during Prefrontal Cortex Development in Humans, Chimpanzees, and Macaques.” *RNA* 24 (4): 585–96. <https://doi.org/10.1261/rna.064931.117>.

» Mazin, Pavel, Jieyi Xiong, Xiling Liu, Zheng Yan, Xiaoyu Zhang, Mingshuang Li, Liu He, et al. 2013. “Widespread Splicing Changes in Human Brain Development and Aging.” *Molecular Systems Biology* 9: 633. <https://doi.org/10.1038/msb.2012.67>.

» McAllister, A. K., D. C. Lo, and L. C. Katz. 1995. “Neurotrophins Regulate Dendritic Growth in Developing Visual Cortex.” *Neuron* 15 (4): 791–803. [https://doi.org/10.1016/0896-6273\(95\)90171-x](https://doi.org/10.1016/0896-6273(95)90171-x).

» McConnell, Susan K. 1995. “Constructing the Cerebral Cortex: Neurogenesis and Fate Determination.” *Neuron* 15 (4): 761–68. [https://doi.org/10.1016/0896-6273\(95\)90168-X](https://doi.org/10.1016/0896-6273(95)90168-X).

» McEvelly, Robert J., Marcela Ortiz de Diaz, Marcus D. Schonemann, Farideh Hooshmand, and Michael G. Rosenfeld. 2002. “Transcriptional Regulation of Cortical Neuron Migration by POU Domain Factors.” *Science (New York, N.Y.)* 295 (5559): 1528–32. <https://doi.org/10.1126/science.1067132>.

» McFarland, Karen N., Steven R. Wilkes, Sarah E. Koss, Kodi S. Ravichandran, and James W. Mandell. 2006. “Neural-Specific Inactivation of ShcA Results in Increased Embryonic Neural Progenitor Apoptosis and Microencephaly.” *Journal of Neuroscience* 26 (30): 7885–97. <https://doi.org/10.1523/JNEUROSCI.3524-05.2006>.

» McKee, Adrienne E., Emmanuel Minet, Charlene Stern, Shervin Riahi, Charles D. Stiles, and Pamela A. Silver. 2005. “A Genome-Wide *In Situ* Hybridization Map of RNA-Binding Proteins Reveals Anatomically Restricted Expression in the Developing Mouse Brain.” *BMC Developmental Biology* 5 (1): 14.

» McKenna, William L., Christian F. Ortiz-Londono, Thomas K. Mathew, Kendy Hoang, Sol Katzman, and Bin Chen. 2015. “Mutual Regulation between *Satb2* and *Fezf2* Promotes Subcerebral Projection Neuron Identity in the Developing Cerebral Cortex.” *Proceedings of the National Academy of Sci-*

ences of the United States of America 112 (37): 11702–7. <https://doi.org/10.1073/pnas.1504144112>.

» McManus, C Joel, and Brenton R Graveley. 2011. “RNA Structure and the Mechanisms of Alternative Splicing.” *Current Opinion in Genetics & Development, Differentiation and gene regulation*, 21 (4): 373–79. <https://doi.org/10.1016/j.gde.2011.04.001>.

» Medina, Diego L., Carla Sciarretta, Anna Maria Calella, Oliver Von Bohlen Und Halbach, Klaus Unsicker, and Liliana Minichiello. 2004. “TrkB Regulates Neocortex Formation through the Shc/PLC-gamma-Mediated Control of Neuronal Migration.” *The EMBO Journal* 23 (19): 3803–14. <https://doi.org/10.1038/sj.emboj.7600399>.

» Meisner, Nicole-Claudia, and Witold Filipowicz. 2011. “Properties of the Regulatory RNA-Binding Protein HuR and Its Role in Controlling MiRNA Repression.” *Advances in Experimental Medicine and Biology* 700: 106–23. [https://doi.org/10.1007/978-1-4419-7823-3\\_10](https://doi.org/10.1007/978-1-4419-7823-3_10).

» Menn, B, S Timsit, G Calothy, and F Lamballe. 1998. “Differential Expression of TrkC Catalytic and Noncatalytic Isoforms Suggests That They Act Independently or in Association.” *The Journal of Comparative Neurology* 401 (1). [https://doi.org/10.1002/\(sici\)1096-9861\(19981109\)401:1<47::aid-cne4>3.0.co;2-c](https://doi.org/10.1002/(sici)1096-9861(19981109)401:1<47::aid-cne4>3.0.co;2-c).

» Menn, B., S. Timsit, A. Represa, S. Mateos, G. Calothy, and F. Lamballe. 2000. “Spatiotemporal Expression of Noncatalytic TrkC NC2 Isoform during Early and Late CNS Neurogenesis: A Comparative Study with TrkC Catalytic and P75NTR Receptors.” *The European Journal of Neuroscience* 12 (9): 3211–23. <https://doi.org/10.1046/j.1460-9568.2000.00215.x>.

» Merkin, Jason, Caitlin Russell, Ping Chen, and Christopher B. Burge. 2012. “Evolutionary Dynamics of Gene and Isoform Regulation in Mammalian Tissues.” *Science* 338 (6114): 1593–99. <https://doi.org/10.1126/science.1228186>.

» Middlemas, D. S., R. A. Lindberg, and T. Hunter. 1991. “TrkB, a Neural Receptor Protein-Tyrosine Kinase: Evidence for a Full-Length and Two Truncated Receptors.” *Molecular and Cellular Biology* 11 (1): 143–53. <https://doi.org/10.1128/mcb.11.1.143-153.1991>.

» Mihalas, Anca B., Gina E. Elsen, Francesco Bedogni, Ray A. M. Daza, Kevyn A. Ramos-Laguna, Sebastian J. Arnold, and Robert F. Hevner. 2016. “Intermediate Progenitor Cohorts Differentially Generate Cortical Layers and Require Tbr2 for Timely Acquisition of Neuronal Subtype Identity.” *Cell Reports* 16 (1): 92–105. <https://doi.org/10.1016/j.celrep.2016.05.072>.

» Mihalas, Anca B., and Robert F. Hevner. 2018. “Clonal Analysis Reveals Laminar Fate Multipotency and Daughter Cell Apoptosis of Mouse Cortical Intermediate Progenitors.” *Development (Cambridge, England)* 145 (17): dev164335. <https://doi.org/10.1242/dev.164335>.

» Miles, Lee B., Sebastian Dworkin, and Charbel Darido. 2017. “Alternative Splicing and Start Sites: Lessons from the Grainyhead-like Family.” *Developmental Biology* 429 (1): 12–19. <https://doi.org/10.1016/j.ydbio.2017.06.018>.

» Miranda, A. S. de, J. L. V. M. de Barros, and Antonio Lucio Teixeira. 2020. “Is Neurotrophin-3 (NT-3): A Potential Therapeutic Target for Depression and Anxiety?” *Expert Opinion on Therapeutic Targets* 24 (12): 1225–38. <https://doi.org/10.1080/14728222.2020.1846720>.

- » Miska, Eric A, Ezequiel Alvarez-Saavedra, Matthew Townsend, Akira Yoshii, Nenad Šestan, Pasko Rakic, Martha Constantine-Paton, and H Robert Horvitz. 2004. "Microarray Analysis of MicroRNA Expression in the Developing Mammalian Brain." *Genome Biology* 5 (9): R68. <https://doi.org/10.1186/gb-2004-5-9-r68>.
- » Miyamoto, Yoshiaki, Ling Chen, Masahiro Sato, Masahiro Sokabe, Toshitaka Nabeshima, Tony Pawson, Ryuichi Sakai, and Nozomu Mori. 2005. "Hippocampal Synaptic Modulation by the Phosphotyrosine Adapter Protein ShcC/N-Shc via Interaction with the NMDA Receptor." *The Journal of Neuroscience* 25 (7): 1826–35. <https://doi.org/10.1523/JNEUROSCI.3030-04.2005>.
- » Mizutani, Ken-ichi, and Tetsuichiro Saito. 2005. "Progenitors Resume Generating Neurons after Temporary Inhibition of Neurogenesis by Notch Activation in the Mammalian Cerebral Cortex." *Development (Cambridge, England)* 132 (6): 1295–1304. <https://doi.org/10.1242/dev.01693>.
- » Mockenhaupt, Stefan, and Eugene V. Makeyev. 2015. "Non-Coding Functions of Alternative Pre-mRNA Splicing in Development." *Seminars in Cell & Developmental Biology* 47–48 (December): 32–39. <https://doi.org/10.1016/j.semcd.2015.10.018>.
- » Molyneaux, Bradley J., Paola Arlotta, Tostomu Hirata, Masahiko Hibi, and Jeffrey D. Macklis. 2005. "Fezl Is Required for the Birth and Specification of Corticospinal Motor Neurons." *Neuron* 47 (6): 817–31. <https://doi.org/10.1016/j.neuron.2005.08.030>.
- » Molyneaux, Bradley J., Paola Arlotta, Joao R. L. Menezes, and Jeffrey D. Macklis. 2007. "Neuronal Subtype Specification in the Cerebral Cortex." *Nature Reviews Neuroscience* 8 (6): 427–37. <https://doi.org/10.1038/nrn2151>.
- » Montiel, Juan F., and Francisco Aboitiz. 2015. "Pallial Patterning and the Origin of the Isocortex." *Frontiers in Neuroscience* 9 (October). <https://doi.org/10.3389/fnins.2015.00377>.
- » Mora-Bermúdez, Felipe, Farhath Badsha, Sabina Kanton, J. Gray Camp, Benjamin Vernot, Kathrin Köhler, Birger Voigt, et al. 2016. "Differences and Similarities between Human and Chimpanzee Neural Progenitors during Cerebral Cortex Development." *eLife* 5 (September): e18683. <https://doi.org/10.7554/eLife.18683>.
- » Moreno, Nerea, Agustín González, and Sylvie Rétaux. 2009. "Development and Evolution of the Subpallium." *Seminars in Cell & Developmental Biology* 20 (6): 735–43. <https://doi.org/10.1016/j.semcd.2009.04.007>.
- » Morimoto-Suzuki, Nao, Yusuke Hirabayashi, Kelsey Tyssowski, Jun Shinga, Miguel Vidal, Haruhiko Koseki, and Yukiko Gotoh. 2014. "The Polycomb Component Ring1B Regulates the Timed Termination of Subcerebral Projection Neuron Production during Mouse Neocortical Development." *Development (Cambridge, England)* 141 (22): 4343–53. <https://doi.org/10.1242/dev.112276>.
- » Muhr, Jonas, Enrique Graziano, Sara Wilson, Thomas M Jessell, and Thomas Edlund. 1999. "Convergent Inductive Signals Specify Midbrain, Hindbrain, and Spinal Cord Identity in Gastrula Stage Chick Embryos." *Neuron* 23 (4): 689–702. [https://doi.org/10.1016/S0896-6273\(01\)80028-3](https://doi.org/10.1016/S0896-6273(01)80028-3).
- » Muiños-Gimeno, Margarita, Monica Guidi, Birgit Kagerbauer, Rocío Martín-Santos, Ricard Navinés, Pino Alonso, José M. Menchón, Mònica Gratacòs, Xavier Estivill, and Yolanda Espinosa-Parrilla. 2009. "Allele Variants in Functional MicroRNA Target Sites of the Neurotrophin-3 Receptor Gene

(NTRK3) as Susceptibility Factors for Anxiety Disorders.” *Human Mutation* 30 (7): 1062–71. <https://doi.org/10.1002/humu.21005>.

» Mukherjee, Neelanjan, David L. Corcoran, Jeffrey D. Nusbaum, David W. Reid, Stoyan Georgiev, Markus Hafner, Manuel Ascano, Thomas Tuschl, Uwe Ohler, and Jack D. Keene. 2011. “Integrative Regulatory Mapping Indicates That the RNA-Binding Protein HuR Couples Pre-mRNA Processing and mRNA Stability.” *Molecular Cell* 43 (3): 327–39. <https://doi.org/10.1016/j.molcel.2011.06.007>.

» Mukhtar, T., and V. Taylor. 2018. “Untangling Cortical Complexity During Development., Untangling Cortical Complexity During Development.” *Journal of Experimental Neuroscience, Journal of Experimental Neuroscience* 12, 12: 1179069518759332–1179069518759332. <https://doi.org/10.1177/1179069518759332>, [10.1177/1179069518759332](https://doi.org/10.1177/1179069518759332).

» Mulligan, Kimberly A., and Benjamin N. R. Cheyette. 2012. “Wnt Signaling in Vertebrate Neural Development and Function.” *Journal of Neuroimmune Pharmacology* 7 (4): 774–87. <https://doi.org/10.1007/s11481-012-9404-x>.

» Naftelberg, Shiran, Ignacio E. Schor, Gil Ast, and Alberto R. Kornbliht. 2015. “Regulation of Alternative Splicing Through Coupling with Transcription and Chromatin Structure.” *Annual Review of Biochemistry* 84 (1): 165–98. <https://doi.org/10.1146/annurev-biochem-060614-034242>.

» Najafi, Hadi, Mohadeseh Naseri, Javad Zahiri, Mehdi Totonchi, and Majid Sadeghizadeh. 2019. “Identification of the Molecular Events Involved in the Development of Prefrontal Cortex Through the Analysis of RNA-Seq Data From BrainSpan.” *ASN Neuro* 11 (December): 1759091419854627. <https://doi.org/10.1177/1759091419854627>.

» Nakamura, Takeshi, Sumie Muraoka, Reiko Sanokawa, and Nozomu Mori. 1998. “N-Shc and Sck, Two Neuronally Expressed Shc Adapter Homologs: THEIR DIFFERENTIAL REGIONAL EXPRESSION IN THE BRAIN AND ROLES IN NEUROTROPHIN AND Src SIGNALING \*.” *Journal of Biological Chemistry* 273 (12): 6960–67. <https://doi.org/10.1074/jbc.273.12.6960>.

» Nakazawa, Toru, Itsuko Nakano, Masahiro Sato, Takeshi Nakamura, Makoto Tamai, and Nozomu Mori. 2002. “Comparative Expression Profiles of Trk Receptors and Shc-Related Phosphotyrosine Adapters during Retinal Development: Potential Roles of N-Shc/ShcC in Brain-Derived Neurotrophic Factor Signal Transduction and Modulation.” *Journal of Neuroscience Research* 68 (6): 668–80. <https://doi.org/10.1002/jnr.10259>.

» Naro, Chiara, Eleonora Cesari, and Claudio Sette. 2021. “Splicing Regulation in Brain and Testis: Common Themes for Highly Specialized Organs.” *Cell Cycle (Georgetown, Tex.)*, February, 1–10. <https://doi.org/10.1080/15384101.2021.1889187>.

» Nieto, Marta, Edwin S. Monuki, Hua Tang, Jaime Imitola, Nicole Haubst, Samia J. Khoury, Jim Cunningham, Magdalena Gotz, and Christopher A. Walsh. 2004. “Expression of Cux-1 and Cux-2 in the Subventricular Zone and Upper Layers II-IV of the Cerebral Cortex.” *The Journal of Comparative Neurology* 479 (2): 168–80. <https://doi.org/10.1002/cne.20322>.

» Nilsen, Timothy W., and Brenton R. Graveley. 2010. “Expansion of the Eukaryotic Proteome by Alternative Splicing.” *Nature* 463 (7280): 457–63. <https://doi.org/10.1038/nature08909>.

» Nowak, Dawid G., Elianna Mohamed Amin, Emma S. Rennel, Coralie Hoareau-Aveilla, Melissa

Gammons, Gopinath Damodoran, Masatoshi Hagiwara, et al. 2010. "Regulation of Vascular Endothelial Growth Factor (VEGF) Splicing from Pro-Angiogenic to Anti-Angiogenic Isoforms." *The Journal of Biological Chemistry* 285 (8): 5532–40. <https://doi.org/10.1074/jbc.M109.074930>.

» Nowakowski, Tomasz J., Aparna Bhaduri, Alex A. Pollen, Beatriz Alvarado, Mohammed A. Mostajo-Radji, Elizabeth Di Lullo, Maximilian Haeussler, et al. 2017. "Spatiotemporal Gene Expression Trajectories Reveal Developmental Hierarchies of the Human Cortex." *Science* 358 (6368): 1318–23. <https://doi.org/10.1126/science.aap8809>.

» Oberst, Polina, Gulistan Agirman, and Denis Jabaudon. 2019. "Principles of Progenitor Temporal Patterning in the Developing Invertebrate and Vertebrate Nervous System." *Current Opinion in Neurobiology, Neuronal Identity*, 56 (June): 185–93. <https://doi.org/10.1016/j.conb.2019.03.004>.

» Oughtred, Rose, Jennifer Rust, Christie Chang, Bobby-Joe Breitkreutz, Chris Stark, Andrew Willemis, Lorrie Boucher, et al. 2021. "The BioGRID Database: A Comprehensive Biomedical Resource of Curated Protein, Genetic, and Chemical Interactions." *Protein Science: A Publication of the Protein Society* 30 (1): 187–200. <https://doi.org/10.1002/pro.3978>.

» Paletzki, Ronald F., and Charles R. Gerfen. 2019. "Basic Neuroanatomical Methods." *Current Protocols in Neuroscience* 90 (1): e84. <https://doi.org/10.1002/cpns.84>.

» Palko, Mary Ellen, Vincenzo Coppola, and Lino Tessarollo. 1999. "Evidence for a Role of Truncated TrkC Receptor Isoforms in Mouse Development." *The Journal of Neuroscience* 19 (2): 775–82. <https://doi.org/10.1523/JNEUROSCI.19-02-00775.1999>.

» Pan, Qun, Ofer Shai, Leo J. Lee, Brendan J. Frey, and Benjamin J. Blencowe. 2008. "Deep Surveying of Alternative Splicing Complexity in the Human Transcriptome by High-Throughput Sequencing." *Nature Genetics* 40 (12): 1413–15. <https://doi.org/10.1038/ng.259>.

» Pandit, Shatakshi, Yu Zhou, Lily Shiue, Gabriela Coutinho-Mansfield, Hairi Li, Jinsong Qiu, Jie Huang, Gene W. Yeo, Manuel Ares, and Xiang-Dong Fu. 2013. "Genome-Wide Analysis Reveals SR Protein Cooperation and Competition in Regulated Splicing." *Molecular Cell* 50 (2): 223–35. <https://doi.org/10.1016/j.molcel.2013.03.001>.

» Parthasarathy, Srinivas, Swathi Srivatsa, Anjana Nityanandam, and Victor Tarabykin. 2014. "Ntf3 Acts Downstream of Sip1 in Cortical Postmitotic Neurons to Control Progenitor Cell Fate through Feedback Signaling." *Development (Cambridge, England)* 141 (17): 3324–30. <https://doi.org/10.1242/dev.114173>.

» Parthasarathy, Srinivas, Swathi Srivatsa, A Ioana Weber, Nikolaus Gräber, Olga V Britanova, Ekaterina Borisova, Paraskevi Bessa, Mateusz C Ambrozkiwicz, Marta Rosário, and Victor Tarabykin. 2021. "TrkC-T1, the Non-Catalytic Isoform of TrkC, Governs Neocortical Progenitor Fate Specification by Inhibition of MAP Kinase Signaling." *Cerebral Cortex*, no. bhab172 (July). <https://doi.org/10.1093/cercor/bhab172>.

» Paz, Inbal, Idit Kosti, Manuel Ares, Melissa Cline, and Yael Mandel-Gutfreund. 2014. "RBPmap: A Web Server for Mapping Binding Sites of RNA-Binding Proteins." *Nucleic Acids Research* 42 (Web Server issue): W361–67. <https://doi.org/10.1093/nar/gku406>.

» Paz, Sean, Adrian R. Krainer, and Massimo Caputi. 2014. "HIV-1 Transcription Is Regulated

by Splicing Factor SRSF1.” *Nucleic Acids Research* 42 (22): 13812–23. <https://doi.org/10.1093/nar/gku1170>.

» Pilaz, Louis-Jan, John J. McMahon, Emily E. Miller, Ashley L. Lennox, Aussie Suzuki, Edward Salmon, and Debra L. Silver. 2016. “Prolonged Mitosis of Neural Progenitors Alters Cell Fate in the Developing Brain.” *Neuron* 89 (1): 83–99. <https://doi.org/10.1016/j.neuron.2015.12.007>.

» Polioudakis, Damon, Luis de la Torre-Ubieta, Justin Langerman, Andrew G. Elkins, Xu Shi, Jason L. Stein, Celine K. Vuong, et al. 2019. “A Single-Cell Transcriptomic Atlas of Human Neocortical Development during Mid-Gestation.” *Neuron* 103 (5): 785–801.e8. <https://doi.org/10.1016/j.neuron.2019.06.011>.

» Pontious, Adria, Tom Kowalczyk, Chris Englund, and Robert F. Hevner. 2008. “Role of Intermediate Progenitor Cells in Cerebral Cortex Development.” *Developmental Neuroscience* 30 (1–3): 24–32. <https://doi.org/10.1159/000109848>.

» Postigo, Antonio, Anna Maria Calella, Bernd Fritsch, Marlies Knipper, David Katz, Andreas Eilers, Thomas Schimmang, Gary R. Lewin, Rüdiger Klein, and Liliana Minichiello. 2002. “Distinct Requirements for TrkB and TrkC Signaling in Target Innervation by Sensory Neurons.” *Genes & Development* 16 (5): 633–45. <https://doi.org/10.1101/gad.217902>.

» Puehringer, Dirk, Nadiya Orel, Patrick Lüningschrör, Narayan Subramanian, Thomas Herrmann, Moses V Chao, and Michael Sendtner. 2013. “EGF Transactivation of Trk Receptors Regulates the Migration of Newborn Cortical Neurons.” *Nature Neuroscience* 16 (4): 407–15. <https://doi.org/10.1038/nn.3333>.

» Puelles, L. 2013. “Chapter 10 - Plan of the Developing Vertebrate Nervous System: Relating Embryology to the Adult Nervous System (Prosomere Model, Overview of Brain Organization).” In *Patterning and Cell Type Specification in the Developing CNS and PNS*, edited by John L. R. Rubenstein and Pasko Rakic, 187–209. Oxford: Academic Press. <https://doi.org/10.1016/B978-0-12-397265-1.00118-0>.

» Quesnel-Vallières, Mathieu, Manuel Irimia, Sabine P. Cordes, and Benjamin J. Blencowe. 2015. “Essential Roles for the Splicing Regulator NSR100/SRRM4 during Nervous System Development.” *Genes & Development* 29 (7): 746–59. <https://doi.org/10.1101/gad.256115.114>.

» Quesnel-Vallières, Mathieu, Robert J. Weatheritt, Sabine P. Cordes, and Benjamin J. Blencowe. 2019. “Autism Spectrum Disorder: Insights into Convergent Mechanisms from Transcriptomics.” *Nature Reviews Genetics* 20 (1): 51–63. <https://doi.org/10.1038/s41576-018-0066-2>.

» Rajagopal, Rithwick, Zhe-Yu Chen, Francis S. Lee, and Moses V. Chao. 2004. “Transactivation of Trk Neurotrophin Receptors by G-Protein-Coupled Receptor Ligands Occurs on Intracellular Membranes.” *Journal of Neuroscience* 24 (30): 6650–58. <https://doi.org/10.1523/JNEUROSCI.0010-04.2004>.

» Rakic, P. 1971. “Guidance of Neurons Migrating to the Fetal Monkey Neocortex.” *Brain Research* 33 (2): 471–76. [https://doi.org/10.1016/0006-8993\(71\)90119-3](https://doi.org/10.1016/0006-8993(71)90119-3).

» Rakic, P.. 1972. “Mode of Cell Migration to the Superficial Layers of Fetal Monkey Neocortex.” *The Journal of Comparative Neurology* 145 (1): 61–83. <https://doi.org/10.1002/cne.901450105>.

» Rakic, Pasko. 2009. “Evolution of the Neocortex: A Perspective from Developmental Biology.” *Na-*

ture Reviews. Neuroscience 10 (10): 724–35. <https://doi.org/10.1038/nrn2719>.

» Ramsköld, Daniel, Eric T. Wang, Christopher B. Burge, and Rickard Sandberg. 2009. “An Abundance of Ubiquitously Expressed Genes Revealed by Tissue Transcriptome Sequence Data.” *PLOS Computational Biology* 5 (12): e1000598. <https://doi.org/10.1371/journal.pcbi.1000598>.

» Rash, Brian G., James B. Ackman, and Pasko Rakic. 2016. “Bidirectional Radial Ca<sup>2+</sup> Activity Regulates Neurogenesis and Migration during Early Cortical Column Formation.” *Science Advances* 2 (2): e1501733. <https://doi.org/10.1126/sciadv.1501733>.

» Ray, Debashish, Hilal Kazan, Kate B. Cook, Matthew T. Weirauch, Hamed S. Najafabadi, Xiao Li, Serge Gueroussov, et al. 2013. “A Compendium of RNA-Binding Motifs for Decoding Gene Regulation.” *Nature* 499 (7457): 172–77. <https://doi.org/10.1038/nature12311>.

» Reillo, Isabel, Camino de Juan Romero, Adrián Cárdenas, Francisco Clascá, María Ángeles Martínez-Martínez, and Víctor Borrell. 2017. “A Complex Code of Extrinsic Influences on Cortical Progenitor Cells of Higher Mammals.” *Cerebral Cortex* 27 (9): 4586–4606. <https://doi.org/10.1093/cercor/bhx171>.

» Renn, Cynthia L, Carmen C Leitch, and Susan G Dorsey. 2009. “*In Vivo* Evidence That Truncated TrkB.T1 Participates in Nociception.” *Molecular Pain* 5 (October): 61. <https://doi.org/10.1186/1744-8069-5-61>.

» Rockenstein, E. M., L. McConlogue, H. Tan, M. Power, E. Masliah, and L. Mucke. 1995. “Levels and Alternative Splicing of Amyloid Beta Protein Precursor (APP) Transcripts in Brains of APP Transgenic Mice and Humans with Alzheimer’s Disease.” *The Journal of Biological Chemistry* 270 (47): 28257–67. <https://doi.org/10.1074/jbc.270.47.28257>.

» Rodrigues, Deivid C., Marat Mufteev, Robert J. Weatheritt, Ugljesa Djuric, Kevin C. H. Ha, P. Joel Ross, Wei Wei, et al. 2020. “Shifts in Ribosome Engagement Impact Key Gene Sets in Neurodevelopment and Ubiquitination in Rett Syndrome.” *Cell Reports* 30 (12): 4179-4196.e11. <https://doi.org/10.1016/j.celrep.2020.02.107>.

» Rose, Christine R., Robert Blum, Bruno Pichler, Alexandra Lepier, Karl W. Kafitz, and Arthur Konnerth. 2003. “Truncated TrkB-T1 Mediates Neurotrophin-Evoked Calcium Signalling in Glia Cells.” *Nature* 426 (6962): 74–78. <https://doi.org/10.1038/nature01983>.

» Rosenberg, Alexander B., Charles M. Roco, Richard A. Muscat, Anna Kuchina, Paul Sample, Zizhen Yao, Lucas T. Graybuck, et al. 2018. “Single-Cell Profiling of the Developing Mouse Brain and Spinal Cord with Split-Pool Barcoding.” *Science (New York, N.Y.)* 360 (6385): 176–82. <https://doi.org/10.1126/science.aam8999>.

» Rouaux, Caroline, and Paola Arlotta. 2013. “Direct Lineage Reprogramming of Post-Mitotic Callosal Neurons into Corticofugal Neurons *in Vivo*.” *Nature Cell Biology* 15 (2): 214–21. <https://doi.org/10.1038/ncb2660>.

» Sagi, Orli, Arie Budovsky, Marina Wolfson, and Vadim E. Fraifeld. 2015. “ShcC Proteins: Brain Aging and Beyond.” *Ageing Research Reviews* 19 (January): 34–42. <https://doi.org/10.1016/j.arr.2014.11.002>.

- » Saito, Yuhki, Soledad Miranda-Rottmann, Matteo Ruggiu, Christopher Y. Park, John J. Fak, Ru Zhong, Jeremy S. Duncan, et al. 2016. “NOVA2-Mediated RNA Regulation Is Required for Axonal Pathfinding during Development.” *ELife* 5 (May): e14371. <https://doi.org/10.7554/eLife.14371>.
- » Sanford, Jeremy R., Xin Wang, Matthew Mort, Natalia VanDuyn, David N. Cooper, Sean D. Mooney, Howard J. Edenberg, and Yunlong Liu. 2009. “Splicing Factor SFRS1 Recognizes a Functionally Diverse Landscape of RNA Transcripts.” *Genome Research* 19 (3): 381–94. <https://doi.org/10.1101/gr.082503.108>.
- » Sato, Hanae, Nao Hosoda, and Lynne E. Maquat. 2008. “Efficiency of the Pioneer Round of Translation Affects the Cellular Site of Nonsense-Mediated mRNA Decay.” *Molecular Cell* 29 (2): 255–62. <https://doi.org/10.1016/j.molcel.2007.12.009>.
- » Schreiner, Dietmar, Jovan Simicevic, Erik Ahrné, Alexander Schmidt, and Peter Scheiffele. 2015. “Quantitative Isoform-Profiling of Highly Diversified Recognition Molecules.” Edited by Ben Barres. *ELife* 4 (May): e07794. <https://doi.org/10.7554/eLife.07794>.
- » Schuurmans, Carol, and François Guillemot. 2002. “Molecular Mechanisms Underlying Cell Fate Specification in the Developing Telencephalon.” *Current Opinion in Neurobiology* 12 (1): 26–34. [https://doi.org/10.1016/S0959-4388\(02\)00286-6](https://doi.org/10.1016/S0959-4388(02)00286-6).
- » Seuntjens, Eve, Anjana Nityanandam, Amaya Miquelajauregui, Joke Debruyne, Agata Stryjewska, Sandra Goebbels, Klaus-Armin Nave, Danny Huylebroeck, and Victor Tarabykin. 2009. “Sip1 Regulates Sequential Fate Decisions by Feedback Signaling from Postmitotic Neurons to Progenitors.” *Nature Neuroscience* 12 (11): 1373–80. <https://doi.org/10.1038/nn.2409>.
- » Shashikant, Tanvi, and Charles A. Etness. 2019. “Genome-Wide Analysis of Chromatin Accessibility Using ATAC-Seq.” *Methods in Cell Biology* 151: 219–35. <https://doi.org/10.1016/bs.mcb.2018.11.002>.
- » Shelton, D. L., J. Sutherland, J. Gripp, T. Camerato, M. P. Armanini, H. S. Phillips, K. Carroll, S. D. Spencer, and A. D. Levinson. 1995. “Human Trks: Molecular Cloning, Tissue Distribution, and Expression of Extracellular Domain Immunoadhesins.” *Journal of Neuroscience* 15 (1): 477–91. <https://doi.org/10.1523/JNEUROSCI.15-01-00477.1995>.
- » Srinivasan, Karpagam, Dino P. Leone, Rosalie K. Bateson, Gergana Dobрева, Yoshinori Kohwi, Terumi Kohwi-Shigematsu, Rudolf Grosschedl, and Susan K. McConnell. 2012. “A Network of Genetic Repression and Derepression Specifies Projection Fates in the Developing Neocortex.” *Proceedings of the National Academy of Sciences of the United States of America* 109 (47): 19071–78. <https://doi.org/10.1073/pnas.1216793109>.
- » Stahl, Ronny, Tessa Walcher, Camino De Juan Romero, Gregor Alexander Pilz, Silvia Cappello, Martin Irmeler, José Miguel Sanz-Aquela, et al. 2013. “Trnp1 Regulates Expansion and Folding of the Mammalian Cerebral Cortex by Control of Radial Glial Fate.” *Cell* 153 (3): 535–49. <https://doi.org/10.1016/j.cell.2013.03.027>.
- » Stark, Chris, Bobby-Joe Breitkreutz, Teresa Reguly, Lorrie Boucher, Ashton Breitkreutz, and Mike Tyers. 2006. “BioGRID: A General Repository for Interaction Datasets.” *Nucleic Acids Research* 34 (Database issue): D535–539. <https://doi.org/10.1093/nar/gkj109>.

- » Stenzel, Denise, Michaela Wilsch-Bräuninger, Fong Kuan Wong, Heike Heuer, and Wieland B. Huttner. 2014. “Integrin Av $\beta$ 3 and Thyroid Hormones Promote Expansion of Progenitors in Embryonic Neocortex.” *Development* 141 (4): 795–806. <https://doi.org/10.1242/dev.101907>.
- » Su, Chun-Hao, Dhananjaya D, and Woan-Yuh Tarn. 2018. “Alternative Splicing in Neurogenesis and Brain Development.” *Frontiers in Molecular Biosciences* 5 (February). <https://doi.org/10.3389/fmolb.2018.00012>.
- » Su, Chun-Hao, Kuan-Yang Hung, Shih-Chieh Hung, and Woan-Yuh Tarn. 2017. “RBM4 Regulates Neuronal Differentiation of Mesenchymal Stem Cells by Modulating Alternative Splicing of Pyruvate Kinase M.” *Molecular and Cellular Biology* 37 (3). <https://doi.org/10.1128/MCB.00466-16>.
- » Sun, Tao, and Robert F. Hevner. 2014. “Growth and Folding of the Mammalian Cerebral Cortex: From Molecules to Malformations.” *Nature Reviews Neuroscience* 15 (4): 217–32. <https://doi.org/10.1038/nrn3707>.
- » Sykes, Alex M., and Wieland B. Huttner. 2013. “Prominin-1 (CD133) and the Cell Biology of Neural Progenitors and Their Progeny.” In *Prominin-1 (CD133): New Insights on Stem & Cancer Stem Cell Biology*, edited by Denis Corbeil, 89–98. *Advances in Experimental Medicine and Biology*. New York, NY: Springer. [https://doi.org/10.1007/978-1-4614-5894-4\\_6](https://doi.org/10.1007/978-1-4614-5894-4_6).
- » Tacke, R., and J. L. Manley. 1995. “The Human Splicing Factors ASF/SF2 and SC35 Possess Distinct, Functionally Significant RNA Binding Specificities.” *The EMBO Journal* 14 (14): 3540–51.
- » Taliaferro, J. Matthew, Marina Vidaki, Ruan Oliveira, Sara Olson, Lijun Zhan, Tanvi Saxena, Eric T. Wang, et al. 2016. “Distal Alternative Last Exons Localize MRNAs to Neural Projections.” *Molecular Cell* 61 (6): 821–33. <https://doi.org/10.1016/j.molcel.2016.01.020>.
- » Tang, Yong, Jens R. Nyengaard, Didima M. G. De Groot, and Hans Jørgen G. Gundersen. 2001. “Total Regional and Global Number of Synapses in the Human Brain Neocortex.” *Synapse* 41 (3): 258–73. <https://doi.org/10.1002/syn.1083>.
- » Tarabykin, Victor, Anastassia Stoykova, Natalia Usman, and Peter Gruss. 2001. “Cortical Upper Layer Neurons Derive from the Subventricular Zone as Indicated by Svet1 Gene Expression.” *Development* 128 (11): 1983–93. <https://doi.org/10.1242/dev.128.11.1983>.
- » Telley, L., G. Agirman, J. Prados, N. Amberg, S. Fièvre, P. Oberst, G. Bartolini, et al. 2019. “Temporal Patterning of Apical Progenitors and Their Daughter Neurons in the Developing Neocortex.” *Science* 364 (6440). <https://doi.org/10.1126/science.aav2522>.
- » Temple, S., and Q. Shen. 2013. “Chapter 14 - Cell Biology of Neuronal Progenitor Cells.” In *Patterning and Cell Type Specification in the Developing CNS and PNS*, edited by John L. R. Rubenstein and Pasko Rakic, 261–83. Oxford: Academic Press. <https://doi.org/10.1016/B978-0-12-397265-1.00076-9>.
- » Terasaka, Tomohiro, Taeshin Kim, Hiral Dave, Bhakti Gangapurkar, Dequina A. Nicholas, Oscar Muñoz, Eri Terasaka, Danmei Li, and Mark A. Lawson. 2019. “The RNA-Binding Protein ELAVL1 Regulates GnRH Receptor Expression and the Response to GnRH.” *Endocrinology* 160 (8): 1999–2014. <https://doi.org/10.1210/en.2019-00203>.
- » Tessarollo, Lino, Pantelis Tsoulfas, Michael J. Donovan, Mary Ellen Palko, Janet Blair-Flynn, Bar-

- bara L. Hempstead, and Luis F. Parada. 1997. "Targeted Deletion of All Isoforms of the TrkC Gene Suggests the Use of Alternate Receptors by Its Ligand Neurotrophin-3 in Neuronal Development and Implicates TrkC in Normal Cardiogenesis." *Proceedings of the National Academy of Sciences* 94 (26): 14776–81.
- » Toma, Kenichi, Takuma Kumamoto, and Carina Hanashima. 2014. "The Timing of Upper-Layer Neurogenesis Is Conferred by Sequential Derepression and Negative Feedback from Deep-Layer Neurons." *Journal of Neuroscience* 34 (39): 13259–76.
- » Toma, Kenichi, Tien-Cheng Wang, and Carina Hanashima. 2016. "Encoding and Decoding Time in Neural Development." *Development, Growth & Differentiation* 58 (1): 59–72. <https://doi.org/10.1111/dgd.12257>.
- » Trivino-Paredes, J. S., P. C. Nahirney, C. Pinar, P. Grandes, and B. R. Christie. 2019. "Acute Slice Preparation for Electrophysiology Increases Spine Numbers Equivalently in the Male and Female Juvenile Hippocampus: A DiI Labeling Study." *Journal of Neurophysiology* 122 (3): 958–69. <https://doi.org/10.1152/jn.00332.2019>.
- » Tsoulfas, Pantelis, Dan Soppet, Enrique Escandon, Lino Tessarollo, José-Luis Mendoza-Ramirez, Arnon Rosenthal, Karoly Nikolics, and Luis F. Parada. 1993. "The Rat TrkC Locus Encodes Multiple Neurogenic Receptors That Exhibit Differential Response to Neurotrophin-3 in PC12 Cells." *Neuron* 10 (5): 975–90. [https://doi.org/10.1016/0896-6273\(93\)90212-A](https://doi.org/10.1016/0896-6273(93)90212-A).
- » Turunen, Janne J, Elina H Niemelä, Bhupendra Verma, and Mikko J Frilander. 2013. "The Significant Other: Splicing by the Minor Spliceosome." *Wiley Interdisciplinary Reviews. RNA* 4 (1): 61–76. <https://doi.org/10.1002/wrna.1141>.
- » Uzquiano, Ana, Ivan Gladwyn-Ng, Laurent Nguyen, Orly Reiner, Magdalena Götz, Fumio Matsuzaki, and Fiona Francis. 2018. "Cortical Progenitor Biology: Key Features Mediating Proliferation versus Differentiation." *Journal of Neurochemistry*, March. <https://doi.org/10.1111/jnc.14338>.
- » Valenzuela, David M., Peter C. Maisonpierre, David J. Glass, Eduardo Rojas, Lorna Nuñez, Yuan Kong, David R. Gies, Trevor N. Stitt, Nancy Y. Ip, and George D. Yancopoulos. 1993. "Alternative Forms of Rat TrkC with Different Functional Capabilities." *Neuron* 10 (5): 963–74. [https://doi.org/10.1016/0896-6273\(93\)90211-9](https://doi.org/10.1016/0896-6273(93)90211-9).
- » Venkataraman, Archana, Thomas J. Whitford, Carl-Fredrik Westin, Polina Golland, and Marek Kubicki. 2012. "Whole Brain Resting State Functional Connectivity Abnormalities in Schizophrenia." *Schizophrenia Research* 139 (1): 7–12. <https://doi.org/10.1016/j.schres.2012.04.021>.
- » Visel, Axel, Christina Thaller, and Gregor Eichele. 2004. "GenePaint.Org: An Atlas of Gene Expression Patterns in the Mouse Embryo." *Nucleic Acids Research* 32 (suppl\_1): D552–56. <https://doi.org/10.1093/nar/gkh029>.
- » Vitali, Ilaria, Sabine Fièvre, Ludovic Telley, Polina Oberst, Sebastiano Bariselli, Laura Frangeul, Natalia Baumann, et al. 2018. "Progenitor Hyperpolarization Regulates the Sequential Generation of Neuronal Subtypes in the Developing Neocortex." *Cell* 174 (5): 1264–1276.e15. <https://doi.org/10.1016/j.cell.2018.06.036>.
- » Voineagu, Irina, Xinchun Wang, Patrick Johnston, Jennifer K. Lowe, Yuan Tian, Steve Horvath,

Jonathan Mill, Rita M. Cantor, Benjamin J. Blencowe, and Daniel H. Geschwind. 2011. “Transcriptomic Analysis of Autistic Brain Reveals Convergent Molecular Pathology.” *Nature* 474 (7351): 380–84. <https://doi.org/10.1038/nature10110>.

» Vuong, Celine K., Douglas L. Black, and Sika Zheng. 2016. “The Neurogenetics of Alternative Splicing.” *Nature Reviews. Neuroscience* 17 (5): 265–81. <https://doi.org/10.1038/nrn.2016.27>.

» Wahl, Markus C., Cindy L. Will, and Reinhard Lührmann. 2009. “The Spliceosome: Design Principles of a Dynamic RNP Machine.” *Cell* 136 (4): 701–18. <https://doi.org/10.1016/j.cell.2009.02.009>.

» Walker, Rebecca L., Gokul Ramaswami, Christopher Hartl, Nicholas Mancuso, Michael J. Gandal, Luis de la Torre-Ubieta, Bogdan Pasaniuc, Jason L. Stein, and Daniel H. Geschwind. 2019. “Genetic Control of Expression and Splicing in Developing Human Brain Informs Disease Mechanisms.” *Cell* 179 (3): 750–771.e22. <https://doi.org/10.1016/j.cell.2019.09.021>.

» Wang, Eric T., Rickard Sandberg, Shujun Luo, Irina Khrebtkova, Lu Zhang, Christine Mayr, Stephen F. Kingsmore, Gary P. Schroth, and Christopher B. Burge. 2008. “Alternative Isoform Regulation in Human Tissue Transcriptomes.” *Nature* 456 (7221): 470–76. <https://doi.org/10.1038/nature07509>.

» Wang, Jinhua, Philip J. Smith, Adrian R. Krainer, and Michael Q. Zhang. 2005. “Distribution of SR Protein Exonic Splicing Enhancer Motifs in Human Protein-Coding Genes.” *Nucleic Acids Research* 33 (16): 5053–62. <https://doi.org/10.1093/nar/gki810>.

» Wang, Lei, Shirui Hou, and Young-Goo Han. 2016. “Hedgehog Signaling Promotes Basal Progenitor Expansion and the Growth and Folding of the Neocortex.” *Nature Neuroscience* 19 (7): 888–96. <https://doi.org/10.1038/nn.4307>.

» Weissman, Tamily A., Patricio A. Riquelme, Lidija Ivic, Alexander C. Flint, and Arnold R. Kriegstein. 2004. “Calcium Waves Propagate through Radial Glial Cells and Modulate Proliferation in the Developing Neocortex.” *Neuron* 43 (5): 647–61. <https://doi.org/10.1016/j.neuron.2004.08.015>.

» Welch, Joshua D., Velina Kozareva, Ashley Ferreira, Charles Vanderburg, Carly Martin, and Evan Z. Macosko. 2019. “Single-Cell Multi-Omic Integration Compares and Contrasts Features of Brain Cell Identity.” *Cell* 177 (7): 1873–1887.e17. <https://doi.org/10.1016/j.cell.2019.05.006>.

» Weyn-Vanhentenryck, Sebastien M., Huijuan Feng, Dmytro Ustianenko, Rachel Duffié, Qinghong Yan, Martin Jacko, Jose C. Martinez, et al. 2018. “Precise Temporal Regulation of Alternative Splicing during Neural Development.” *Nature Communications* 9 (1): 1–17. <https://doi.org/10.1038/s41467-018-04559-0>.

» Wilkinson, Max E., Clément Charenton, and Kiyoshi Nagai. 2020. “RNA Splicing by the Spliceosome.” *Annual Review of Biochemistry* 89 (1): null. <https://doi.org/10.1146/annurev-biochem-091719-064225>.

» Wills, Melanie K. B., and Nina Jones. 2012. “Teaching an Old Dogma New Tricks: Twenty Years of Shc Adaptor Signalling.” *The Biochemical Journal* 447 (1): 1–16. <https://doi.org/10.1042/BJ20120769>.

» Wu, Sheng-Xi, Sandra Goebbels, Kouichi Nakamura, Kazuhiro Nakamura, Kouhei Kometani, Naga-hiro Minato, Takeshi Kaneko, Klaus-Armin Nave, and Nobuaki Tamamaki. 2005. “Pyramidal Neurons of Upper Cortical Layers Generated by NEX-Positive Progenitor Cells in the Subventricular Zone.”

Proceedings of the National Academy of Sciences of the United States of America 102 (47): 17172–77. <https://doi.org/10.1073/pnas.0508560102>.

» Xiao, S H, and J L Manley. 1998. “Phosphorylation-Dephosphorylation Differentially Affects Activities of Splicing Factor ASF/SF2.” *The EMBO Journal* 17 (21): 6359–67. <https://doi.org/10.1093/emboj/17.21.6359>.

» Xie, Zhongcong, Yuanlin Dong, Uta Maeda, Weiming Xia, and Rudolph E. Tanzi. 2007. “RNA Interference Silencing of the Adaptor Molecules ShcC and Fe65 Differentially Affect Amyloid Precursor Protein Processing and A $\beta$  Generation\*.” *Journal of Biological Chemistry* 282 (7): 4318–25. <https://doi.org/10.1074/jbc.M609293200>.

» Xu, Bin, Iuliana Ionita-Laza, J. Louw Roos, Braden Boone, Scarlet Woodrick, Yan Sun, Shawn Levy, Joseph A. Gogos, and Maria Karayiorgou. 2012. “De Novo Gene Mutations Highlight Patterns of Genetic and Neural Complexity in Schizophrenia.” *Nature Genetics* 44 (12): 1365–69. <https://doi.org/10.1038/ng.2446>.

» Xu, Qiang, Barmak Modrek, and Christopher Lee. 2002. “Genome-Wide Detection of Tissue-Specific Alternative Splicing in the Human Transcriptome.” *Nucleic Acids Research* 30 (17): 3754–66.

» Xu, Xiangdong, Dongmei Yang, Jian-Hua Ding, Wang Wang, Pao-Hsien Chu, Nancy D. Dalton, Huan-You Wang, et al. 2005. “ASF/SF2-Regulated CaMKII $\delta$  Alternative Splicing Temporally Reprograms Excitation-Contraction Coupling in Cardiac Muscle.” *Cell* 120 (1): 59–72. <https://doi.org/10.1016/j.cell.2004.11.036>.

» Yap, Karen, Yixin Xiao, Brad A. Friedman, H. Shawn Je, and Eugene V. Makeyev. 2016. “Polarizing the Neuron through Sustained Co-Expression of Alternatively Spliced Isoforms.” *Cell Reports* 15 (6): 1316–28. <https://doi.org/10.1016/j.celrep.2016.04.012>.

» Yates, Andrew D., Premanand Achuthan, Wasiu Akanni, James Allen, Jamie Allen, Jorge Alvarez-Jarreta, M. Ridwan Amode, et al. 2020. “Ensembl 2020.” *Nucleic Acids Research* 48 (D1): D682–88. <https://doi.org/10.1093/nar/gkz966>.

» Yeo, Gene, and Christopher B. Burge. 2004. “Maximum Entropy Modeling of Short Sequence Motifs with Applications to RNA Splicing Signals.” *Journal of Computational Biology* 11 (2–3): 377–94. <https://doi.org/10.1089/1066527041410418>.

» Yoon, Ki-Jun, Francisca Rojas Ringeling, Caroline Vissers, Fadi Jacob, Michael Pokrass, Dennisse Jimenez-Cyrus, Yijing Su, et al. 2017. “Temporal Control of Mammalian Cortical Neurogenesis by M6A Methylation.” *Cell* 171 (4): 877–889.e17. <https://doi.org/10.1016/j.cell.2017.09.003>.

» Yu, Jing, and Andrew P. McMahon. 2006. “Reproducible and Inducible Knockdown of Gene Expression in Mice.” *Genesis (New York, N.Y.: 2000)* 44 (5): 252–61. <https://doi.org/10.1002/dvg.20213>.

» Zaghlool, Ammar, Adam Ameer, Lucia Cavelier, and Lars Feuk. 2014. “Splicing in the Human Brain.” *International Review of Neurobiology* 116: 95–125. <https://doi.org/10.1016/B978-0-12-801105-8.00005-9>.

» Zahr, Siraj K., Guang Yang, Hilal Kazan, Michael J. Borrett, Scott A. Yuzwa, Anastassia Voronova, David R. Kaplan, and Freda D. Miller. 2018. “A Translational Repression Complex in Developing

Mammalian Neural Stem Cells That Regulates Neuronal Specification.” *Neuron* 97 (3): 520-537.e6. <https://doi.org/10.1016/j.neuron.2017.12.045>.

» Zaqout, Sami, and Angela M. Kaindl. 2016. “Golgi-Cox Staining Step by Step.” *Frontiers in Neuroanatomy* 0. <https://doi.org/10.3389/fnana.2016.00038>.

» Zarate, Y. A., M. Steinrath, A. Matthews, W. E. Smith, A. Sun, L. C. Wilson, C. Brain, et al. 2018. “Bone Health and SATB2-Associated Syndrome.” *Clinical Genetics* 93 (3): 588–94. <https://doi.org/10.1111/cge.13121>.

» Zhang, Haijun, Yafei Chang, Longbin Zhang, Seung-Nam Kim, Gaizka Otaegi, Zhen Zhang, Yan-zhen Nie, et al. 2019. “Upregulation of MicroRNA MiR-9 Is Associated with Microcephaly and Zika Virus Infection in Mice.” *Molecular Neurobiology* 56 (6): 4072–85. <https://doi.org/10.1007/s12035-018-1358-4>.

» Zhang, Qiong, Ying Huang, Lei Zhang, Yu-Qiang Ding, and Ning-Ning Song. 2019. “Loss of Satb2 in the Cortex and Hippocampus Leads to Abnormal Behaviors in Mice.” *Frontiers in Molecular Neuroscience* 12: 33. <https://doi.org/10.3389/fnmol.2019.00033>.

» Zhang, Xiang H.-F., and Lawrence A. Chasin. 2004. “Computational Definition of Sequence Motifs Governing Constitutive Exon Splicing.” *Genes & Development* 18 (11): 1241–50. <https://doi.org/10.1101/gad.1195304>.

» Zhang, Xiaochang, Ming Hui Chen, Xuebing Wu, Andrew Kodani, Jean Fan, Ryan Doan, Manabu Ozawa, et al. 2016. “Cell Type-Specific Alternative Splicing Governs Cell Fate in the Developing Cerebral Cortex.” *Cell* 166 (5): 1147-1162.e15. <https://doi.org/10.1016/j.cell.2016.07.025>.

» Zhang, Zuo, and Adrian R. Krainer. 2004. “Involvement of SR Proteins in mRNA Surveillance.” *Molecular Cell* 16 (4): 597–607. <https://doi.org/10.1016/j.molcel.2004.10.031>.

» Zhao, Yawei, Ting Zhu, Xueying Zhang, Qingyang Wang, Jiyan Zhang, Wenbin Ji, and Yuanfang Ma. 2015. “Splicing Factor 2/Alternative Splicing Factor Contributes to Extracellular Signal regulated Kinase Activation in Hepatocellular Carcinoma Cells.” *Molecular Medicine Reports* 12 (3): 3890–94. <https://doi.org/10.3892/mmr.2015.3851>.

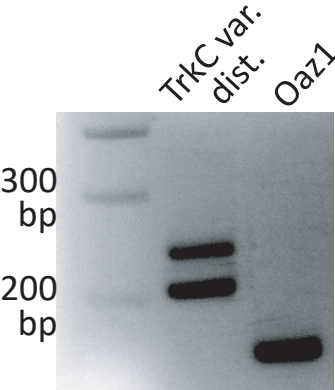
» Zhong, Suijuan, Shu Zhang, Xiaoying Fan, Qian Wu, Liying Yan, Ji Dong, Haofeng Zhang, et al. 2018. “A Single-Cell RNA-Seq Survey of the Developmental Landscape of the Human Prefrontal Cortex.” *Nature* 555 (7697): 524–28. <https://doi.org/10.1038/nature25980>.

» Ziats, M. N., and O. M. Rennert. 2014. “Identification of Differentially Expressed MicroRNAs across the Developing Human Brain.” *Molecular Psychiatry* 19 (7): 848–52. <https://doi.org/10.1038/mp.2013.93>.

» Zimmer, Céline, Marie-Catherine Tiveron, Rolf Bodmer, and Harold Cremer. 2004. “Dynamics of Cux2 Expression Suggests That an Early Pool of SVZ Precursors Is Fated to Become Upper Cortical Layer Neurons.” *Cerebral Cortex (New York, N.Y.: 1991)* 14 (12): 1408–20. <https://doi.org/10.1093/cercor/bhh102>.

» Zuo, P., and J. L. Manley. 1994. “The Human Splicing Factor ASF/SF2 Can Specifically Recognize Pre-mRNA 5’ Splice Sites.” *Proceedings of the National Academy of Sciences* 91 (8): 3363–67. <https://doi.org/10.1073/pnas.91.8.3363>.

# SUPPLEMENTARY INFORMATION



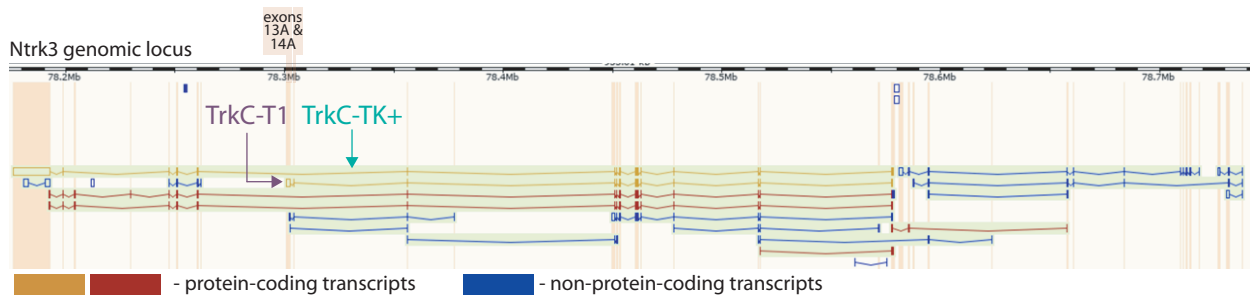
**Supplementary Figure 1. N2A cells express both TrkC-T1 (upper band) and TrkC-TK+ (lower band). Oaz1 PCR product shown as positive control for cDNA quality.**

Name	Expression in WT N2A cells	
	Value	Rank
<i>Hprt</i>	10.4868	94
<i>Actb</i>	12.779	100
<i>Celf1</i>	10.8063	95
<i>Celf2</i>	4.54326	3
<i>Elavl1</i>	11.5004	98
<i>Hnrnp2</i>	9.20938	84
<i>Hnrnp1</i>	10.6235	94
<i>Khdrbs3</i>	4.95731	17
<i>Mbnl1</i>	10.667	94
<i>Mbnl2</i>	10.6811	95
<i>Mbnl3</i>	4.82421	11
<i>Nova1</i>	8.95551	81
<i>Nova2</i>	7.49943	68
<i>Ptbp1</i>	10.8611	96
<i>Ptbp2</i>	10.6078	94
<i>Rbfox2</i>	9.36738	85
<i>Rbm22</i>	9.25504	84
<i>Rbm47</i>	4.55413	3
<i>Rbm5</i>	9.40558	85
<i>Srpk1</i>	10.9143	96
<i>Srrm2</i>	11.1425	97
<i>Srsf1</i>	10.061	91
<i>Srsf2</i>	11.695	99
<i>Srsf3</i>	9.27605	84
<i>Srsf4</i>	9.28704	84
<i>Srsf5</i>	8.57685	78
<i>Srsf6</i>	9.61914	87
<i>Srsf7</i>	8.98895	81
<i>Srsf9</i>	9.28325	84
<i>Srsf10</i>	11.1348	97
<i>Srsf11</i>	9.5474	87
<i>Srsf12</i>	5.11726	25
<i>Tra2a</i>	9.68302	88
<i>U2af1</i>	8.96652	81

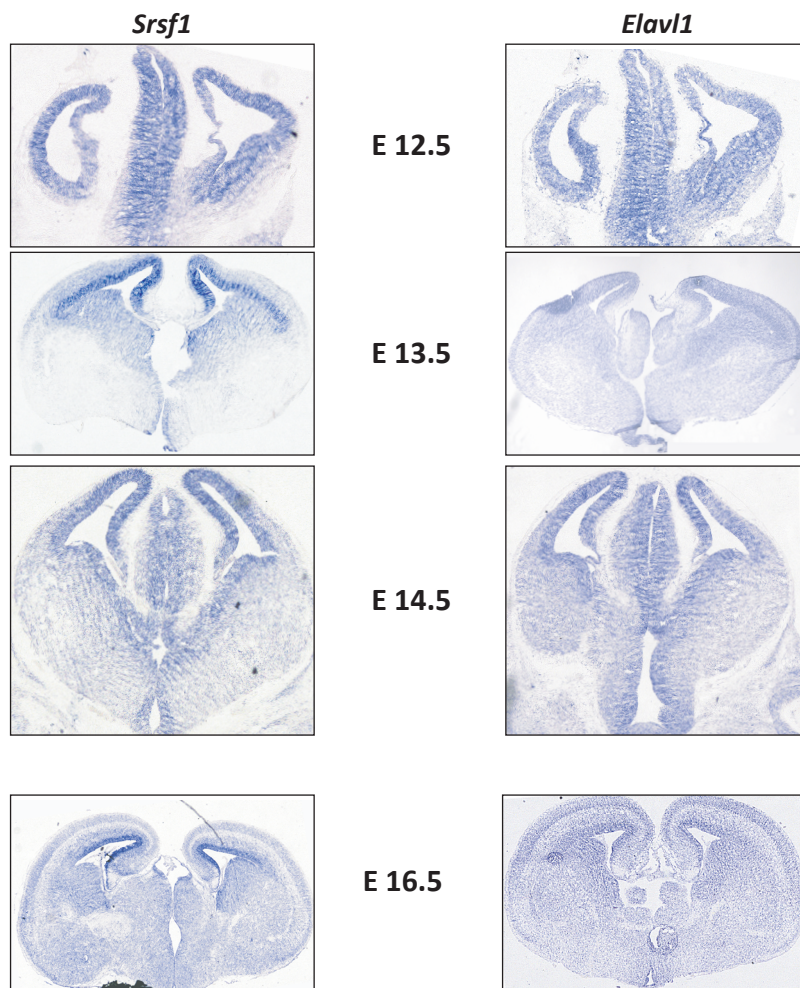
**Supplementary Table 1 Expression levels of targetted splicing factors in N2A cells.** Data obtained from querying the dataset of wild type N2A cells from Chakrabarti et al. (GSE45160 on GEO at NCBI, Chakrabarti et al., 2013). *Hprt* and *Actb* are shown as controls for highly expressed genes.

siRNA	Average	Std.dev	Percent change from ctrl
ctrl	40.511	1.866	0.000
Rbm47	42.244	2.496	-4.278
Elavl1	71.546	3.815	-76.609
Rbm22	55.113	2.175	-36.043
Tra2a	48.314	2.404	-19.261
Ptbp1	42.277	1.222	-4.358
Srsf1	25.294	1.204	37.562
Ptbp2	40.941	3.234	-1.062
Hnrnp1	52.111	4.075	-28.634
U2af1	47.383	3.496	-16.962
Khdrbs3	40.443	6.939	0.168
Rbm5	40.256	8.920	0.631
Hnrnp2	48.881	0.646	-20.661
utr	50.063	9.110	-23.579
Ctrl	26.469	1.818	0.000
Mbn1	24.491	0.068	7.476
Mbn2	26.096	0.223	1.412
Mbn3	26.587	0.254	-0.446
Nova1	23.458	1.677	11.376
Nova2	22.022	0.946	16.803
Ptbp1	22.092	2.541	16.537
Ptbp2	25.097	0.480	5.184
Rbfox2	25.075	2.358	5.270
Celf1	26.164	0.781	1.155
Celf2	25.561	0.637	3.430
untr.	24.091	1.033	8.986
ctrl	27.261	0.818	0.000
SRSF1	13.139	1.792	51.803
SRSF2	27.087	0.024	0.638
SRSF3	24.269	2.332	10.974
SRSF4	26.874	1.067	1.420
SRSF5	20.797	4.755	23.711
SRSF6	19.053	0.118	30.109
SRSF7	24.704	1.969	9.379
SRSF9	26.110	1.978	4.222
SRSF10	20.243	2.477	25.744
SRSF11	25.540	0.385	6.310
SRSF12	30.351335	0.4632971	-11.3375083
SRPK1	20.94467	0.017774	23.16887155
SRRM2	26.654089	1.6461143	2.225062899
untr.	22.552332	22.552332	17.27150167

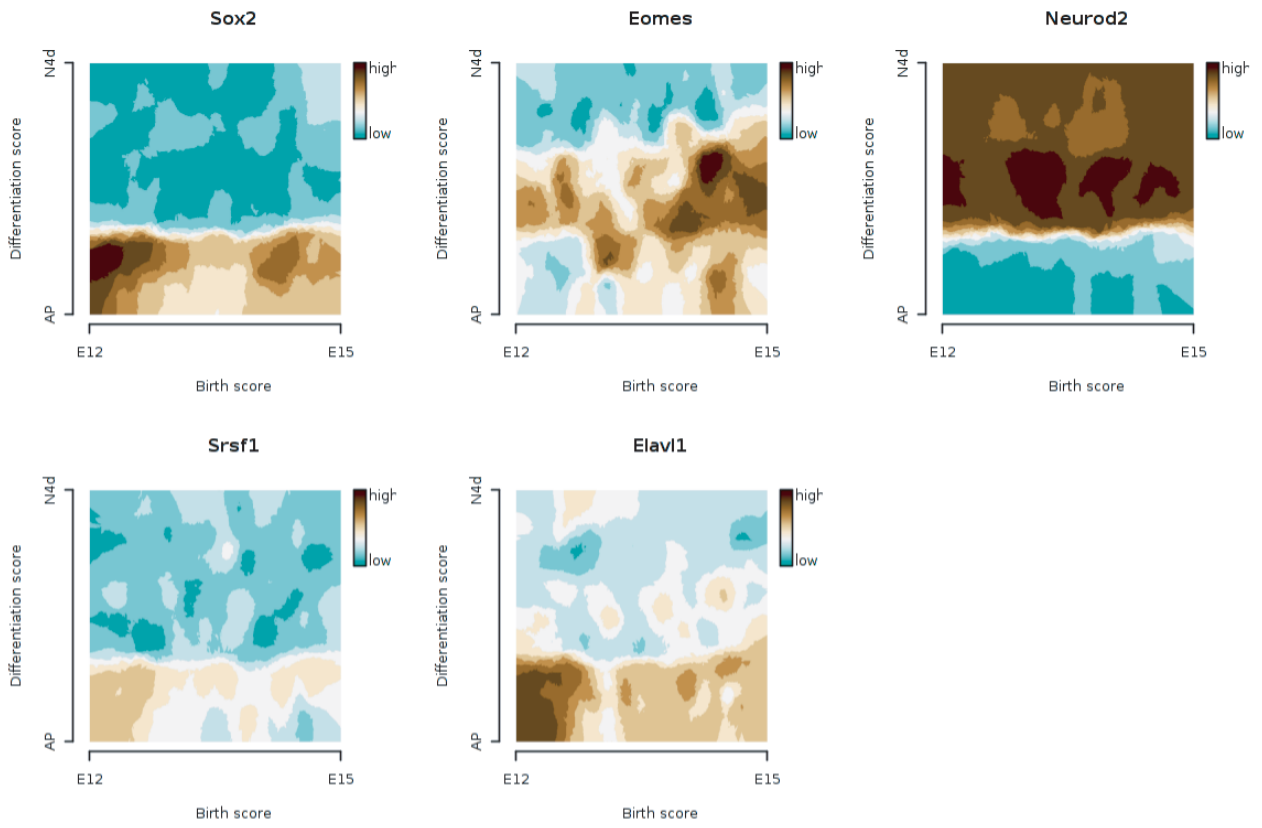
**Supplementary Table 2** PSI values for the splicing factor knockdowns shown in Figure 2.7, as reported to the control (siCtrl).



**Supplementary Figure 2 Transcripts from the murine Ntrk3 (TrkC) locus annotated in the Ensembl genome browser.** TrkC-TK+ and TrkC-T1 are indicated. No other transcript variants are described that skip exon 13A but retain exon 14A.



**Supplementary Figure 3 Panoramic overviews over the brains resulting from in situ hybridization with probes directed against *Srsf1* and *Elavl1*, as shown in Figure 2.12 and Figure 2.13.**



**Supplementary Figure 4 Expression of Srsf1 and Elavl1 as shown in the single-cell RNA sequencing dataset from Telley et al., 2019.** Upper row presents expression profiles of genes characteristic for apical radial glia (Sox2), intermediate progenitors (Eomes) and postmitotic neurons (Neurod2).

